FOSSIL ENERGY

DOE/ID/13421-1
OSTI ID: 8240

EVALUATION OF RESERVOIR WETTABILITY AND ITS EFFECTS ON OIL RECOVERY

Annual Report
August 1998

By
Jill S. Buckley

Date Published: July 1999

Work Performed Under Contract No. DE-FC22-96ID13421

New Mexico Institute of Mining and Technology
Socorro, New Mexico

National Petroleum Technology Office
U. S. DEPARTMENT OF ENERGY
Tulsa, Oklahoma

DOE/ID/13421-1
Distribution Category UC-122

Evaluation of Reservoir Wettability and Its Effects On Oil Recovery

July 1999

Work Performed Under Contract DE-FC22-96ID13421

Prepared for
U.S. Department of Energy
Assistant Secretary for Fossil Energy

Purna Halder, Project Manager
National Petroleum Technology Office
P.O. Box 3628
Tulsa, OK 74101

Prepared by
Petroleum Recovery Research Center
New Mexico Institute of Mining and Technology
801 Leroy Place
Socorro, NM 87801

TABLE OF CONTENTS

LIST OF FIGURES

LIST OF TABLES

ABSTRACT

We report on the second year of the project, "Evaluation of Reservoir Wettability and its Effect on Oil Recovery." The objectives of this five-year project are (1) to achieve improved understanding of the surface and interfacial properties of crude oils and their interactions with mineral surfaces, (2) to apply the results of surface studies to improve predictions of oil production from laboratory measurements, and (3) to use the results of this research to recommend ways to improve oil recovery by waterflooding.

Progress has been made in several important areas. In Part 1, we have been testing improved methods of oil characterization for prediction of their wettability-altering potential. Four medium gravity crude oils have been characterized in section 1.1 by their "G-AB" profiles, where G is API gravity, A is acid number and B is base number. The oils in this group have varying amounts of asphaltenes, but all have sufficiently low gravity so that surface precipitation is not anticipated to dominate their interactions with solid surfaces. We find that the oil in this group with the highest ratio of base number to acid number gave the greatest alteration of wetting on mica surfaces, when the brine chosen favored acid/base interactions. Less wetting alteration was observed for the other three oils with all combinations of brine.

Another important contribution in the oil characterization area of this project is the use of refractive index to quantify solvent quality of an oil with respect to its asphaltene fraction. The theoretical basis and application of the refractive index approach are reported in section 1.2 of this report.

In Part 2 of this project we seek to improve the available tools for the assessment of wetting alteration by interactions between crude oils, brine, and rock surfaces. Many of our standard measurements have used glass slides as the test surface. Muscovite mica potentially has many advantages over glass as a surface standard. In the study reported in section 2.1 we demonstrate that our mechanistic insight developed using glass test surfaces applies to mica as well. At elevated temperatures, tests with mica may actually be more predictive of interactions with rock surfaces than glass surface tests have been.

Finally, in section 2.2 we have used crude oil in combination with brines of varying composition to alter the surface wetting of square glass capillary tubes. In these capillaries, displacement by spontaneous imbibition can be observed directly and related to the mixed-wet conditions.

presented at the 1998 International Symposium on Wettability and its Effect on Oil Recovery in Trondheim, 22-24 June.

Mixed wetting in square tubes (section 2.2) was studied by visiting scholar Kristine Spildo, a Ph.D. student from the Chemistry Department at the University of Bergen. Support for Ms. Spildo was provided by Statoil (Norway) through the VISTA program. This work is the basis of a paper, "Mixed Wetting in Square Capillaries," presented at the 1998 International Symposium on Wettability and its Effect on Oil Recovery in Trondheim, 22-24 June.

EXECUTIVE SUMMARY

We report on the second year of the project, "Evaluation of Reservoir Wettability and its Effect on Oil Recovery." The objectives of this five-year project are (1) to achieve improved understanding of the surface and interfacial properties of crude oils and their interactions with mineral surfaces, (2) to apply the results of surface studies to improve predictions of oil production from laboratory measurements, and (3) to use the results of this research to recommend ways to improve oil recovery by waterflooding. During the second year of this project we have tested the generality of the proposed mechanisms by which crude oil components can alter wetting. Using these mechanisms, we have begun a program of characterizing crude oils with respect to their wettability altering potential. Wettability assessment has been improved by replacing glass with mica as a standard surface material and crude oils have been used to alter wetting in simple square glass capillary tubes in which the subsequent imbibition of water can be followed visually.

In Part 1 of this project we consider the various mechanisms by which crude oils alter wetting and test the simplest possible oil characterization schemes consistent with our goal of predicting the circumstances under which a given oil will alter wetting. We can separate the interaction mechanisms of importance in reservoir rocks into those attributable to the ionic interactions of petroleum acids and bases and the colloidal interactions that occur as the asphaltenes become more aggregated and less well dispersed in the oil.

Petroleum Acids and Bases: By choosing medium gravity oils, we can isolate those which have neither a large concentration of asphaltenes, nor such poor solvency that any asphaltenes are near the onset of precipitation. These medium gravity oils can vary widely in their acidic and basic characteristics. We find that both numbers must be considered to evaluate an oil. An oil with high base number, low acid number, and very little asphaltene was found to alter the wetting of mica surfaces to a greater extent (especially when the brine was very low in ionic strength) than one with much more asphaltene, but less basic character.

The Onset of Asphaltene Precipitation: We have shown that the onset of asphaltene precipitation of a given pair of oil and precipitant occurs at a nearly constant value of refractive

index. In this report we show in detail the theoretical background for use of the refractive index to quantify the solvent quality of an oil for its asphaltenes. We apply this analysis to a wide range of crude oils and show how standard PVT analyses can be used to calculate refractive index during depressurization of an oil.

Wetting Assessment: Part 2 of this project is devoted to improving our ability to assess wetting of surfaces and porous media exposed to crude oils. The first major improvement consists of replacing glass as a standard surface with mica. Some of the advantages of mica include its molecularly flat cleavage surface and the analogy in surface structure between mica and clay minerals. We show that the interaction mechanisms found originally to pertain to glass surfaces are also important for mica. We also find some important differences between glass and mica treated at elevated temperature with crude oils that may help to explain some of the discrepancies between surface and porous media tests that have been noted in the past.

Finally, we have used crude oil to alter the wetting of a very simple porous medium, i.e. square glass capillary tubes. Mixed-wet conditions can be produced if there is an initial water saturation in the corners of the tube during exposure to oil. Direct visual observation of spontaneous imbibition into tubes with varying wettability is reported.

ACKNOWLEDGMENTS

This work is supported by the US Department of Energy under Cooperative Agreement DEFC22-96ID13421, by the State of New Mexico, and by industrial support from Mobil, Norsk Hydro, and Unocal.

Crude oil samples were supplied by Arco, Elf Aquitaine, Shell, and Statoil.

Project contributors include:

Jill Buckley	Senior Scientist, Head Petrophysics and Surface Chemistry Group
Virginia Chang	Research Associate
Mary Downes	Research Assistant
Yu Liu	Research Associate
Rashid Al-Maamari	PhD student in Petroleum Engineering
Sue Von Drasek	MS student, Geochemistry
Ling Liu	MS student in Chemistry
Kristine Spildo	Visiting Scholar, PhD student in Chemistry at U. Bergen, Norway
Jianxin Wang	PhD student in Petroleum Engineering
Kay Brower	Prof. Emeritus, Chemistry, NMIMT
Norman Morrow	Prof. Petroleum & Chem. Eng., U. Wyoming

The asphaltene study (section 1.2) was a cooperative effort with George Hirasaki and Baldev Gill of the Chemical Engineering Department at Rice University. It was the basis of a paper at the 1997 spring AIChE meeting in Houston. The paper, "Asphaltene Precipitation and Solvent Properties of Crude Oils," by J.S. Buckley, G.J. Hirasaki, Y. Liu, S. Von Drasek, J.X. Wang, and B.S. Gill, has been published in *Petroleum Science and Technology* (1998) **16**, No. 3&4, 251-285.

The report on adhesion and adsorption of crude oils on mica (section 2.1) was based on the thesis work of Ling Liu, who completed an M.S. in Chemistry at NMIMT in May, 1997. It is the basis of a paper, "Alteration of Wetting of Mica Surfaces," by L. Liu and J.S. Buckley

INTRODUCTION

Objectives

The objectives of this five-year project are threefold:

1. achieve improved understanding of the surface and interfacial properties of crude oils and their interactions with mineral surfaces,

2. apply the results of surface studies in the laboratory to improve predictions of oil production, and

3. use the results of this research to recommend ways to improve oil recovery by waterflooding.

Both existing methods of wettability assessment and new methods developed in the course of this research will applied to advance our understanding of oil reservoir wettability and how wetting affects oil recovery.

Contents of this Report

This report details the results of the second year of this five-year project, beginning with a brief review of some definitions of mixed wetting, mechanisms of interaction between crude oil, brine, rock (so-called COBR interactions), and standard methods of wettability assessment.

During year two of this project, advances in Part 1—oil characterization—have included characterization of specific crude oils and extension of the theory regarding asphaltenes and their onset of precipitation.

In Part 2 of this project—wettability measurement—the effects of COBR interactions on wetting alteration of specific materials are the focus. This report include the conclusions of our study of COBR interactions with mica surfaces, showing both similarities and some interesting differences from previous studies with glass. Also reported is a preliminary study on creating mixed-wet conditions in square glass capillary tubes.

Part 3 of this project is concerned with applying the lessons learned from our studies of COBR interactions and wetting alteration to improvements in waterflood oil recovery. Part 3 will extend throughout the remainder of the project.

Definitions

Mixed wetting

In mixed-wet porous media, not all pore surfaces have the same wetting. Differences might arise because of the distribution of various pore lining minerals (Dalmatian or fractional wetting as suggested by Brown and Fatt, 1956) or because of limitations imposed by the initial fluid distribution (as suggested first by Salathiel, 1973). Both of these situations are included in the definition of mixed wetting. A porous medium that is mixed-wet may imbibe both water and oil, either water or oil, or it may imbibe neither phase.

It is important to note that multiphase flow through mixed-wet porous media is influenced both by the degree and distribution of wetting. The effect of wetting in mixed-wet media cannot be inferred by interpolations between strongly water-wet and strongly oil-wet studies. Thus, a more fundamental picture of the distribution and degree of wetting is essential to development of the ability to predict oil recovery from surface studies.

Water film stability

Whether or not components from the oil phase can adsorb on solid surfaces and alter their wetting properties depends, first, on whether stable water films exist between oil and solid. The stability of thin water films between oil and solid depends on DLVO and other forces arising from properties of the solid/brine and oil/brine interfaces (Buckley *et al.*, 1989). In previous studies of COBR interactions we have shown that regions of stability and instability can be delineated by observing adhesion (or non-adhesion) of a drop of crude oil to a smooth solid surface under brine (Buckley *et al.*, 1997). **Figure 1** shows these regions of stability and instability for A-93 crude oil from Prudhoe Bay and clean borosilicate glass surfaces. Standard adhesion tests (by procedures explained later in this review) were used to define those regions where brine pH and NaCl concentration produced stable and unstable water films. Comparison of adhesion tests at room

temperature with tests at elevated temperature (80°C) showed that there is a region of brine composition where stability depends on temperature. In most cases, adhesion was observed at low temperature, whereas the high temperature tests showed non-adhesion.

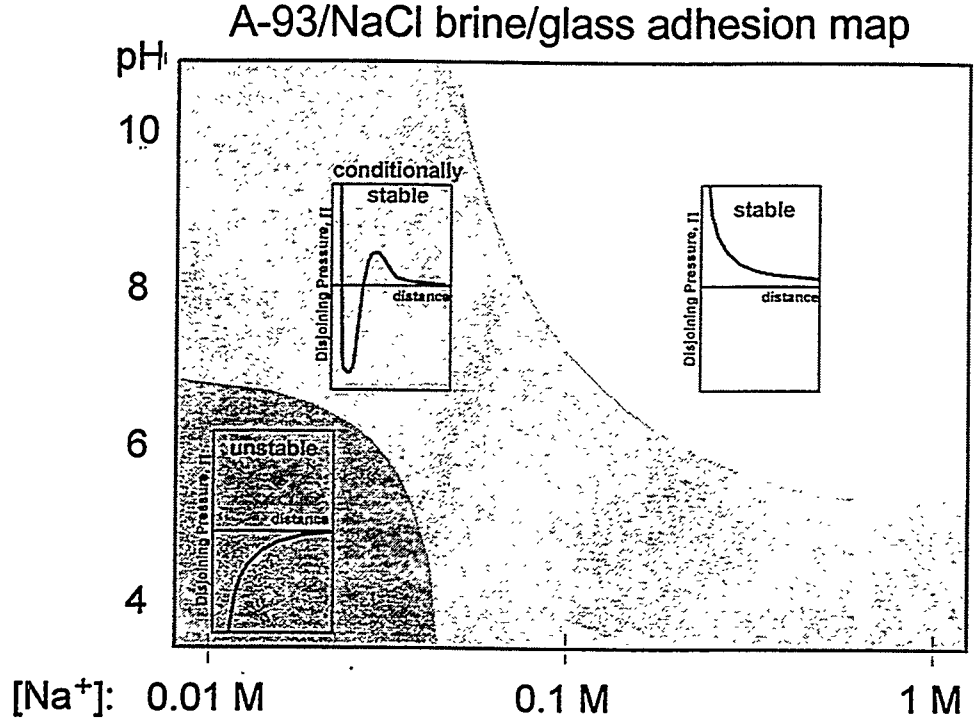

Figure 1. Regions of stability and instability of water films for drops of A-93 crude oil contacted with clean glass surfaces under brines of varying pH and NaCl concentration. Stable films result in non-adhesion whereas unstable films result in adhesion of the crude oil drop to the surface. In the region denoted as conditionally stable, low temperature adhesion and high temperature non-adhesion were observed. The disjoining pressure curves are illustrations only. Disjoining pressure was not measured in these experiments (after Buckley *et al.*, 1997).

Crude oil components that can adsorb and alter wetting

Acids and bases

The strong pH dependence exhibited by crude oils in their adhesion to solid surfaces (e.g., Fig. 1) is evidence for the contribution of acidic and basic species in the oil to adhesion phenomena. Other strongly pH-dependent phenomena include electrophoretic mobility and

interfacial tension. Acid and base numbers provide a rough guide to the contribution to wetting alteration of these polar components in the oil (ASTM-664-89; ASTM-2896-88; Buckley *et al.*, 1998).

Asphaltenes and resins

Crude oils are complex mixtures of hundreds of components ranging in size from one carbon atom to one hundred or even more. Beyond the first few members of each homologous series, individual species cannot be readily separated and identified by standard techniques. Instead, crude oils are often characterized by dividing components into a few groups based on physical and chemical separations.

Some of the heaviest, most polar components, implicated in wetting alteration, are insoluble in low molecular weight paraffins (e.g. ASTM D2007-80). They can be removed by precipitation with an excess of *n*-pentane or *n*-heptane. The remainder of the oil can be separated chromatographically on the basis of polarity, with saturates as the least polar fraction followed by the aromatic hydrocarbons. The final fraction, called resins or polars, consists of hydrocarbons with small percentages of polar heteroatoms (mainly oxygen, nitrogen, and sulfur).

Asphaltenes exist in crude oil as aggregates, whose size can change continuously with changes in temperature, pressure, or oil composition, as demonstrated by measurements with small-angle x-ray (SAXS) and neutron (SANS) scattering (Espinat and Ravey, 1993; Thiyagarajan, 1995). It is necessary to understand the nature of asphaltene dispersion in oil because their effect on wetting may vary as their state of aggregation changes.

Wetting on smooth surfaces

Contact angles

The most fundamental measure of wetting is a contact angle between two fluids which partially wet a solid surface, as shown in **Fig. 2.** By convention, we report the angle through the water phase. In practice, equilibrium contact angles are never measured with crude oil because there can be hysteresis between water-advancing and water-receding conditions caused by roughness in the surface and by chemisorption and physisorption between oil components and the

solid surface. Contact angles are measured in our laboratory by the captive drop technique (Gaudin, 1964).

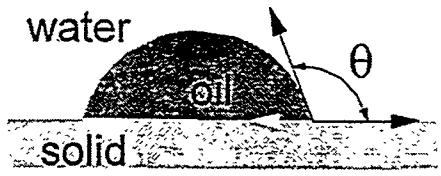

Figure 2. Contact angle is the angle between the tangent to the droplet at the three-phase line and the solid surface, measured here through the water phase.

Adhesion

Observations of large hysteresis between receding and advancing conditions led to development of an adhesion test first described by Morrow, *et al.* (1986) and given a rational basis in DLVO theory by Buckley, *et al.* (1989). The test itself is deceptively simple. A drop of oil is formed under water at the tip of either a microburet or syringe held as rigidly as possible to avoid vibration during changes in drop volume. The volume of the oil droplet can vary, but it is usually quite small (a few μl or less). Variations in contact angle with drop volume are of secondary importance in these measurements. The oil droplet is allowed to contact a smooth solid surface, also submerged in the aqueous phase. After some period of contact between oil and solid (usually two minutes), the drop is drawn back into the needle or buret tip. At that stage, very different phenomena have been observed, as illustrated in **Fig. 3**, for the two extremes of possible outcomes.

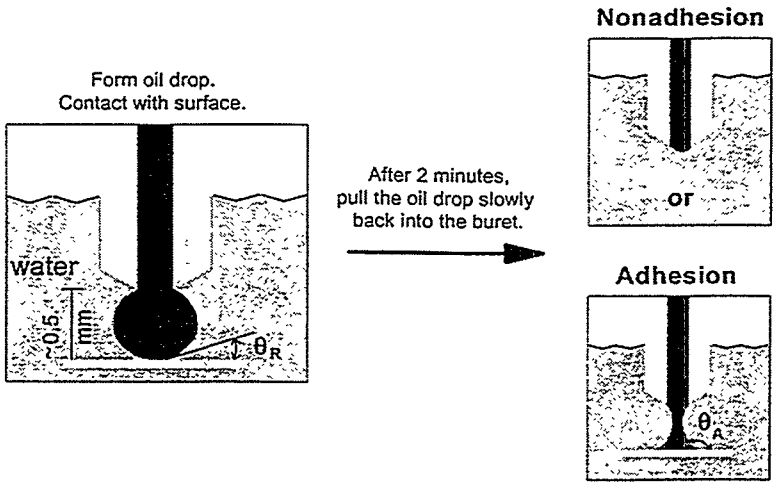

Figure 3. Illustration of adhesion and non-adhesion between an oil droplet and a solid surface under water or brine.

When the oil drop does not adhere, there is very little difference between advancing and receding contact angles (θ_A and θ_R, respectively). At the other extreme, the three-phase contact line is pinned, and, as the volume of the oil drop is reduced, the shape of the drop is distorted, as shown in the case labeled adhesion. Further reduction in the drop volume results in separation of the adhering drop from the oil in the buret. Drops of oil up to about 0.5 µl in volume may remain on the surface. Using this simple distinction between adhering and non-adhering conditions, a map of brine compositions can be made with distinctions drawn between areas of adhesion and non-adhesion. A typical example is shown in **Fig. 4**. Intermediate conditions are often observed in which very small droplets adhere, or θ_A is high and a larger oil droplet adheres. With time, however, the contact angle begins to decrease and eventually the drop is released and floats to the surface.

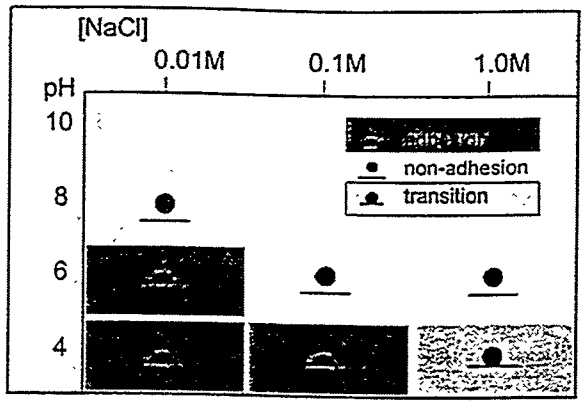

Figure 4. A typical adhesion map delineates conditions of NaCl concentration and pH under which adhesion occurs. In this example, the crude oil is A-93. The test was performed at 80°C.

Of course, this arbitrary division according to the extremes of adhesion and non-adhesion is an oversimplification. A great deal of additional detail can be observed in these tests. The three-phase line is not always pinned, but may slip at a well-defined advancing contact angle. The volume and final contact angle of adhering drops can vary. In principle, the adhering drop might spread. This situation has been observed only once (i.e., for one crude oil in contact with a single brine composition) in many hundreds of these measurements with dozens of different crude oils. Variations in the standard procedure (for example, allowing longer contact times) can provide additional information, but the standard procedure provides a fixed starting point in this universe of variables.

Adsorption

In order to observe much longer periods of interaction between smooth solid surfaces, brines, and crude oils, a second standard test has been developed (Buckley and Morrow, 1991; Liu and Buckley, 1997). An outline of the standard procedure adopted for this adsorption test is shown in **Fig. 5.**

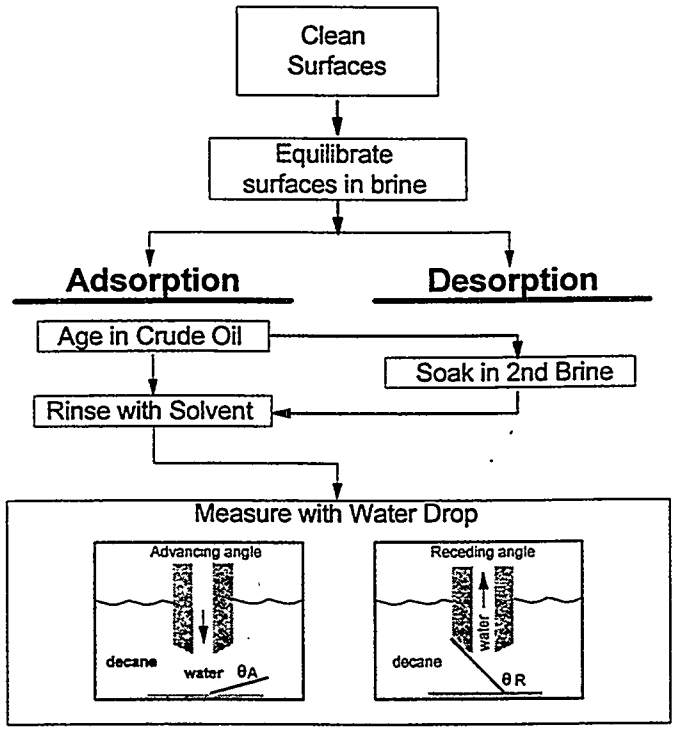

Figure 5. Standard procedures for adsorption and desorption tests.

After cleaning and equilibrating in brine, the solid pieces are removed and allowed to drain, but not to dry, before being immersed in crude oil. Variables include brine and oil compositions, aging time, and temperature. At the end of the oil-aging period, samples are removed and washed gently with solvent to remove bulk oil. Toluene has been used as the standard solvent; cyclohexane gives nearly the same results. Fluids that are poor asphaltene solvents—decane, for example—are avoided since they make the surfaces uniformly oil-wet. After washing, the treated surface is immersed in just such a poor asphaltene solvent so that further changes do not occur as water advancing and receding contact angles are measured (Fig. 5).

An additional step, immersing the treated surface in another brine solution and aging it again, shows the extent to which the adsorbed components can be removed. Desorption varies with time, temperature, and brine composition.

Mechanisms of interaction

The main categories of crude oil/brine/solid interactions identified thus far, using both adhesion and adsorption measurements on glass surfaces, include:

- **polar** interactions that predominate in the absence of a water film between oil and solid,
- **surface precipitation**, dependent mainly on crude oil solvent properties with respect to the asphaltenes,
- **acid/base** interactions that control surface charge at oil/water and solid/water interfaces, and
- **ion-binding** or specific interactions between charged sites and higher valency ions.

Polar interactions

Clean, dry surfaces have been aged in a variety of crude oils and their asphaltene fractions. Under these conditions, interactions that alter surface wetting can occur between polar functional groups in the oil and polar surface sites. The advancing angles (θ_A) measured with decane and water are intermediate and the extent of interaction changes little with either aging time or aging temperature.

Surface precipitation

Crude oils vary in their ability to solvate their asphaltenes. Some indicators of poor solvent quality are low refractive index (discussed in detail in section 1.2) or high API gravity (low density). If the oil is a poor solvent for the asphaltenes, the tendency for wetting alteration is enhanced (Buckley *et al.*, 1997). The effect of precipitation is readily illustrated if, after aging in crude oil, surfaces are washed with decane instead of toluene. Because decane induces asphaltene precipitation, the surface immediately becomes oil-wet. Receding angles (θ_R) are high and hysteresis between θ_A and θ_R is small.

Acid/base interactions

Water plays an important role in mediating oil/solid interactions. In the presence of water, both the solid and oil interfaces become charged. Polar functional groups belonging to both the mineral and crude oil phases can behave as acids (giving up a proton and becoming negatively charged) and bases (gaining a proton and a positive charge) (Cuiec, 1975). There are two major ways in which the phenomenon of surface charge impacts COBS interactions:

(1) *Net charge affects water film stability.* The influence of DLVO forces in stabilizing a thin film of water between mineral and oil is most significant when the brine phase salinity is low and composed of monovalent ions. Under these conditions, the main variable influencing surface charge and thus water film stability is pH, since the acid/base equilibria and thus the extent of surface charge are all governed by pH.

(2) *Ionized acidic and/or basic sites influence adsorption.* Collapse of the water film is only the first step in wetting alteration. At this stage, crude oil components at the oil/brine interface can adsorb on the solid surface. Silica surfaces are negatively charged above pH 2; positively charged nitrogen bases can adsorb (Anderson, 1986). Calcite surfaces are positively charged below a pH of about 9.5; acidic species adsorb (Morrow *et al.*, 1973; Thomas *et al.*, 1993).

Ion-binding interactions

When present, Ca^{2+} ions mask the purely acid/base interactions. Several interactions are possible:

oil—Ca—oil mineral—Ca—mineral oil—Ca—mineral

The first two can limit wettability alteration while the last promotes it. pH is no longer the major determining factor in adhesion experiments (Buckley and Morrow, 1991), nor is adhesion a good indicator of interactions that occur with longer exposure times. Longer exposure adsorption tests show that strong interactions can occur, but the interactions are very dependent on temperature (Liu and Buckley, 1997). High hysteresis, similar to that observed for acid/base interactions, has been observed. Interactions via ion binding appear to be somewhat more resistant to desorption than acid/base interactions.

Wetting in porous media

Standard core preparation procedures

Cylindrical cores are cut with a diamond core bit using tap water for cooling. The cores are allowed to dry for several days in an oven at 80°C, after which nitrogen permeabilities are measured. Selected core plugs are saturated under vacuum in degassed brine and allowed to equilibrate in the brine phase for one week at ambient temperature. At the end of this equilibration time, absolute permeability to brine is measured. Synthetic and outcrop cores thus prepared are strongly water-wet and are ready for use in various kinds of experiments.

For alteration of core wettability, the brine-saturated cores are flooded with crude oil to establish an initial water saturation. An initial measurement of oil permeability is made. The value of initial water saturation, aging time, and aging temperature are the main variables associated with the extent of wetting alteration at this stage. Cores with oil and connate water are submerged in crude oil in a sealed beaker and stored either in an oven or in a water bath at the designated aging temperature. At the end of the aging period, the oil aged in the core is displaced with fresh oil (either the same crude oil of a refined oil) and permeability to oil is remeasured with connate water in place.

Spontaneous imbibition

The use of imbibition measurements to characterize wettability in cores has been common since a test was proposed by Amott (1959) that compared the amount of a phase imbibed spontaneously with the amount of that phase taken up by the same core in a forced displacement. While this is strictly an empirical measure that can be affected by many experimental details, it does provide a framework for comparisons from one sample to another and even from one rock type to another. The procedure used here is similar to that suggested by Cuiec (1991). It combines spontaneous imbibition with viscous forced displacement in a core flood, as opposed to the gravity-driven centrifuge displacement recommended by Amott. An idealized capillary pressure curve is shown in **Fig. 6** with the saturations used to calculate wetting parameters indicated. Since only endpoint saturations are used, measurement of P_c is not required.

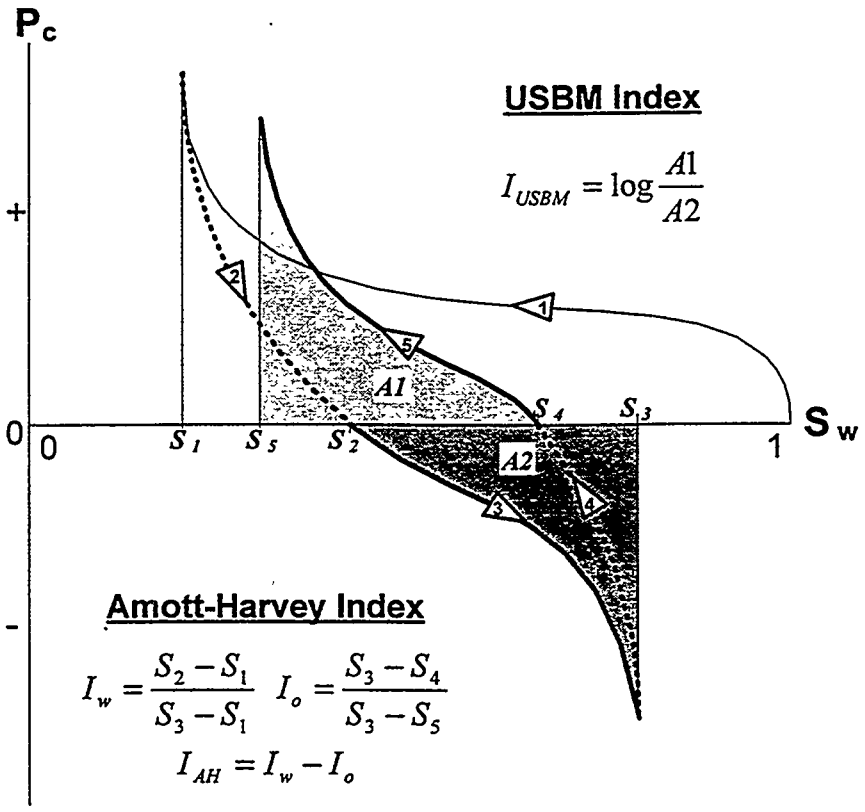

Figure 6. Idealized capillary pressure vs. saturation curve, indicating the values used for calculation of Amott wettability indices (I_w and I_o) and the combined Amott-Harvey Index $I_{w\text{-}o}$.

All steps shown by solid lines in Fig. 6 are viscous displacements with the core confined in a Hassler holder. In the spontaneous imbibition steps (dotted lines), all core surfaces are exposed to the imbibing fluid. Imbibition is monitored either gravimetrically or volumetrically.

PART 1. CHEMICAL EVALUATION OF CRUDE OILS

1.1 COBR Interactions of Some Medium Gravity Crude Oils

1.1.1 Introduction

When both water and oil are present in a rock, ionic interactions between charged pore surface sites and organic acidic and basic functional groups can account for crude oil/brine/rock interactions that alter wetting. These ionic interactions compete with surface precipitation, a colloidal mechanism that depends on oil solvent quality. A set of parameters including *gravity*, *acid* number, and *base* number (G-AB) has suggested for characterizing crude oils with respect to their propensity to alter wetting of a given substrate (Buckley *et al.*, 1998). API gravity represents the influence of solvent quality of the oil (which is related to gravity or density of the oil). Acidity and basicity contribute to ionic interactions between oil components and charged sites on the mineral surface.

Surface precipitation was shown to dominate for oils that are unusually poor solvents for their asphaltenes (for example, Lagrave crude oil). Ionic interactions have been demonstrated using oils with high values of either acid number (Moutray crude oil) or base number (Prudhoe Bay crude oil). The G-AB profiles of these three oil samples are shown in **Fig. 1.1-1**. API gravity is plotted on the vertical axis. Acid and base numbers are indicated by the horizontal bars, with the acid number in the negative direction and the base number in the positive direction. Note that the acid numbers, which have the same units as base numbers, but are often of smaller magnitude, have been multiplied by a weighting factor of four.

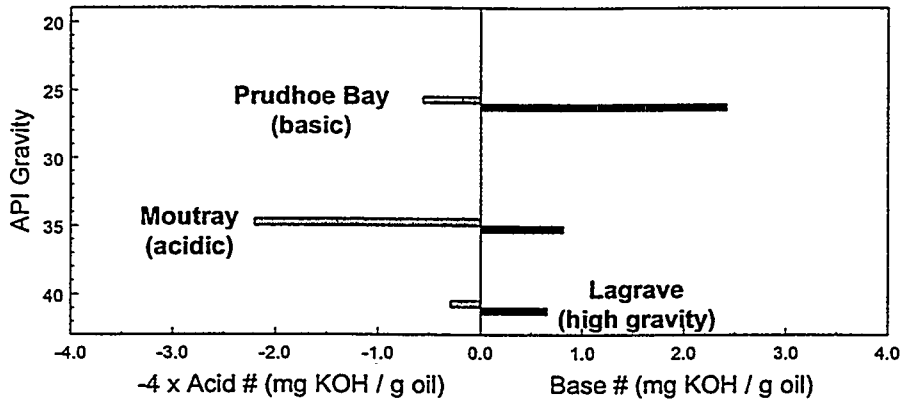

Figure 1.1-1. G-AB profiles of selected crude oils. Prudhoe Bay oil exemplifies a basic oil, Moutray is acidic, and Lagrave is a high gravity oil with asphaltenes that are approaching the onset of instability.

Most oils do not fall into one of these simple categories. If both acid and base numbers are low, ionic interactions may not be significant. Similarly, if both acid and base numbers are high, ionic interactions may be less important than if only one or the other dominates. As yet, it is not possible to put limits on the G-AB parameters to predict the extent of various types of interactions. More information is needed between the extremes represented by the oils in Fig. 1.1-1. In this report, evaluations of the ionic COBR interactions of four medium gravity oils, ranging in gravity from 27° to 31° API, are reported. In this study, rock surfaces are represented by muscovite mica. The validity of using mica to study COBR interactions with crude oils is examined in section 2.1 of this report.

1.1.2 Experimental materials and method

1.1.2.1 Muscovite mica surfaces

Muscovite mica was used as the solid substrate in this study. Properties and layer charge characteristics of the samples (from Ward's Natural Science Establishment, Inc. and S & J Trading, Inc.) are shown in **Tables 1.1-1** and **1.1-2** (Liu, 1997).

Table 1.1-1. Properties of muscovite mica samples.

Composition	Crystallograph	Physical Description	Deposit
$KAl_2(Si,Al)O_{10}(OH,F)$	Monoclinic, 2/m	{001} perfect cleavage colorless, transparent	Stoneham Maine

Table 1.1-2. Layer charge characteristics of muscovite mica samples.

Lattice Dimension (A)	ξ (eq / mol)	C_i (meq / g)	σ_o (C / m^2)	A_e (A^2 / charge)
a = 5.19, b = 9.00	1	2.2	0.343	23.4

For surfaces aged at high temperatures, mica has advantages over quartz or borosilicate glass because there is less change in the surface with time (Liu, 1997). Mica has the additional advantages of being both molecularly smooth and similar in surface structure to illite.

1.1.2.2 Organic solvents and water

Decane (99+%) and toluene (99.8%, HPLC grade) were purchased from Aldrich. Decane and toluene were further purified by passing through dual-packed columns of activated silica gel and alumina. Water was purified first by deionizing freshly distilled water and then by redistilling it in an all-glass apparatus.

Brines: The chemicals used for buffer preparation were sodium acetate ($NaC_2H_3O_2 \cdot 3H_2O$) and glacial acetic acid ($HC_2H_3O_2$) for pH 4, sodium hydrogenphosphate ($Na_2HPO_4 \cdot 7H_2O$) and sodium dihydrogenphosphate ($NaH_2PO_4 \cdot H_2O$) for pH 6 and pH 8 solutions. Sodium chloride (NaCl) was used for salinity adjustment; 100 ppm sodium azide (NaN_3) was added to buffered solutions used in tests with CS oil to prevent bacterial growth.

The inorganic salts used for aqueous mixed-brine preparation were sodium bicarbonate ($NaHCO_3$), sodium sulfate (Na_2SO_4), sodium chloride, potassium chloride (KCl), calcium chloride ($CaCl_2 \cdot 2H_2O$), and magnesium chloride ($MgCl_2 \cdot 6H_2O$). **Table 1.1-3** summarizes the molar concentrations (*M*) of the salts in each of the CS and Spraberry reservoir brines (RB), and synthetic sea water (SW).

Table 1.1-3. Brine compositions.

	CS-RB (M)	Spraberry-RB (M)	Spraberry-RRB (M)	Synthetic SW (M)
$NaHCO_3$	0.01818			0.00046
Na_2SO_4	0.00019			0.02757
NaCl	0.22638	2.09951	0.02413	0.41073
KCl	0.00144			
$CaCl_2 \cdot 2H_2O$	0.00146	0.05110	0.05868	0.00998
$MgCl_2 \cdot 6H_2O$	0.00099			0.05236
$[Ca^{2+}] / [Na^+]$	0.006	0.024	2.432	0.021
Ionic Strength	0.25391	2.25279	0.20017	0.68093

In addition to the basic recipes in Table 1.1-3, ten-fold and hundred-fold dilutions were tested to show the effect of varying ionic strength. In some cases Ca^{2+} concentration was increased to give additional comparisons with different ratios of divalent to monovalent cation concentrations (**Table 1.1-4**).

Table 1.1-4. Calcium-enriched CS-RB and synthetic SW.

	0.10* CS-RB (M)	0.10* SW (M)
$NaHCO_3$	0.001818	0.000046
Na_2SO_4	0.000019	0.002757
NaCl	0.022638	0.041073
KCl	0.000144	
$CaCl_2 \cdot 2H_2O$	0.013216	0.009998
$MgCl_2 \cdot 6H_2O$	0.000099	0.005236
$[Ca^{2+}] / [Na^+]$	0.540	0.214
Ionic Strength	0.06461	0.09504

1.1.2.3 Crude oils

Four crude oil samples were tested: CS, Gullfaks-96, Mars-97, and Spraberry. **Table 1.1-5** summarizes some physical and chemical properties of each of these oil samples. G-AB parameters are listed in **Table 1.1-6**. There is only a 4° difference in API gravity between the

heaviest and lightest of these four oils. Mars-97 is the only one of these crude oil samples with visible asphaltene in precipitation tests with *n*-heptane. None of these oils has a high acid number; Spraberry has a fairly high base number. The G-AB profiles are shown in **Fig. 1.1-2.**

Table 1.1-5. Physical and chemical properties of crude oils.

	CS	Gullfaks-96	Mars-97	Spraberry
Density @ 25°C (g / mL)	0.8861	0.8856	0.8811	0.8635
RI @ 20°C	1.5029	1.4930	1.4950	1.47824
P_{RI} with n-C_7	n/a	n/a	1.4316	n/a
Asphaltene ppt with n-C_5 (wt%)	1.38	1.13	3.25	0.39
Asphaltene ppt with n-C_7 (wt%)	0.48	0.56	1.86	0.16
H / C	1.742	1.749		
O / C	0.004	0.004		
N / C	0.0039	0.0025		
S / C	0.0018	0.0019		

Table 1.1-6. Crude oil G-AB parameters.

	CS	Gullfaks-96	Mars-97	Spraberry
API gravity @ 60°F	27.0°	28.3°	30.3°	31.1°
Acid Number (mg KOH / g oil)	0.330	0.244	0.368	0.085
Base Number (mg KOH / g oil)	1.16	1.19	1.79	2.65
Base Number/Acid Number	3.5	4.9	4.9	31.2

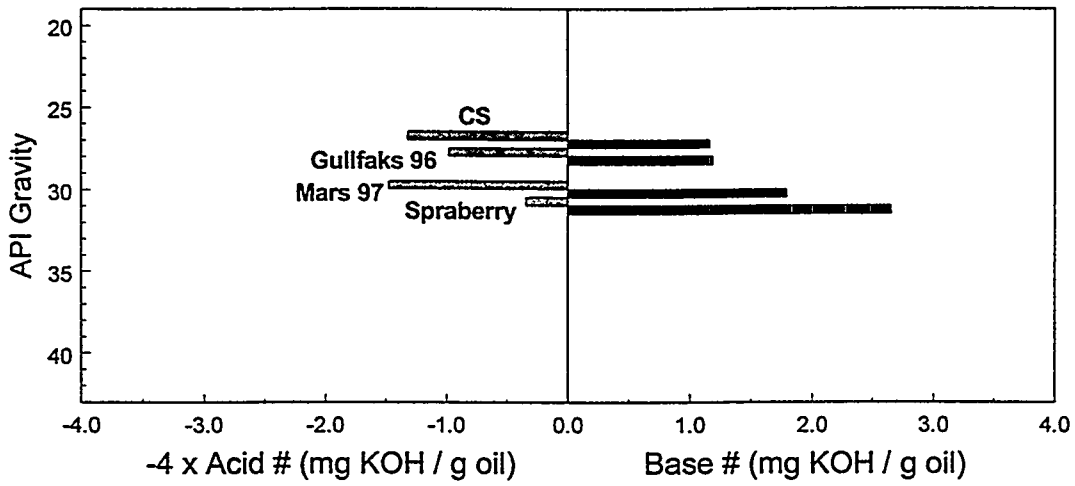

Figure 1.1-2. G-AB profiles of the four medium gravity crude oil samples.

None of these oils is in the poor solvent category, exemplified by the high gravity Lagrave. We expect, therefore, that if they alter wetting, they must do so by ionic interactions, not by surface precipitation of asphaltenes.

Only one of this set of four medium gravity crude oils would be expected to have a significant impact on wetting by ionic interactions. Spraberry has a high base number (2.65 mg KOH/g oil) and a low acid number (0.085 mg KOH/g oil). The remaining three oils have acid and base numbers that fall in the median ranges, with neither base numbers nor acid numbers dominating. We thus expect that CS, Gullfaks-96, and Mars-97 will have minimal effects on the wetting of a silicate surface by any of the mechanisms identified to date. Note that Spraberry is expected to have more influence on wetting even than Mars-97, which has 3.25% *n*-pentane asphaltenes.

1.1.2.4 Contact angle measurements

Freshly cleaved muscovite mica sheets were cut into 10x20mm samples, cleaned, and equilibrated with a selected brine for up to 24 hours. Those aged in buffered NaCl brines were used for adhesion tests.

Mica pieces equilibrated with mixed brines were then transferred wet to a crude oil and aged from one to 21 days, at aging temperatures of 25°C and 55° or 60°C. After aging, these mica samples were removed from the oil, rinsed with toluene, and immersed in decane. Contact angles were measured by the captive drop technique using a contact angle goniometer (Gaertner Scientific Corp.) to observe the water/oil contact line for water advancing and receding on mica. Adhesion and adsorption test protocols are illustrated in **Fig. 1.1-3.**

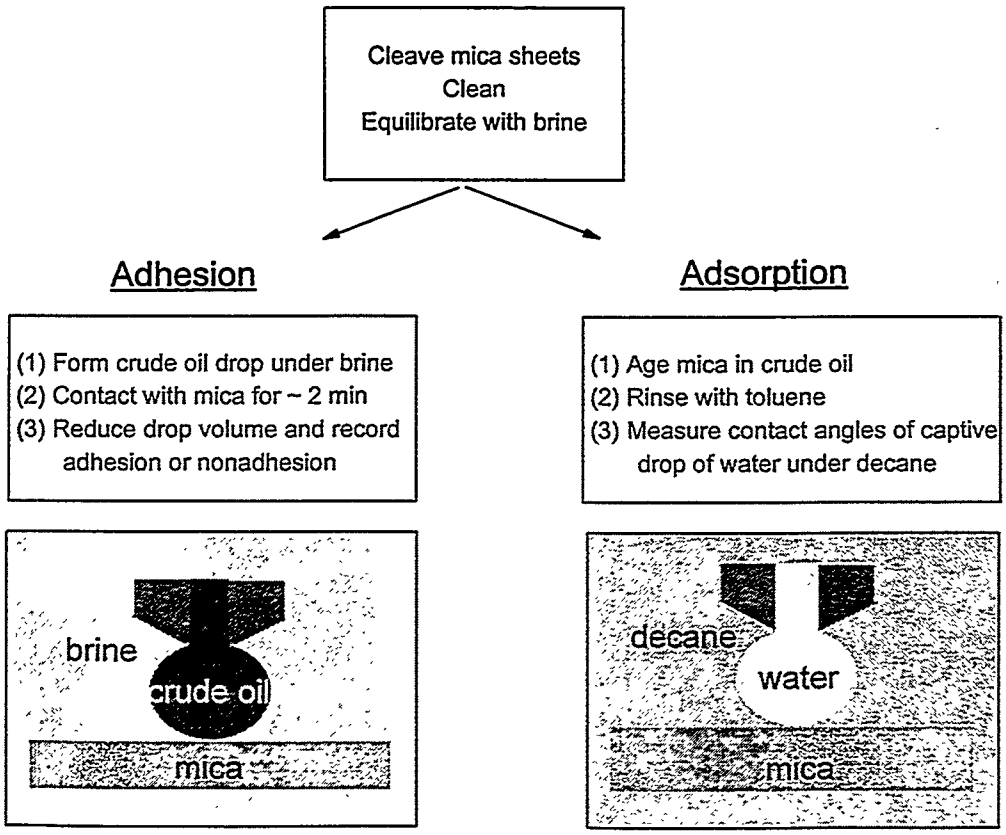

Figure 1.1-3. Illustration of adhesion, observed with a drop of crude oil briefly contacting clean mica under brine, and adsorption tests, in which contact angles are measured using decane and water as probe fluids on brine and oil treated surfaces.

1.1.3 Results and discussion

1.1.3.1 Adhesion—buffered NaCl brines

Acid/base interactions that depend on brine pH and ionic strength are evaluated by the adhesion test. Results are shown in **Figs. 1.1-4** to **1.1-7**. These interactions occur rapidly—the typical adhesion test involves only two minutes of contact between oil and brine-covered solid. In some cases, differences between low and high temperature can reflect a widening of the range of metastable conditions at lower temperature that may be related to the transition to colloidal interactions (Buckley *et al.*, 1997).

For the four oils in this report, adhesion mainly occurs when both brine pH and ionic strength are low. Differences between low and high temperature tests are minimal.

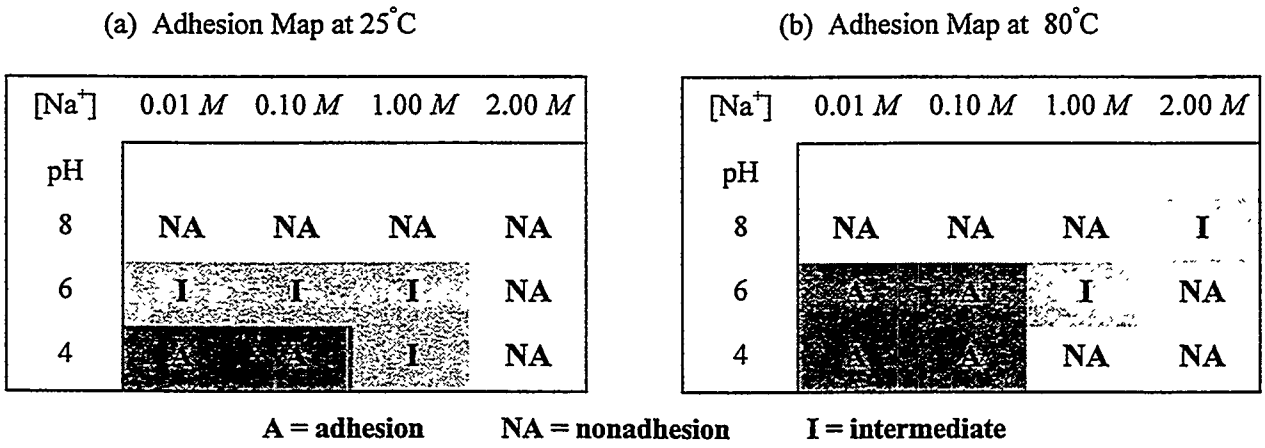

Figure 1.1-4. Adhesion of CS crude oil on mica surfaces as a function of pH and ionic strength.

(a) Adhesion Map at 25°C

[Na^+]	0.01 *M*	0.10 *M*	1.00 *M*	2.00 *M*
pH				
8	NA	NA	I	NA
6	NA	NA	NA	NA
4	A	A	NA	NA

(b) Adhesion Map at 60°C

[Na^+]	0.01 *M*	0.10 *M*	1.00 *M*	2.00 *M*
pH				
8	NA	NA	NA	NA
6	NA	NA	NA	NA
4	A	I	NA	NA

A = adhesion NA = nonadhesion I = intermediate

Figure 1.1-5. Adhesion of Gullfaks-96 oil on mica surfaces as a function of pH and ionic strength.

(a) Adhesion Map at 25°C

[Na^+]	0.01 *M*	0.10 *M*	1.00 *M*	2.00 *M*
pH				
8	NA	NA	NA	A
6	I	NA	NA	I
4	A	A	NA	NA

(b) Adhesion Map at 60°C

[Na^+]	0.01 *M*	0.10 *M*	1.00 *M*	2.00 *M*
pH				
8	NA	NA	NA	NA
6	A	NA	NA	NA
4	A	A	NA	A

A = adhesion NA = nonadhesion I = intermediate

Figure 1.1-6. Adhesion of Mars-97 crude oil on mica surfaces as a function of pH and ionic strength.

(a) Adhesion Map at 25°C

[Na^+]	0.01 *M*	0.10 *M*	1.00 *M*	2.00 *M*
pH				
8	NA	NA	NA	NA
6	A	I	NA	NA
4	A	A	NA	NA

(b) Adhesion Map at 60°C

[Na^+]	0.01 *M*	0.10 *M*	1.00 *M*	2.00 *M*
pH				
8	NA	NA	NA	NA
6	A	I	NA	NA
4	A	A	NA	NA

A = adhesion NA = nonadhesion I = intermediate

Figure 1.1-7. Adhesion of Spraberry crude oil on mica surfaces as a function of pH and ionic strength.

1.1.3.2 Adsorption—contact angles on surfaces treated with mixed brines and oil

Of more practical importance are the interactions that occur in the presence of brines containing divalent and multivalent ions. Wettability-altering interactions under these conditions are not yet predictable. Typically, they occur more slowly than simple acid/base interactions. The effects of exposure times of one day and three weeks, at room temperature and elevated temperature, have been evaluated with measurements of contact angles between probe fluids (decane and water) after exposure of the mica surfaces to brine and oil. Results for surfaces treated at 25°C are summarized in **Table 1.1-7**; **Table 1.1-8** lists the results for surfaces aged at 55 or 60°C.

Table 1.1-7. Decane/water contact angles on brine- and oil-treated mica aged at 25°C.

Crude Oil	Mixed-Brine	Dilutions	Ionic Strength	pH	Aging time Days	θ_A	θ_R	$\theta_A - \theta_R$
CS	CS RB	1.00	0.25391	8.07	1	30	20	10
					21	24	16	8
		0.10	0.02539	8.14	1	22	17	5
					21	43	24	20
		0.01	0.00254	7.41	1	37	24	14
					21	51	26	25
		0.10*	0.06461	7.70	1	39	26	13
					21	54	26	27
Gullfaks-96	Synthetic Sea Water	1.00	0.68093	7.42	1	32	17	14
					21	49	23	26
		0.10	0.06809	6.83	1	40	20	20
					21	45	23	21
		0.01	0.00681	6.31	1	36	19	17
					21	54	20	34
		0.10*	0.09504	6.83	1	47	25	21
					21	56	22	34
Mars-97	Synthetic Sea Water	1.00	0.68093	7.72	1	34	19	15
					21	20	13	7
		0.10	0.06809	7.01	1	41	21	20
					21	59	26	33
		0.01	0.00681	6.53	1	35	19	16
					21	52	23	29
		0.10*	0.09504	6.88	1	37	20	18
					21	45	22	22
Spraberry	Spraberry RB	1.00	2.25279	6.22	1	22	16	7
					21	34	20	15
		0.10	0.22528	6.31	1	27	17	10
					21	26	16	10
		0.01	0.02253	6.24	1	68	26	42
					21	73	31	42
Spraberry	Spraberry RB (reduced NaCl)	1.00	0.20017	6.37	1	29	17	12
					21	52	30	22
		0.10	0.02002	6.43	1	45	21	24
					21	75	27	48
		0.01	0.00200	6.81	1	69	26	43
					21	55	26	28

* Composition in Table 1.1-4.

Table 1.1-8. Decane/water contact angles on brine- and oil-treated mica aged at 55-60°C.[1]

Crude Oil	Mixed-Brine	Dilutions	Ionic Strength	pH	Aging time Days	θ_A	θ_R	$\theta_A - \theta_R$
CS	CS RB	1.00	0.25391	8.07	1	34	25	10
					21	51	24	27
		0.10	0.02539	8.14	1	52	29	23
					21	58	26	31
		0.01	0.00254	7.41	1	39	25	14
					21	50	26	24
		0.10*	0.06461	7.70	1	37	27	11
					21	40	26	15
Gullfaks-96	Synthetic Sea Water	1.00	0.68093	7.42	1	45	23	23
					21	63	20	43
		0.10	0.06809	6.83	1	28	17	11
					21	42	14	27
		0.01	0.00681	6.31	1	51	22	29
					21	68	21	48
		0.10*	0.09504	6.83	1	38	21	17
					21	61	22	39
Mars-97	Synthetic Sea Water	1.00	0.68093	7.72	1	22	15	7
					21	28	14	15
		0.10	0.06809	7.01	1	44	19	25
					21	21	15	6
		0.01	0.00681	6.53	1	23	14	9
					21	71	27	44
		0.10*	0.09504	6.88	1	25	18	7
					21	34	16	17
Spraberry	Spraberry RB	1.00	2.25279	6.22	1	40	19	21
					21	24	17	8
		0.10	0.22528	6.31	1	34	18	16
					21	32	19	13
		0.01	0.02253	6.24	1	78	38	41
					21	122	65	57
Spraberry	Spraberry RB (reduced NaCl)	1.00	0.20017	6.37	1	50	27	24
					21	58	27	31
		0.10	0.02002	6.43	1	75	34	41
					21	140	80	60
		0.01	0.00200	6.81	1	101	53	48
					21	154	80	74

[1] Aging temperature was 60°C for all samples except the CS oil-treated surfaces, which were aged at 55°C.
* Composition in Table 1.1-4.

1.1.3.2a CS crude oil and CS reservoir brine

Values of both acid and base numbers for CS oil are intermediate, as is their ratio (Table 1.1-6). These values can be compared to data previously published for other oils (Buckley *et al.*, 1998). There is no visible asphaltene precipitate in mixtures with *n*-heptane over a wide range of volume fractions. Thus, there is no obvious signal that would predict strong alteration of wetting with this medium gravity oil.

Mica samples aged in CS crude oil remained preferentially water-wet even after 21 days of aging at high temperature (**Fig. 1.1-8**). Little effect was apparent from changing either ionic strength or the ratio of Ca^{2+} to Na^{+}. Other studies with this oil, both on flat surfaces and in Berea sandstone cores, have also shown it to yield preferentially water-wet conditions (Xie *et al.*, 1997).

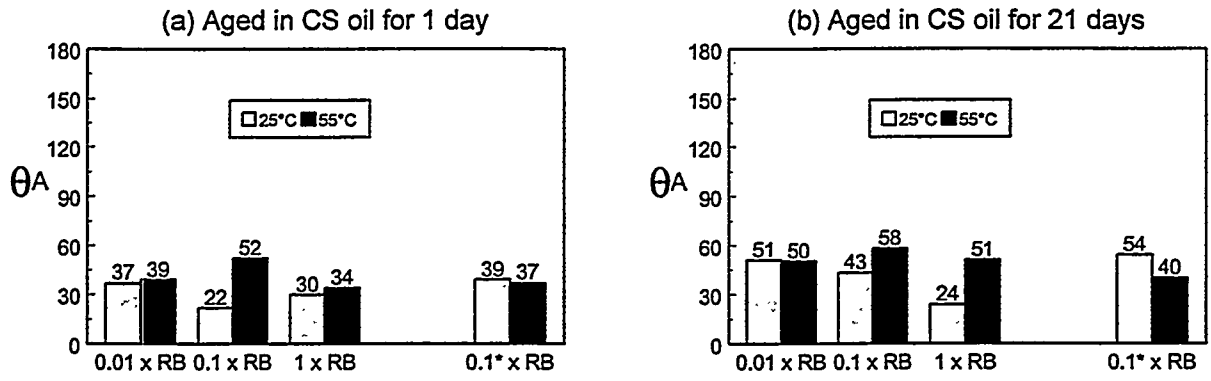

Figure 1.1-8. Water-advancing contact angles for mica surfaces aged first in CS reservoir brine (RB) and its dilutions, then in CS crude oil after (a) 1 day and (b) 21 days at 25°C and

1.1.3.2b Gullfaks-96 crude oil and synthetic sea water brine

Gullfaks-96 has values of acid and base number that are similar to CS oil. Like CS, it has no visible asphaltene precipitate in mixtures with *n*-heptane over a wide range of volume fractions.

Sea water is the brine most readily available for injection offshore. It is therefore a reasonable choice for a general mixed brine composition, for use when a reservoir-specific brine

composition is not available. **Figure 1.1-9** shows that muscovite mica samples pretreated with SW and its dilutions all remain preferentially water-wet after long exposure to Gullfaks-96.

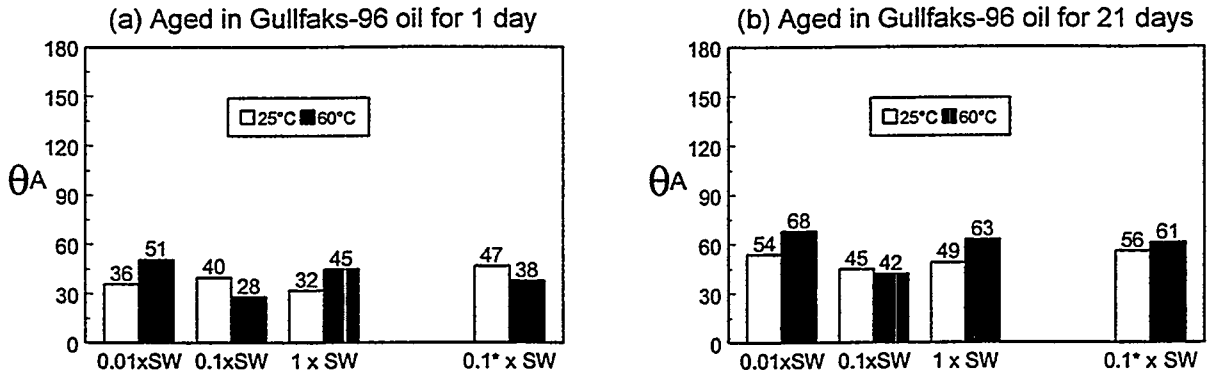

Figure 1.1-9. Water-advancing contact angles for mica surfaces aged first in synthetic sea water (SW) and its dilutions, then in Gullfaks-96 crude oil after (a) 1 day and (b) 21 days at 25°C and 60°C.

1.1.3.2c Mars-97 crude oil and synthetic sea water brine

Mars-97 crude oil has slightly higher values of both acid and base numbers than either CS or Gullfaks-96. The principal difference between Mars and the other oils in this report is that it contains more asphaltene. **Figure 1.1-10** shows refractive indices (RI) of mixtures of Mars-97 and *n*-heptane; the onset of asphaltene precipitation occurs at a P_{RI} of 1.432, well below the RI of the oil. Colloidal contributions to wetting alteration should not be a major factor under these conditions.

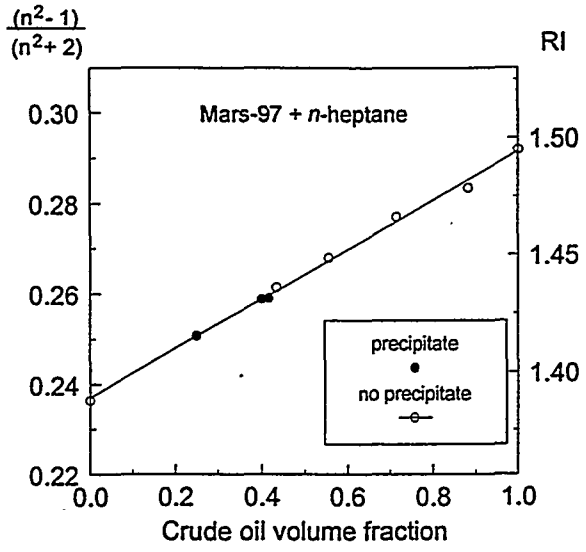

Figure 1.1-10. Refractive index of mixtures of Mars-97 crude oil and *n*-heptane and the onset of asphaltene precipitation.

As shown in **Fig. 1.1-11**, surfaces exposed to synthetic sea water, then aged in Mars-97 oil for up to three weeks remained preferentially water-wet. These results are consistent with those for CS and Gullfaks-96, both of which have similar acid and base numbers. There is no obvious effect of the different amounts of asphaltenes.

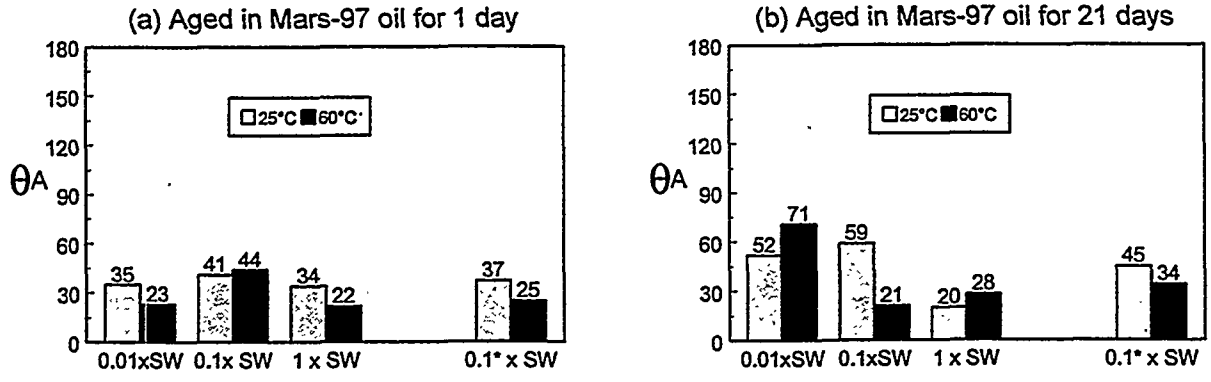

Figure 1.1-11. Water-advancing contact angles for mica surfaces aged first in synthetic sea water (SW) and its dilutions, then in Mars-97 crude oil after (a) 1 day and (b) 21 days at 25°C

1.1.3.2d Spraberry crude oil, Spraberry RB, and RRB

The lightest of the four oil samples tested, Spraberry oil, has the highest base number and a low acid number so that the ratio of base to acid numbers is quite high. On that basis, it might be expected to have the greatest propensity to alter wetting of a negatively charged surface by acid/base interactions. There is some tendency for mica surfaces aged in Spraberry oil to become less water-wet, if treated first with the most dilute brine (**Fig. 1.1-12**). Wetting alteration is more pronounced using dilutions of reduced NaCl reservoir brine (**Fig. 1.1-13**).

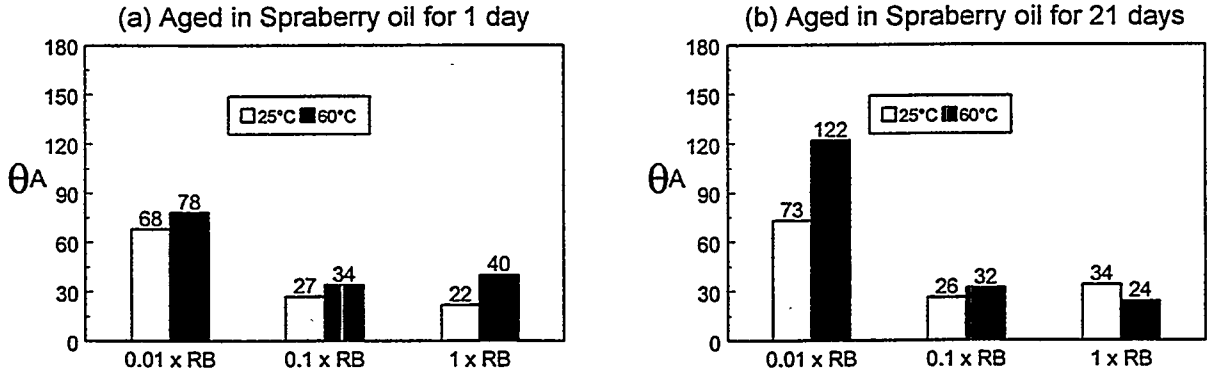

Figure 1.1-12. Water-advancing contact angles for mica surfaces aged in Spraberry reservoir brine (RB) and its dilutions followed by Spraberry crude oil after (a) 1 day and (b) 21 days at 25°C and 60°C.

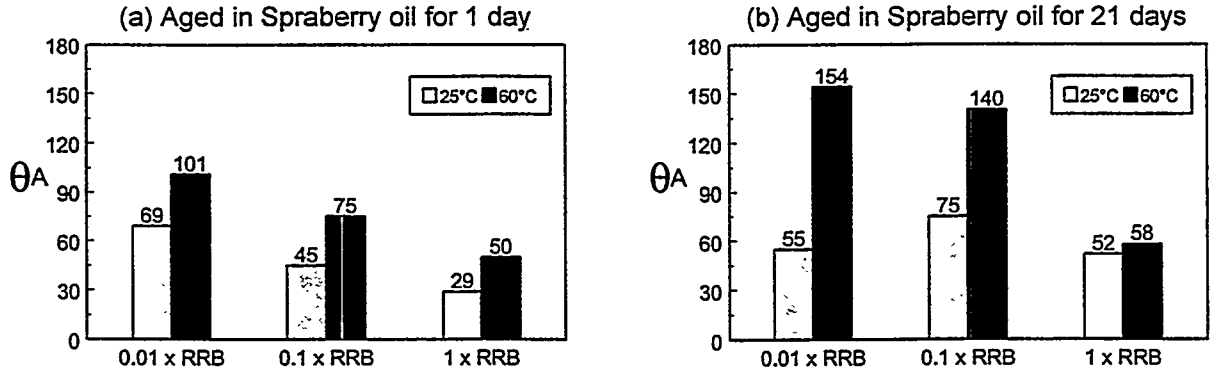

Figure 1.1-13. Water-advancing contact angles for mica surfaces aged in reduced NaCl Spraberry reservoir brine (RRB) and its dilutions followed by Spraberry crude oil after (a) 1 day and (b) 21 days at 25°C and 60°C.

Although the ratios of divalent to monovalent ions are different in the Spraberry and reduced NaCl Spraberry brines, they can be compared on the basis of ionic strength, as shown in

Fig. 1.1-14. A slight trend for higher contact angles at lower ionic strength is apparent in samples aged at 25°C; a much stronger trend is evident for samples aged in oil at 60°C.

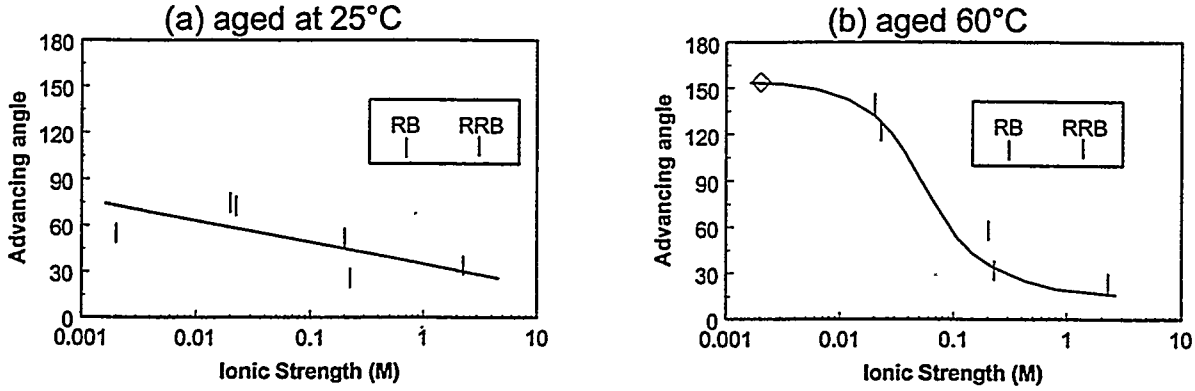

Figure 1.1-14. Water-advancing contact angles for mica surfaces aged in dilutions of Spraberry reservoir brine (RB) and reduced NaCl Spraberry reservoir brine (RRB) followed by Spraberry crude oil after 21 days (a) at 25°C and (b) at 60°C.

1.1.4 Summary

The results of wettability tests with these four medium gravity oil samples are consistent with expectations based on their G-AB profiles. Surface precipitation should not be an important factor for any of these samples. Spraberry, with a high base number and low acid number, participates in acid/base interactions with the acidic mica surface. These interactions are strongest when ionic strength is low.

As additional experience is gained with oils that have an increasingly wide range of G-AB profiles, we expect to be able to define more closely the properties associated with oils that have the highest and lowest propensity to alter wetting of solid surfaces.

1.2 Asphaltene Precipitation and Solvent Properties of Crude Oils

Including contributions from G.J. Hirasaki and B.S. Gill

Dept. of Chemical Engineering, Rice University, Houston, TX

1.2.1 Introduction

There is significant commercial interest in understanding the conditions under which asphaltene precipitation occurs during pressure depletion, CO_2 flooding, or natural gas flooding of petroleum reservoirs. Simple and reliable methods are needed to characterize crude oils and to predict the conditions at which precipitation occurs.

Thermodynamic models for predicting asphaltene precipitation traditionally have used the Hildebrand solubility parameter (Hildebrand and Scott, 1964) to estimate the heat of solution (Hirschberg *et al.*, 1984; Leontaritis and Mansoori, 1987; Burke *et al.*, 1990; MacMillan *et al.*,1995; Cimino *et al.*, 1995a, 1995b; Rassamdana *et al.*, 1996; Victorov and Firoozabadi, 1996; Pan and Firoozabadi, 1996). In these models, the heat of asphaltene-crude oil interaction, ΔH^M, is a function of the difference between the solubility parameter of the asphaltene (δ_a) and that of the remaining components of the crude oil (δ_s).

$$\Delta H^M \propto (\delta_a - \delta_s)^2 \qquad (1.2\text{-}1)$$

where the subscript a denotes asphaltene and the subscript s denotes the remaining components of the oil or the "solvent."

The Flory-Huggins model describes the intermolecular interactions with a dimensionless interaction parameter, χ.

$$\chi = \frac{V_s}{RT}\left(\delta_a - \delta_s\right)^2 \qquad (1.2\text{-}2)$$

This term represents the heat or excess energy of solute-solvent interactions. The models' predictions are limited by the accuracy of this term. The solubility parameter of the oil is estimated by approximating the cohesive energy density from the equation-of-state fit to live oil PVT data.

1.2.2 Assumption regarding London dispersion interactions

We assume that the dominant intermolecular interaction energy governing asphaltene precipitation is the London dispersion contribution to the van der Waals forces. London dispersion interactions occur between all molecules, including nonpolar ones; their occurrence is due to induced polarization. The London dispersion properties of a material can be characterized by the wavelength dependence of the refractive index (RI) or the "dispersion" of visible light. Polar interactions (dipole, ionic, charge transfer, hydrogen bonding, etc.), which are commonly used to describe asphaltene-resin interactions, are assumed to be of secondary importance. In the work that follows, the resin fraction of the crude oil will not receive special treatment. Resins will be considered to be components of the "solvent" fraction and the asphaltenes will be treated as the "solute." Electronic polarizability, related to aromaticity, is an important resin property in this model.

In support of this assumption, we observe that nonpolar materials of similar molecular size and structure can be either solvents or precipitants for asphaltenes, depending on their degree of polarizability. Consider, for example, the 7-carbon compounds, *n*-heptane (RI=1.3878) and toluene (RI=1.4961). The former is a precipitant and the latter is a solvent for asphaltenes. Also consider liquid carbon dioxide, CO_2 (RI=1.195) and carbon disulfide, CS_2 (RI=1.6319). The former is a precipitant and the latter is a solvent for asphaltenes. Thus, the induced polarizability, as quantified by the RI, appears to be important in determining the ability of hydrocarbons to serve as a precipitant or as a solvent for asphaltenes.

Further support is provided by the solubility parameter mapping of Wiehe (1996) which shows that asphaltene insolubility is dominated by aromaticity and molecular weight, not by polar or hydrogen bonding interactions.

The assumption of dominance of London dispersion forces would certainly not be true if significant amounts of polar materials were added to the crude oil mixture. However, since polar components are relatively minor compared to the amount of hydrocarbon in crude oils, we will ignore the contribution of polar interactions in this analysis.

The interaction energy between asphaltene molecules in a solvent medium with only London dispersion interactions (assuming the adsorption frequency of the asphaltene and the solvent are the same) is as follows (Israelachvili, 1991, Eq. 6.35):

$$w(r) = -\frac{\sqrt{3}h\nu_e}{4}\frac{\left(n_a^2 - n_s^2\right)^2}{\left(n_a^2 + 2n_s^2\right)^{3/2}}\frac{a_a^6}{r^6} \qquad (1.2\text{-}3)$$

$$= -\frac{C}{r^6}, \quad r > 2a_a$$

$$C = \frac{\sqrt{3}h\nu_e a_a^6}{4}\frac{\left(n_a^2 - n_s^2\right)^2}{\left(n_a^2 + 2n_s^2\right)^{3/2}} \qquad (1.2\text{-}4)$$

where h is Planck's constant, ν_e is the absorption frequency in the ultraviolet, n_a and n_s are the refractive indices of asphaltene and the solvent (extrapolated to zero frequency), a_a is the equivalent radius of the asphaltene molecule, r is distance between the centers of the molecules, and C is the coefficient of the distance dependence. The interaction energy is now expressed as a function of the differences between the squares of the refractive indices rather than the difference between the solubility parameters of asphaltene and solvent.

For a molecule of asphaltene interacting with the surface of a macroscopic body of asphaltene across a solvent medium, the energy is as follows (Israelachvili, 1991, Eq. 10.2):

$$w(D) = -\frac{\pi C\rho_a}{6D^3} \quad (\text{molecule} - \text{surface}) \qquad (1.2\text{-}5)$$

where D is the distance of the molecule from the surface and ρ_a is the number density of asphaltene molecules in the macroscopic body. If the interaction is between two spherical

aggregates of asphaltene or between a spherical aggregate and the surface of a macroscopic body of asphaltene, then the energy of interaction is as follows (Israelachvili, 1991, Eq. 10.5):

$$W(D) = -\frac{\pi^2 C \rho_a^2 R}{6D} \quad \text{(sphere – sphere or sphere – surface)} \qquad (1.2\text{-}6)$$

where R is the radius of the spherical particle. If the interaction is between two parallel surfaces of macroscopic bodies of asphaltene, the interaction energy per unit area is as follows (Israelachvili, 1991, Eq. 10.8):

$$W(D) = -\frac{\pi C \rho_a^2}{12D^2} \quad \text{(surface – surface, per unit area)} \qquad (1.2\text{-}7)$$

Hirasaki (1993) used a generalization of these concepts to predict the contact angles of non-polar materials on Teflon and the spreading of non-polar materials at the gas/water interface.

The solubility parameter will be approximated by the van Laar-Lorenz approach using the van der Waals equation of state (EOS) cohesion parameter (Hildebrand and Scott, 1964).

$$\delta \approx \frac{a^{1/2}}{V} \qquad (1.2\text{-}8)$$

where a is the van der Waals (vdW) EOS cohesion parameter and V is the molar volume. The vdW cohesion parameter can be expressed in terms of the parameters of the pair interaction energy (Israelachvili, 1991, Eq. 6.10):

$$a = \frac{2\pi N_o^2 C}{3\sigma^3} \qquad (1.2\text{-}9)$$

where σ is the hard sphere diameter. The pair interaction model, Eq. (1.2-3) & (1.2-4), will be used for the parameters in this equation. Let the "solvent" be vacuum (i.e., RI=1.0) and "asphaltene" be the species for which the solubility parameter is to be determined. The resulting expression for the solubility parameter is as follows:

$$\delta = \left(\frac{\sqrt{3}\pi}{384}\frac{h\nu_c}{\sigma^3}\right)^{1/2} \frac{\sigma^3}{V/N_o}\frac{n^2-1}{\left(n^2+2\right)^{3/4}} \qquad (1.2\text{-}10)$$

This equation expresses the solubility parameter in terms of the refractive index.

The correlation between the solubility parameter and the RI at ambient conditions for a number of *n*-alkane and aromatic hydrocarbons (Weast, 1987; Barton, 1991) is illustrated in **Fig. 1.2-1**. The exponent of ¾ in Eq. 1.2-10 has been approximated by an exponent of unity. The comparison shown here is between a function of RI

$$F_{RI} = \frac{n^2-1}{n^2+2} \qquad (1.2\text{-}11)$$

and the corresponding solubility parameters for paraffinic and aromatic hydrocarbons. Ethane and methane deviate from an otherwise linear trend because they are near or above their critical temperatures at ambient conditions.

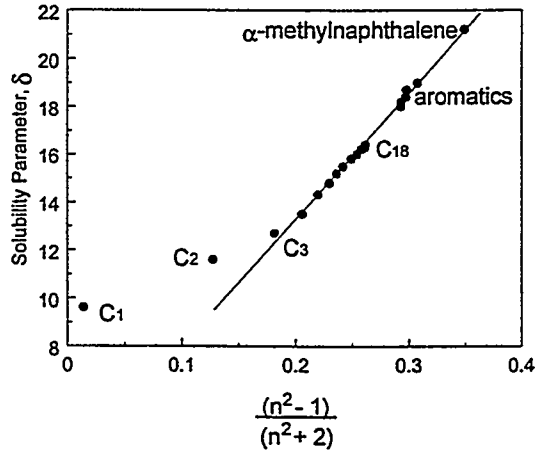

Figure. 1.2-1. Comparison of solubility parameter and F_{RI}.

1.2.3 Composition and density dependence of RI

The refractive index is expressed as a function of composition and density through the Clausius-Mossotti or Lorenz-Lorentz equation (Feynman, *et al.*, 1989; Vedam and Limsuwan, 1978).

$$\frac{3}{4\pi}\left(\frac{n^2-1}{n^2+2}\right)=\sum_i \frac{C_i \alpha_i}{4\pi \varepsilon_o N_o} \tag{1.2-12}$$

where C_i is the molar concentration of species i, α_i is the electronic polarizibility of species i, ε_o is the permittivity of free space, and N_o is Avogadro's number. This can be expressed in terms of the RI at some reference condition.

$$\left(\frac{n^2-1}{n^2+2}\right)=\sum_i \frac{C_i}{C_i^o}\left(\frac{n^2-1}{n^2+2}\right)_i^o \tag{1.2-13}$$

This expression describes the composition and density dependence of the RI. The coefficients of the C_i term are molar refractions. At ambient conditions and with ideal volume of mixing, the ratio, C_i / C_i^o is equal to the volume fraction of component i in the mixture. The molar refraction of a mixture can be expressed as a function of the mole fractions and molar refractions of its components by dividing Eq. 1.2-13 by the total molar concentration, C_Σ.

$$\begin{aligned}\frac{1}{C_\Sigma}\left(\frac{n^2-1}{n^2+2}\right)&=\sum_i \frac{X_i}{C_i^o}\left(\frac{n^2-1}{n^2+2}\right)_i^o \\ C_\Sigma&=\sum_i C_i \\ X_i&=\frac{C_i}{C_\Sigma}\end{aligned} \tag{1.2-14}$$

The validity of the Lorenz-Lorentz equation to describe the density dependence of RI was investigated by Vedam and Limsuwan (1978). For example, **Fig. 1.2-2** compares the calculated and measured change in RI of *n*-octane with pressure. The observation that the calculated RI is greater than the measured RI implies that the electronic polarizability and molar refraction are not strictly independent of density.

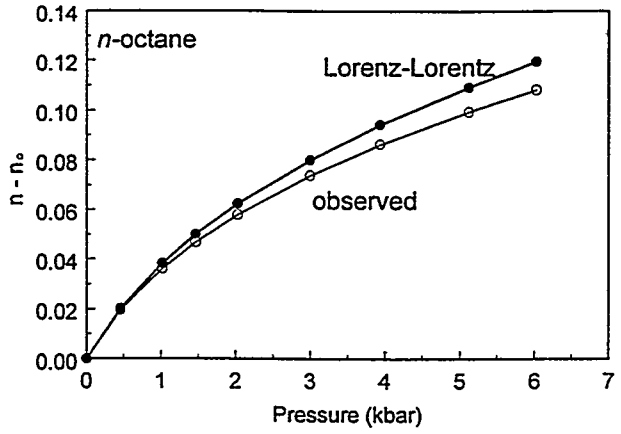

Figure. 1.2-2. Comparison of calculated and measured RI values for *n*-octane.

Live crude oil can be treated as a mixture of stock tank oil and separator gas. The RI of the live oil can be calculated from the formation volume factor, $B_o(P)$,(RB/STB), the solution gas/oil ratio, $R_s(P)$,(scf/STB), the RI of the stock tank oil, and the molar refraction of the separator gas.

$$\left(\frac{n^2-1}{n^2+2}\right)(P) = \frac{1}{B_o}\left(\frac{n^2-1}{n^2+2}\right)_{STO} + 7.52\times10^{-6}\frac{R_s}{B_o}\frac{1}{C^o_{gas}}\left(\frac{n^2-1}{n^2+2}\right)^o_{gas} \qquad (1.2\text{-}15)$$

The factor of 7.52×10^{-6} in the second term on the right-hand-side of Eq. 1.2-15 converts R_s from scf/bbl to moles/cm^3.

The molar refraction of the components of the separator gas can be calculated from group contributions (Weast, 1987).

$$\frac{1}{C^o_{gas}}\left(\frac{n^2-1}{n^2+2}\right)^o_{gas} = R_{gas} = \sum_i X_i R_i \qquad (1.2\text{-}16)$$

where X_i is the mole fraction and R_i is the molar refraction of component *i*.

Refractive indices calculated from molar refractions and values reported from measurements (Weast, 1987) are compared for a number of *n*-alkanes and aromatic hydrocarbons in **Fig. 1.2-3**. The agreement is very good for all except styrene.

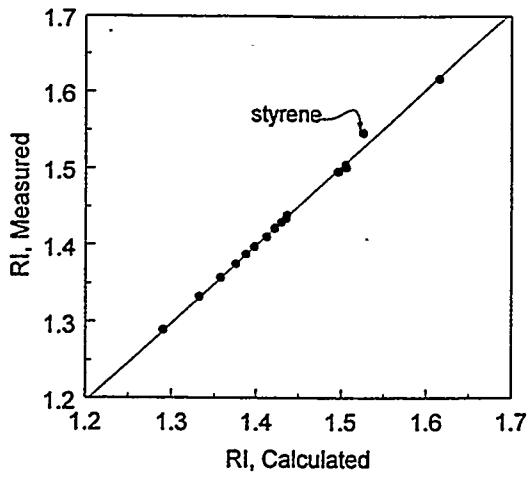

Figure 1.2-3. Comparison of calculated and measured RI.

1.2.4 Frequency dependence of RI

The expression for the intermolecular interactions in Eq. 1.2-3 has the RI, extrapolated to zero frequency, as a parameter. Often, the RI is available only at the frequency of the sodium-D line. **Fig. 1.2-4** is a Cauchy plot (Hough and White, 1980) of selected hydrocarbons. The slope is used to determine the absorption frequency, and the intercept gives the RI extrapolated to zero frequency. The value of RI at the sodium-D line is indicated. The curves are nearly parallel. Thus, since it is the difference between RI values that is related to the interaction energy, the values of RI measured at the frequency of the sodium-D line can be used to approximate the RI extrapolated to zero frequency.

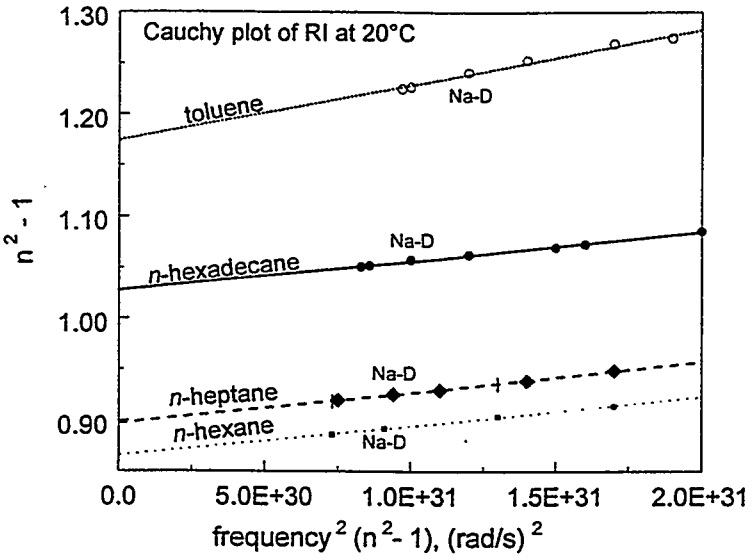

Figure 1.2-4. Dielectric polarizability is determined from RI as a function of frequency.

The frequency dependence of RI for asphaltenes probably does not parallel those for the transparent hydrocarbon shown in Fig. 1.2-4. Asphaltenes are black, indicating that they absorb in the range of visible wavelengths. Since they absorb at a lower frequency than the transparent hydrocarbons, they should have a larger Cauchy plot slope, contradicting the assumption implicit in Eq. 1.2-3 that asphaltene and solvent absorption frequencies are the same and that the Cauchy plots are parallel.

1.2.5 Precipitation of model systems

We have hypothesized that London dispersion interactions dominate asphaltene precipitation. Therefore, we have selected coronene as a model compound. Coronene is hexabenzobenzene, a flat molecule with six benzene rings surrounding a central benzene ring. It is a polyaromatic hydrocarbon with no polar functionality. We expect that coronene has an RI greater than 1.6, based on data for similar materials (see **Tables 1.2-1** and **1.2-2** below).

Table 1.2-1. Density and RI of polyaromatic compounds. (Weast, 1987)

Name	Formula	m.p., °C	Density	RI
naphthalene	$C_{10}H_8$	80.5	$0.962^{100/4}$	1.5898^{85}
			1.0253	1.4003^{24}
α-methylnaphthalene	α-$CH_3C_{10}H_7$	-22	$1.0202^{20/4}$	1.617^{20}
1,2,5 trimethylnaphthalene	1,2,5-$(CH_3)_3C_{10}H_5$	33.5	$1.0103^{22/4}$	1.6093^{22}
α-phenylnaphthalene	α-$C_6H_5C_{10}H_7$	45	$1.096^{20/4}$	1.6664^{20}
phenanthrene	$C_{14}H_{10}$	101	0.9800^{4}	1.5943
anthracene	$C_{14}H_{10}$	216	$1.283^{25/4}$	
1-methylanthracene	1-$CH_3C_{14}H_9$	85-6	$1.0471^{99/4}$	$1.680^{99/4}$
fluorathene	$C_{16}H_{10}$		$1.252^{0/4}$	
pyrene	$C_{16}H_{10}$	156	$1.271^{23/4}$	
coronene	$C_{24}H_{12}$	438-40	1.371	

Table 1.2-2. Solubility parameters. (Barton, 1991)

Name	Solubility Parameter $MPa^{1/2}$	RI
naphthalene	20.3	1.5898^{85}
α-methylnaphthalene	21.2	1.617^{20}
phenanthrene	20.0	1.5943
anthracene	20.3	
average of above	20.4	1.60
carbon disulfide	20.5	1.6319^{20}

The solubility parameters of the model compounds above are close to the values of 19.5 and 20.5 $MPa^{1/2}$ estimated for asphaltenes by Hirschberg *et al.* (1984) and Burke *et al.* (1990), respectively. If these compounds are analogues for asphaltenes, then the estimated RI for asphaltene is about 1.6.

Approximately 3 mg/ml of coronene were dissolved in toluene (RI=1.496); *n*-heptane (RI=1.3878) was added as the precipitant. Precipitation occurred when the volume fraction of *n*-heptane was 0.61 and the mixture RI decreased below 1.4275. This value of RI at the onset of precipitation is very similar to experimental observations with crude oils, shown in the next

section. Unlike crude oils, however, the precipitation is sudden and crystalline material precipitates. Nevertheless, this experiment demonstrates that decreasing RI is sufficient to precipitate a polycylic, aromatic hydrocarbon in a system with no polar interactions.

1.2.6 Refractive index of crude oils

1.2.6.1 Measurements

The RI of crude oil samples was measured at 20°C using an Abbe refractometer with a sodium lamp. Two problems were encountered. Volatile oils may lose light components during the measurement, and heavier oils may be too opaque to be measured.

For volatile oils, several measurements were made with each sample, as recommended in ASTM D1218-92. Initial measurements provided a first estimate of the RI. The refractometer was then set at this initial value and the final measurement was made very quickly to minimize the extent of evaporation.

For opaque oils, RI was estimated by extrapolating F_{RI} (defined in Eq. 1.2-11) of oil/hydrocarbon mixtures, as shown in **Fig. 1.2-5**. The fit to a straight line for F_{RI} as a function of volume fraction of crude oil in the crude oil-plus-*n*-heptane mixture is excellent.

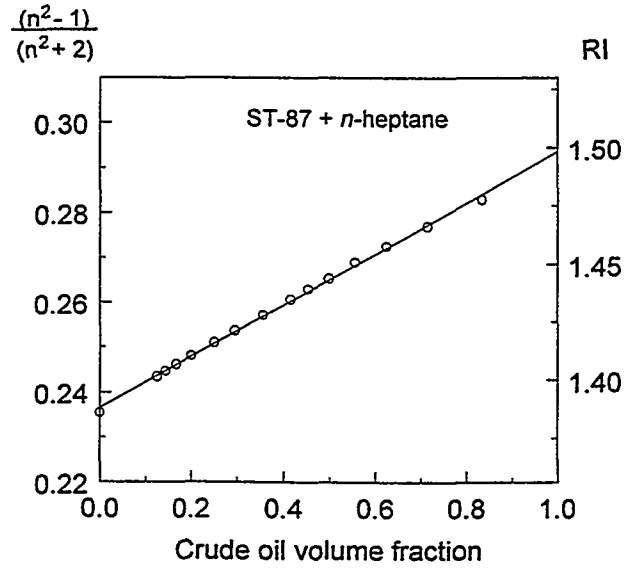

Figure 1.2-5. F_{RI} and RI of mixtures of ST-87 crude oil with *n*-heptane. No asphaltenes precipitated from any of these mixtures.

Fig. 1.2-6 shows measured values of F_{RI} and RI for Lagrave crude oil mixtures with *n*-heptane. In this case, the oil is light enough to permit direct measurement of its RI so the measured and extrapolated values can be compared. Each mixture is examined microscopically for the presence of asphaltene precipitate; open circles indicate mixtures with no asphaltenes. For the asphaltene-free mixtures, F_{RI} is a linear function of the volume fraction of crude oil. The straight line shown is a least-squares fit to the F_{RI} data for the Lagrave oil sample, pure *n*-heptane, and asphaltene-free mixtures of the two. Measured and extrapolated values of RI for this oil (1.470) are indistinguishable.

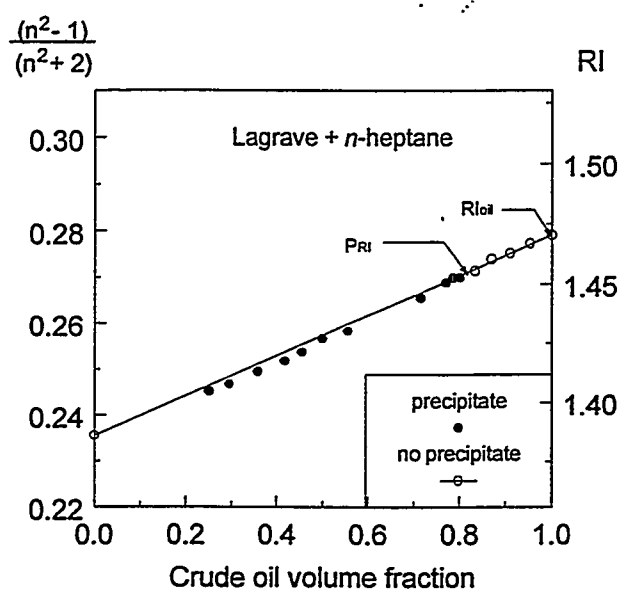

Figure 1.2-6. F_{RI} and RI of mixtures of Lagrave crude oil with *n*-heptane. Mixtures with RI < 1.453 contain precipitated asphaltene.

1.2.6.2 RI of mixtures containing precipitate

Mixtures with RI < P_{RI} (RI at onset of precipitation) contain varying amounts of precipitate. **Fig. 1.2-7** shows refractive index measurements for two crude oils and *n*-heptane; mixtures containing precipitate are indicated by solid symbols and those with no precipitate are shown with open symbols. Straight lines are least-squares fits to the open symbol data points only. In the case of A-93, mixtures containing precipitate do not deviate appreciably from the linear relationship between RI and volume fraction of crude oil in the oil-heptane mixture. The oil from California is quite different, with a large deviation for mixtures containing precipitate. Lagrave crude oil (Fig. 1.2-5) is an intermediate example.

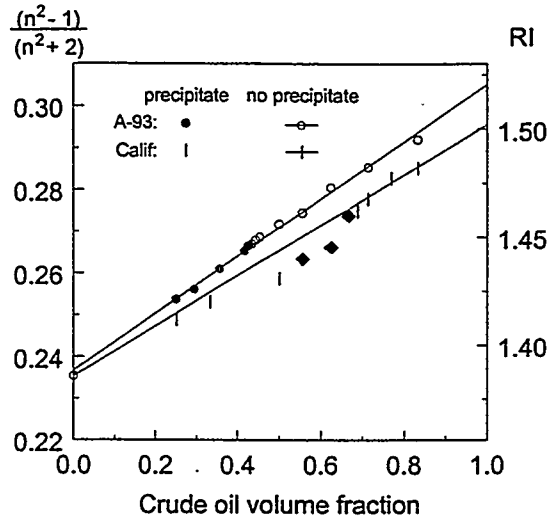

Figure 1.2-7. F_{RI} and RI of mixtures of A-93 and California crude oils with *n*-heptane. Mixtures containing precipitate may deviate from linear relationship between F_{RI} and volume fraction of crude oil in the mixture.

1.2.6.3 Refractive index at the onset of precipitation, P_{RI}

Microscopic examination established that mixtures of Lagrave crude oil and heptane with RI less than 1.453 contained asphaltene precipitate. Thus the RI at the onset of precipitation (P_{RI}) is 1.453 for Lagrave mixed with *n*-heptane. **Table 1.2-3** summarizes the results of RI measurements and microscopic examination for 11 crude oils.

Table 1.2-3. RI and P_{RI} data for mixtures of crude oils with *n*-heptane.

Crude Oil	API gravity (°)	n-C_5 asphaltenes %	RI	$f_{V,oil}$ at pptn	P_{RI}	Δ_{RI} = (RI - P_{RI})
A-93	25.5	10.9	1.522	0.43	1.446	0.076
A-95	25.2	5.0	1.518	0.43	1.445	0.074
California	28.5		1.503	0.70	1.465	0.038
EMSU	32.0	1.2	1.484	0.43	1.429	0.055
Lagrave	41.3	3.8	1.470	0.82	1.454	0.016
Moutray	35.2	1.8	1.484	0.45	1.432	0.052
Oklahoma	26.0		1.568	0.23	1.427	0.141
Schuricht	24.6	9.9	1.514	0.47	1.448	0.066
Heavy CA	19.0	6.8	1.565	0.24	1.431	0.135
SQ-95	37.2	2.9	1.476	0.16	1.402	0.074
Tensleep	31.2	3.4	1.486	>1.00	1.490	-0.004

A fairly wide range of oils are represented in Table 1.2-3. API gravity ranges from 19° to more than 41°. RI varies from a low of 1.47 to a high of almost 1.57. RI and API gravity are roughly correlated, with some exceptions, as shown in **Fig. 1.2-8.**

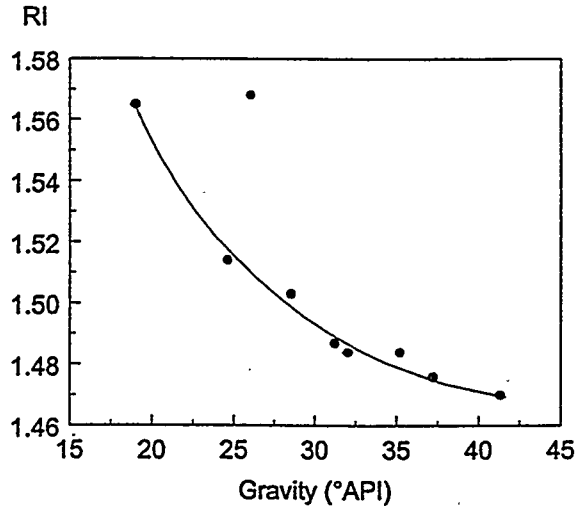

Figure 1.2-8. As API gravity increases, RI of crude oils decreases.

Although the oils have a wide range of RI, P_{RI} varies over a narrower range, as shown in **Fig. 1.2-9** for 10 crude oils. The standard deviation of P_{RI} for this set of crude oils is only about half that for the oil RI values; average P_{RI} is ~1.44. The range of asphaltene content in these samples is very broad, from a low of 1.2 to a high of 10.9 wt%. There is no correlation evident between asphaltene content and either RI or P_{RI}.

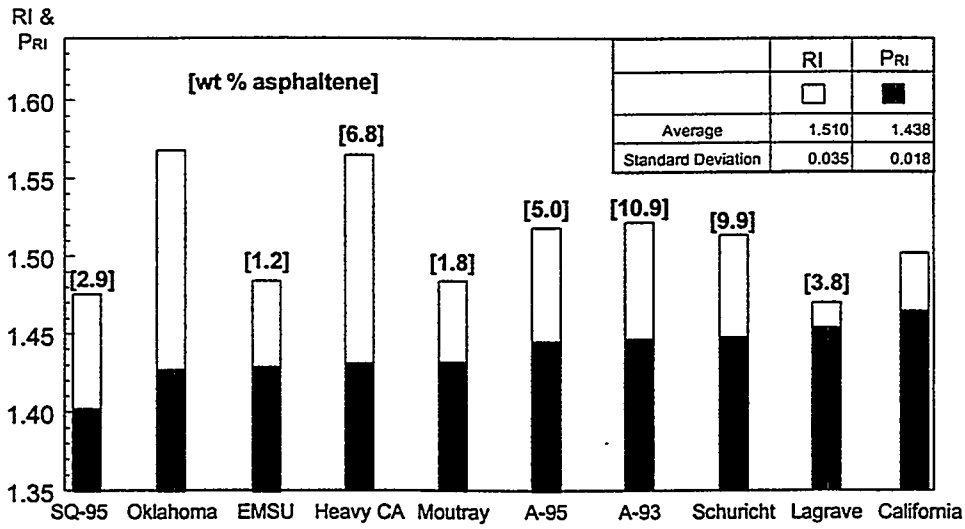

Figure 1.2-9. Comparison of RI and P_{RI}.

1.2.6.4 P_{RI}—calculation from measurements at infinite dilution

The values of both RI and P_{RI} vary from one crude oil to another. For a given set of crude oil and precipitant, however, P_{RI} is approximately constant (Buckley, 1996). Addition of a hydrocarbon solvent, such as toluene, changes the volume fraction of precipitant required to initiate precipitation, but not the refractive index at which it occurs.

Destabilization at a constant ratio of solvent-to-precipitant has been reported by many observers (Heithaus, 1962; Bichard, 1969; Hotier and Robin, 1983; Reichert *et al.*, 1986; Dubey and Waxman, 1991; Cimino *et al.*, 1995b). Often, the volume of solvent greatly exceeds the amount of oil or bitumen in these tests. A constant solvent-to-precipitant ratio is observed since they are effectively working at infinite dilution. RI is determined by the ratio of solvent-to-precipitant. When the oil itself makes a significant contribution to mixture RI, the ratio can vary, but precipitation occurs at the same value of RI for a particular combination of oil and precipitant.

Assuming infinite dilution, the ratios reported in the literature can be used to calculate a value of RI at the onset of precipitation, which we will call P_{RI}*. For a binary mixture of nonpolar molecules, RI can be calculated using Eq. 1.2-14 above.

Cimino *et al.* (1995b) precipitated asphaltenes with pentane from toluene and tetralin solutions. **Table 1.2-4** shows the values used to calculate P_{RI}* from their published onset of precipitation data. These values of P_{RI}* are in the same range as observations of various crude oils with no added solvent and *n*-heptane as precipitant shown in Table 1.2-3.

Table 1.2-4. P_{RI}* Calculated from onset of precipitation at infinite dilution. (Cimino *et al.*, 1995)

	n-pentane	toluene	tetralin
M (g/mole)	72.15	92.14	132.21
ρ (g/cm^3)	0.6262	0.8669	.9702
RI	1.3579	1.4961	1.5413
precipitating mixture	201 g	296 g	
	240 g		258 g
P_{RI}*		1.43	1.42

The results of similar calculations using the data of Hotier and Robin (1983) are shown in **Fig. 1.2-10** as P_{RI}* as a function of number of carbon atoms in the precipitant. Many different solvents were used; the data for benzene, toluene, and xylene are shown here. P_{RI} is in the range of 1.42 - 1.43 for this oil (identified only as fuel oil K), when heptane is the precipitant.

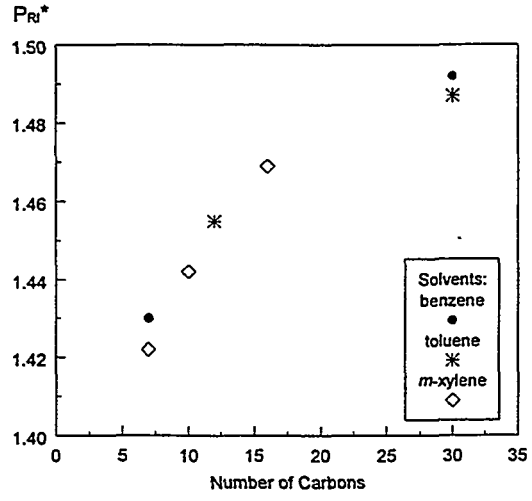

Figure 1.2-10. P_{RI}* as a function of precipitant chain length (from data of Hotier and Robin, 1983).

1.2.6.5 Addition of aromatic solvents

As reported previously (Buckley, 1996), addition of aromatic or other hydrocarbon solvents has minimal effect on P_{RI}. The fractions of various components in the mixture vary, concentration of the asphaltene fraction, and ratio of precipitant to solvent all vary, but the RI at the onset of precipitation is constant.

The effect of aromatic solvents, toluene and α-methylnaphthlene (AMN), on the volume fraction of oil at the onset of precipitation is illustrated in **Fig. 1.2-11**. Compared to toluene, AMN has a higher RI and thus permits a greater dilution with the precipitant before precipitation occurs. Thus AMN is an analog of a resin in its solvating power for the asphaltenes even though AMN has no polar functionality.

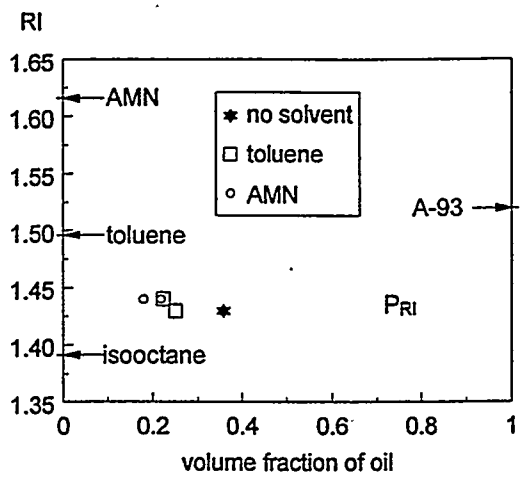

Figure 1.2-11. Onset of precipitation of asphaltenes induced by isooctane from A-93 crude oil and its mixtures with toluene and α-methylnaphthalene. (data from Buckley, 1996)

1.2.6.6 Comparison of P_{RI} for precipitants of varying molecular size

P_{RI} varies with the size of added precipitant, as shown in **Fig. 1.2-12** for A-93 crude oil precipitated with *n*-alkanes from pentane to pentadecane. For the lighter compounds (pentane and hexane especially), volatility of the precipitant necessitates measurements in a closed system. RI was estimated in these cases by linear interpolation between RI of the pure precipitant and that of the crude oil using the volume fractions at the onset of precipitation.

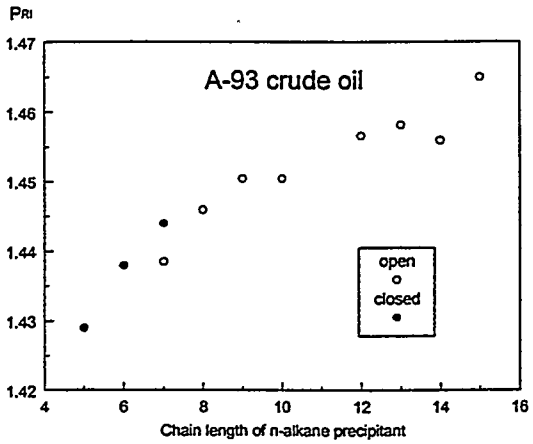

Figure 1.2-12. P_{RI} as a function of precipitant size.

This variation of P_{RI} with the size of the precipitant can be interpreted with the help of the expression for the Flory-Huggins parameter χ in Eq. 1.2-2. This dimensionless parameter is a function of both the solvent solubility parameter and the solvent molecular volume. The solvent

in our case is the mixture of the crude oil and added precipitant. If the onset of precipitation occurs at a critical value of χ, then a solvent with a larger molecular volume must also have a larger solubility parameter at the onset of precipitation. Given the correlation demonstrated previously between solubility parameter and RI, precipitants with larger molecular volumes should initiate precipitation at higher RI, consistent with the results shown in Figs. 1.2-10 and 1.2-12.

1.2.6.7 RI of asphaltene

An estimate of the RI of the asphaltene fraction has been made by extrapolation from RI measurements for mixtures of asphaltenes that were first precipitated from A-93 crude oil with *n*-hexane, then redissolved in toluene (**Fig. 1.2-13**). Volume fractions were calculated based on a measured asphaltene density of 1.2 g/ml. The extrapolated value of RI is about 1.72, assuming no volume change on mixing.

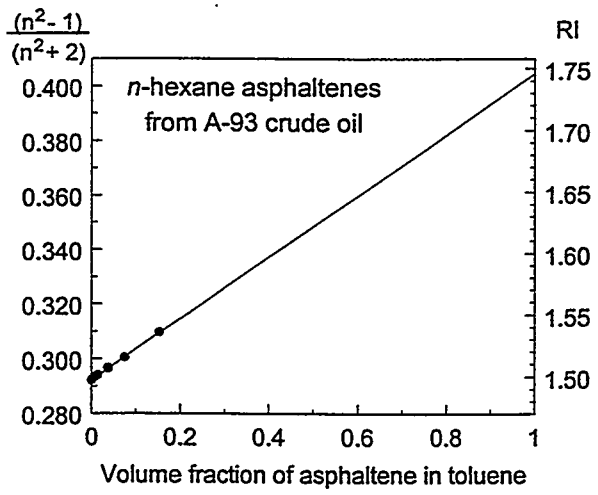

Figure 1.2-13. F_{RI} and RI of asphaltenes precipitated from A-93 crude oil by n-hexane.

This estimate is somewhat higher than the RI of material adsorbed from a crude oil of 1.67 reported by Christenson and Israelachvili (1987). RI can only be measured for fairly dilute solutions because the mixtures become opaque with increasing asphaltene concentration. A long extrapolation is required, reducing the certainty of the calculated value. The density was measured by displacement of water with asphaltene; that value also is uncertain. Different measurement methods give a range of density results for asphaltenes (Parkash *et al.*, 1979). If the density were 1.0 g/ml, the estimate of asphaltene RI would be reduced to 1.7.

As discussed in the section on the frequency dependence of RI above, the RI at the sodium-D line may not be appropriate for asphaltenes because of the slope of the Cauchy plot and because the adsorption frequency of asphaltenes may be substantially different from other components of the crude oil. An alternative to measurements is to estimate RI of asphaltenes from analogous polyaromatic compounds (see Table 1.2-1).

1.2.6.8 Asphaltene/maltene/precipitant model of crude oil

Thermodynamic models for the prediction of asphaltene precipitation will require the RI of the asphaltenes and of the remainder of the oil phase or solvent. This solvent pseudocomponent consists of (1) the deasphalted oil (resins, aromatics, and saturates), often known as maltenes, (2) precipitants such as methane, CO_2, or *n*-alkanes, and (3) added solvents such as toluene or AMN.

As an illustration, we can calculate the RI of the maltene fraction of a stock tank oil. The density and RI of asphaltene are assumed to be 1.26 g/cm^3 and 1.61, respectively for this calculation. The step is to convert asphaltene content from weight % , w_a, to volume fraction, $f_{V(asphaltene)}$.

$$f_{V(asphaltene)} = \frac{w_a \rho_o}{100 \rho_a} \tag{1.2-17}$$

The maltene RI is determined by extrapolation to zero volume fraction of asphaltene as shown in **Fig. 1.2-14**; determinations for three crude oils are illustrated in **Table 1.2-5**.

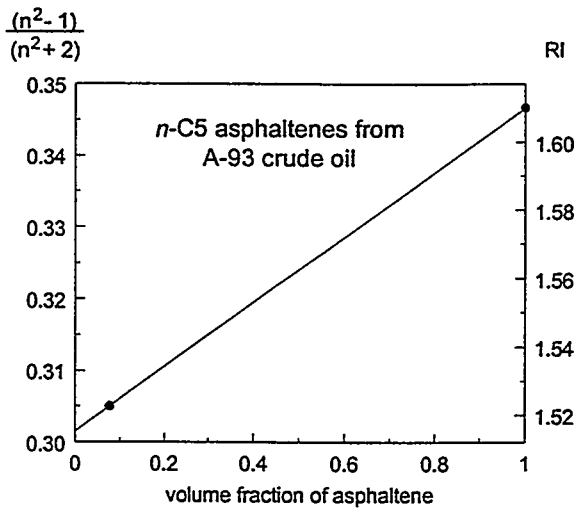

Figure 1.2-14. RI of maltenes calculated by extrapolation for A-93 crude oil.

Table 1.2-5. Estimation of maltene RI.

Crude Oil	Asphaltene Fraction, wt %	Asphaltene Volume Fraction	RI of STO	RI of maltenes
Heavy CA	6.8%	0.050	1.550	1.547
Alaska-93	10.9%	0.077	1.522	1.515
Lagrave	3.8%	0.025	1.470	1.467

1.2.6.9 RI of live crude oil upon pressure depletion

The RI of a 21.6°API gravity crude oil is modeled during pressure depletion as a binary mixture of stock tank oil (STO) and separator gas. Conventional "black oil" PVT data expresses the concentration of STO in the hydrocarbon liquid as the reciprocal of the formation volume factor, B_o (RB/STB). The dissolved gas is expressed as the solution gas/oil ratio, R_s (scf/STB). The concentration of separator gas in the hydrocarbon liquid is R_s/B_o. The PVT data is illustrated in **Fig. 1.2-15**.

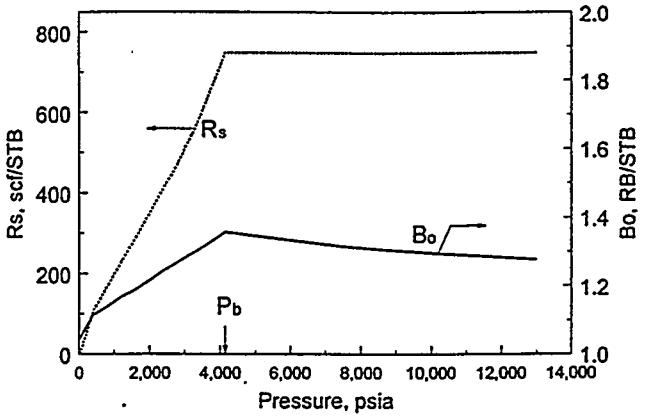

Figure 1.2-15. Black oil PVT data.

No STO was available, so RI could not be measured; it was estimated to be 1.53 from the correlation with API gravity (Fig. 1.2-8). The separator gas was assumed to be methane with a molar refraction of 6.7 cm^3/mole. The calculated RI of the live oil at reservoir temperature during pressure depletion is shown in **Fig. 1.2-16.** For purpose of illustration, suppose that the precipitation RI, P_{RI}, is equal to 1.44, shown by the dashed line. This illustrates that asphaltene precipitation will occur slightly above the bubble point pressure as a result of density reduction and will continue below the bubble point until the RI is increased to a value above the P_{RI} as a result of loss of methane.

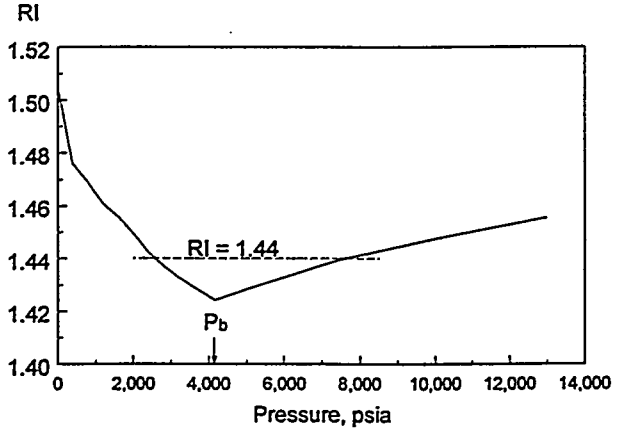

Figure 1.2-16. Calculated RI of crude oil during pressure depletion.

1.2.7 Remaining questions

We have assumed—first in Eq. 1.2-3 and again in substituting RI at the sodium-D line for RI extrapolated to zero frequency—that the asphaltenes have the same absorption frequency as

the maltenes. This assumption is not strictly valid. A better approximation may be gained by determining RI of the asphaltenes as a function of wavelength and using the exact Lifshitz theory to calculate interaction energies.

Asphaltenes have been treated as a single component. In reality, the asphaltenes have a distribution of polarizability or RI and of molecular sizes. More realistic thermodynamic models of asphaltene solvation and precipitation will require treatment of the asphaltenes and resins as distributions of components. The aggregates they form must also be described as having distributions of size and composition.

1.2.8 Summary

- The solubility parameters of several hydrocarbons have the dependence on RI as predicted for London dispersion interactions.
- The density dependence of the RI can be accurately estimated by the Clausius-Mossotti or Lorenz-Lorentz equations over the pressure range of interest in petroleum reservoirs.
- The difference between the RIs of hydrocarbons, extrapolated to zero frequency, can be estimated from the differences between the RIs measured at the sodium-D line if the hydrocarbons have similar absorption frequencies. This may not be valid for asphaltenes since they absorb in the frequencies of visible light.
- The F_{RI} of mixtures of a crude oil or its asphaltenes with hydrocarbon solvents and precipitants are a linear function of the volume fraction of the crude oil as predicted by the Clausius-Mossotti and Lorenz-Lorentz equations. This makes it possible to estimate the RI of the crude oil or asphaltene when it is too opaque to measure directly.
- The RI of live crude oil during pressure depletion can be calculated from the RI of STO, molar refraction of the separator gas, the formation volume factor, B_o, and the solution gas/oil ratio, R_s.

- For a number of crude oils with RI in the range, 1.51 ± 0.04, precipitation with addition of *n*-heptane begins when the mixture RI is less than the average P_{RI} of 1.44 ± 0.02. Note that the value of P_{RI} is more nearly constant than is the RI of the original oils.

- In a model system with the pure hydrocarbons, hexabenzobenzene and toluene, addition of *n*-heptane initiates precipitation when the RI drops below 1.4275. This value of P_{RI} is within the range of values observed for crude oil systems. Thus precipitation phenomena analogous to asphaltene precipitation occurs in a system with no polar interactions. This is evidence that polar interactions are not necessary for asphaltene precipitation.

- The addition of the aromatic solvent, α-methylnaphthalene, to crude oil allows more dilution with isooctane before precipitation occurs, but the values of P_{RI} is unchanged. Thus AMN is an analog of a resin in its solvating power for the asphaltenes even though AMN has no polar groups to contribute to solvation due to polar interactions. This is evidence that the aromatic character of the resins is responsible for the solvating properties of the resins.

PART 2. WETTABILITY ASSESSMENT

2.1 Alteration of Wetting of Mica Surfaces

2.1.1 Introduction

In previous work, glass surfaces have been used for several systematic investigations of crude oil/brine/solid interactions. Microscope slides made of soft glass (Liu and Buckley, 1997) and plates of quartz glass (Xie, 1997) have both been used to observe adhesion and adsorption properties of crude oils.

Several mechanisms by which crude oil components can interact with silicate surfaces have been proposed (Buckley *et al.*, 1998). However, mechanisms demonstrated on smooth glass surfaces are not necessarily predictive of wetting alteration in sandstone cores (Buckley *et al.*, 1996). Quartz is the major mineral component of sandstones and thus has traditionally been considered as a representative substrate for sandstone interactions with crude oils. However, pore surfaces, rather than bulk composition, are the important part of a rock, with respect to interactions with crude oil, and those surfaces may be dominated by minor components such as clays.

Muscovite mica is in many ways an ideal choice to replace glass in surface tests of the wettability altering potential of crude oils. Freshly cleaved surfaces are crystalline, molecularly smooth and readily reproduced. There is a wealth of data about the surface properties of mica. It is the main substrate used for measurements of surface forces (Israelachvili, 1991). Surface charge is determined by the ratio of substitution of Al^{3+} for Si^{4+} in the tetrahedral layers; the naturally occurring counter ion can be readily replaced by ion exchange. Muscovite has a surface structure similar to illite, a common clay mineral in sandstone reservoirs. Muscovite itself is found in reservoir rocks (Hurst, 1985) and may be a more common reservoir mineral than is usually recognized because it can be mistaken for illite in x-ray diffraction studies (Herron *et al.*, 1997).

2.1.2 Mechanisms of wetting alteration

Some mechanisms by which polar crude oil components can adsorb on high energy surfaces and alter wetting were defined in the introductory section of this report. They fall into three general categories, summarized in **Table 2.1-1** (see also Buckley *et al.*, 1998).

Table 2.1-1. Mechanisms of interaction by which crude oil components can adsorb on silicate surfaces.

Interaction category:	Occur between:	Resulting wettability:
polar	oil and dry surfaces	produce low to intermediate contact angles
ionic	oil and wet surfaces	results depend on stability of water film and specific interactions
surface precipitation	colloidal asphaltenes and surfaces	render surfaces oil-wet

Ionic mechanisms can be further subdivided into acid/base interactions that predominate in the absence of divalent or multivalent ions and specific or ion-binding interactions that can occur when higher valency ions are present. In this study, we investigate whether mica surfaces display a similar range of polar and ionic interactions to those defined in Table 2.1-1 for glass.

Mica, like quartz, is negatively charged except at very low pH. Thus, we might expect that the interactions with brine and oil should be similar for mica and quartz. There are differences, however, in surface structure, charging mechanisms, and roughness that may impact interactions. Given the difficulties inherent in studies of complex natural materials such as crude oil, it is necessary to document wetting alteration of mica with some well-studied oils, while samples are still available.

2.1.3 Experimental methods and materials

2.1.3.1 Mica

Samples of mica were obtained from Ward's Natural Science Establishment. These included:

muscovite $\left(KAl_2(Si_3Al)O_{10}(OH,F)_2\right)$ and
biotite $\left(K(Mg,Fe^{2+})_3(Al,Fe^{3+})Si_3O_{10}(OH,F)_2\right)$

Both of these mica minerals exhibit perfect cleavage to produce molecularly smooth surfaces.

2.1.3.2 Aqueous solutions

All solutions were prepared from deionized water, redistilled in glass and reagent grade salts. NaCl solutions with salinities up to 1*M* were weakly buffered using sodium acetate/acetic acid (pH 4) or sodium phosphate salts (pH 6 and 8). The pH values of the 2*M* NaCl solutions were adjusted with HCl or NaOH. For the NaCl solutions, pH and concentration are indicated within braces as {pH, [NaCl]}. The pH of $CaCl_2$ solutions was not adjusted; it ranged from 5.9 to 6.2.

2.1.3.3 Refined oils

Toluene and decane were purified by passing the fluids through a column of silica gel and alumina.

2.1.3.4 Crude oils

Two crude oils were used in these tests. Their properties are summarized in **Table 2.1-2.**

Table 2.1-2. Crude oil properties

	A-93 (Prudhoe Bay)	Moutray (W. Texas)
API Gravity (° API)	22.5	35.2
Acid Number (mg KOH/g oil)[1]	0.14	0.55
Base Number (mg KOH/g oil)[2]	2.42	0.81
n-C_5 asphaltenes (wt%)[3]	10.9	1.79
n-C_7 asphaltenes (wt%)	7.1	0.95
Elemental analysis[4]:		
H/C	1.671	1.803
N/C	0.003	0.002
S/C	0.004	0.002
O/C	0.004	0.006

[1] ASTM D664-89. [2] ASTM D2896-88; Dubey and Doe, 1993. [3] ASTM D2007-80. [4] Huffman Labs

2.1.3.5 Test protocols

The tests used here have been described previously (Liu and Buckley, 1997). Additional details of the testing procedures with mica are also available (Liu, 1997). Briefly, they involve the following observations.

(1) *Adhesion* or non-adhesion of a drop of crude oil was observed as it was withdrawn from a clean, brine-covered surface after a short contact time

between oil and solid. NaCl concentration, pH, and temperature have been identified as important variables in these tests.

(2) Water/decane contact angles were measured to assess the affect of *adsorption* on surfaces exposed first to brine and then to crude oil. Brine composition and oil exposure conditions (time and temperature) have been found to be the main variables affecting adsorption for a given oil and surface. Crude oil was removed by washing with toluene prior to contact angle measurement.

2.1.4 Results and discussion

Two oils that have been extensively tested on glass surfaces (Buckley and Morrow, 1990; Liu and Buckley, 1997; Xie *et al.*, 1997) and in Berea sandstone cores (Morrow *et al.*, 1986; Jadhunandan and Morrow, 1995; Zhou *et al.*, 1995, 1996; Yildiz, 1995; Buckley *et al.*, 1996; Tang and Morrow, 1997) are Moutray crude oil from West Texas and A-93 from Prudhoe Bay, Alaska. These crude oils were selected for a detailed comparison of wettability-altering interactions on mica to those previously reported on soft and quartz glass.

2.1.4.1 Wetting alteration—dry mica

Previous studies on glass have demonstrated wetting changes that occur when dry surfaces are aged in crude oil. The resulting surfaces tend to have water-advancing angles (against decane) that are in the intermediate range ($60° < \theta_A < 120°$) and water-receding angles that are much lower ($\theta_R < 30°$) (Buckley *et al.*, 1998). **Figure 2.1-1** shows the results of comparable experiments on muscovite.

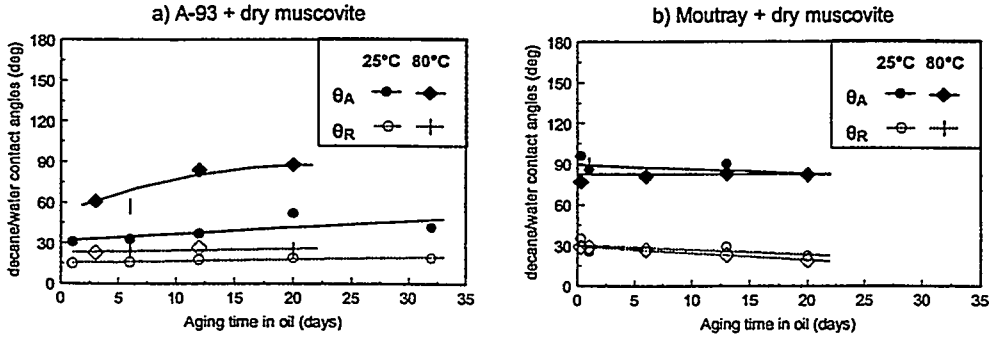

Figure 2.1-1. Contact angles on dry mica surfaces treated with A-93 and Moutray crude oils.

Interactions between dry mica and crude oils produce surfaces that are neither water-wet nor oil-wet. (Note that while the solid surfaces were dried before exposure to oil, water was not rigorously excluded from any of these tests.) Differences between mica surfaces aged at room temperature and at 80°C are evident for A-93 oil, but not for Moutray. Changes with aging time are minimal in both cases. These observations are generally consistent with previously reported results with many different crude oils and glass surfaces where rapid alteration to intermediate conditions that vary little with temperature have been observed.

In the experiments summarized in Fig. 2.1-1, mica surfaces were rinsed with toluene to remove all but the adsorbed oil. Rinsing with a solvent other than toluene would likely produce different contact angles. More paraffinic solvents destabilize asphaltenes, whereas stronger solvents might remove some of the adsorbed material.

2.1.4.2 Wetting alteration of mica in the presence of water

The presence of water complicates crude oil/solid interactions in several ways. Bulk water can shield solid surfaces from contact with high molecular weight compounds in the oil and limit their access to adsorption sites on the solid surface. Stable water films can also prevent adsorption, especially in low salinity, high pH regimes where electrostatic repulsive forces balance van der Waals attraction. If water films are unstable, alteration of wetting can be more pronounced than in the absence of water. The compositions of both oil and brine are key variables in determining the wetting alteration observed on a given surface.

Dependence of water film stability on brine pH and ionic strength indicates the contribution of acid/base interactions and is the basis of standard adhesion tests. Brine pH and NaCl concentrations for which adhesion was observed in two-minute tests with A-93 at 25°C and 80°C on mica are shown in **Fig. 2.1-2**. The adhesive areas are smaller than the corresponding areas on glass. Glass results are indicated in Fig. 2.1-2 by the dotted lines separating adhesion/transition observations from non-adhesion (Buckley *et al.*, 1997).

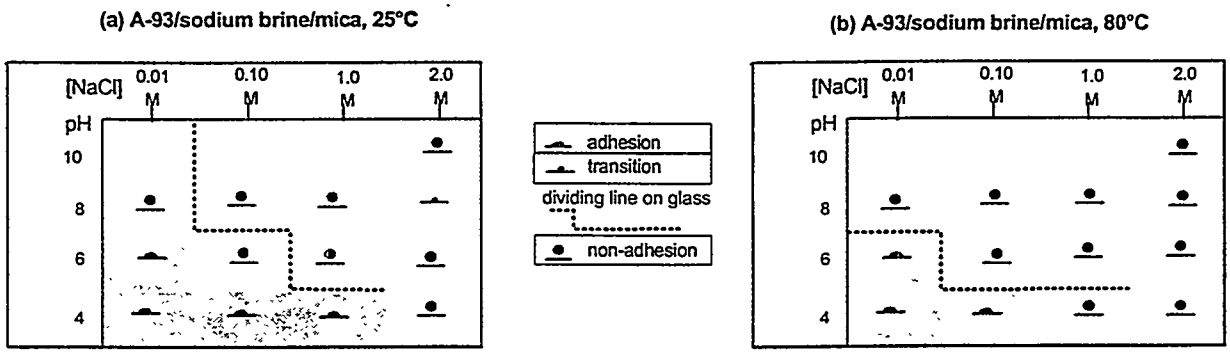

Figure 2.1-2. Adhesion maps for A-93 crude oil on muscovite and biotite mica.

The adhesion tests suggest a tentative outline of conditions where water films are stable (higher pH and higher ionic strength) and where they are unstable (lower pH and lower ionic strength), as illustrated in **Fig. 2.1-3.** Transitional conditions and those that change with temperature are included in the intermediate or conditionally stable region. That region is smaller for mica than for glass; regions that are clearly unstable are comparable.

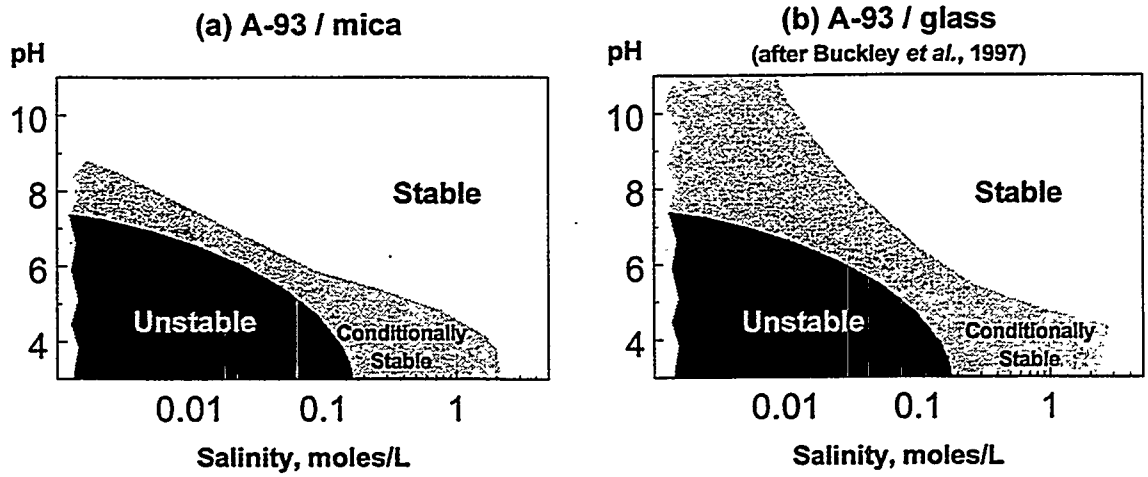

Figure 2.1-3. A-93 water film stability maps based on comparisons of adhesion at 25 and 80°C.

2.1.4.3 Comparison of different mica minerals

Two different mica minerals have been tested. Muscovite is light in color and large areas appear to be smooth. Biotite, which has iron substituted in its inner layers, is darker in color and the samples used in these tests often appeared to be macroscopically rough. Despite these

differences, tests showed that wettability-altering interactions were similar for both types of mica. The examples shown in **Fig. 2.1-4** illustrate that there are only small differences between muscovite and biotite after the first day of aging (Fig. 2.1-4a). Differences are more significant after samples have been aged for about three weeks (Fig. 2.1-4b). In most cases, the contact angles measured on biotite were somewhat higher than those on muscovite.

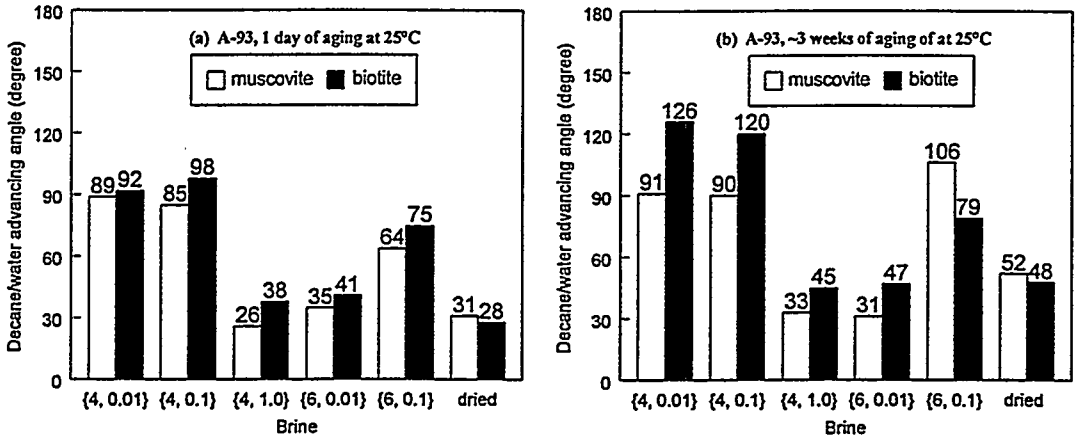

Figure 2.1-4. Muscovite vs. biotite.

2.1.4.4 Effect of roughness

The effect of roughness was tested by selecting two sets of samples, specimens that appeared smooth and those that were obviously rough. As shown in **Fig 2.1-5** for biotite, there were no systematic differences discernible in the contact angles on oil-treated surfaces that could be attributed to this macroscopic-scale roughness.

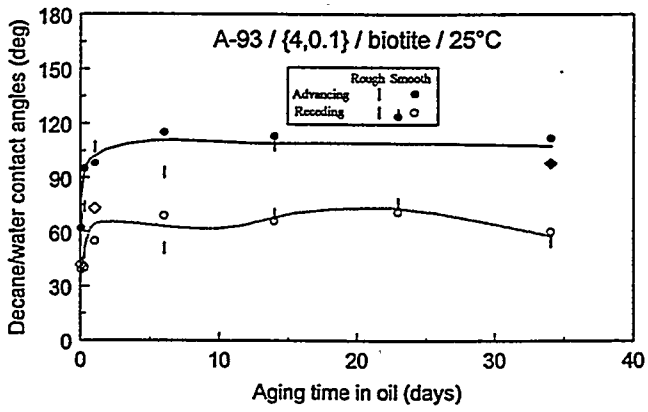

Figure 2.1-5. Comparison of macroscopically rough and smooth biotite samples.

2.1.4.5 Acid/base interactions with A-93, a high base number oil

An oil with a high base number and low acid number should have ample positively charged interfacial sites to enable fairly strong interactions between oil components and the negatively charged mica surface, especially when pH is low. Unstable conditions permit contact of oil with surface and alteration of wettability by adsorption of positively charged crude oil components. As shown in **Fig. 2.1-6**, only the lowest pH and lowest ionic strength brine tested consistently produced contact angles above 90° (Fig. 2.1-6a). At the other extreme are the higher ionic strength brines ([NaCl] = 1*M*), all of which gave low water-advancing angles of about 40° or less (Fig. 2.1-6c). The pH 8 brine with [NaCl] = 0.1 *M* is also in this category. All the other brine compositions tested gave intermediate results that changed with aging temperature (Fig. 2.1-6b). The results in Fig. 2.1-6 lead to a somewhat revised picture of the water-film stability map, as shown in **Fig. 2.1-7**.

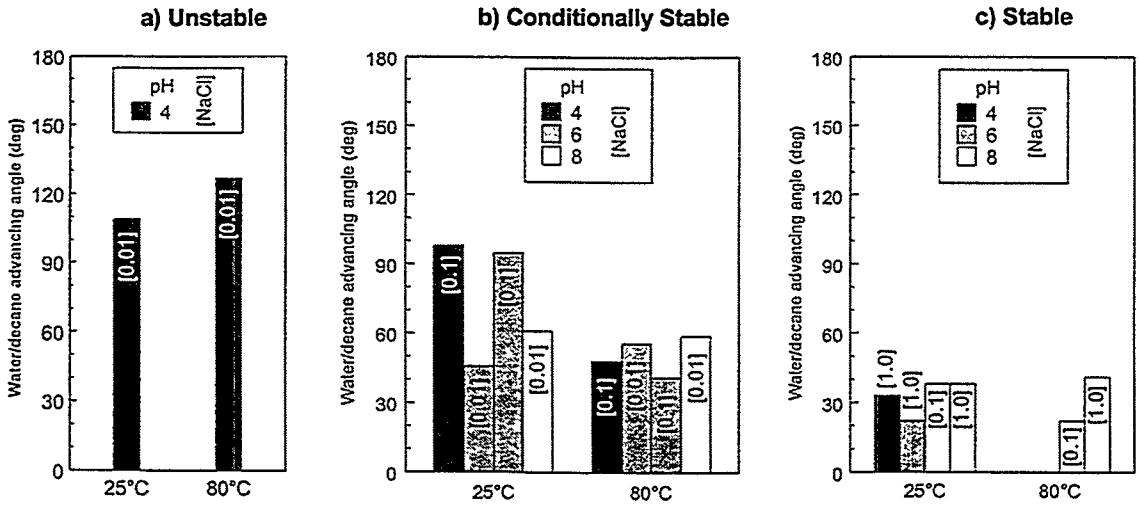

Figure 2.1-6. Alteration of wettability of muscovite aged in brine and A-93 crude oil.

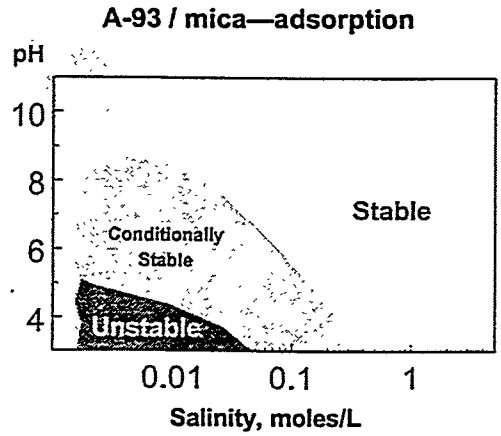

Figure 2.1-7. Water film stability map based on contact angles measured on mica surfaces aged in crude oil.

Comparisons of oil/brine/solid interactions on mica and glass have been reported previously by Basu and Sharma (1997). Using a method proposed by Ducker *et al.* (1994), they have applied atomic forces microscopy (AFM) to the measurement of force/distance relationships for water films between solid and oil. Their crude oil results are comparable to the observations based on adhesion and contact angle measurements. Water-film instability was greater for glass than for mica. They attributed the difference primarily to asperities on the order or 20 to 30 nm on their glass surfaces.

The effect of temperature on interactions between oil, brine, and solid has yet to be clearly explained. Increasing temperature can release an adhering drop of oil. On the other hand, higher contact angles have been reported on glass surfaces aged at 80°C than on similarly treated surfaces aged in oil at room temperature (Liu and Buckley, 1998; Xie *et al.*, 1997). In cores, a similar dilemma exists. Berea sandstone cores aged in oil at elevated temperature often appear to be less water-wet than those aged in the same oil at room conditions (Jadhunandan and Morrow, 1991), but high temperature imbibition experiments produce more water-wet estimates of wetting than in similar cores tested at room temperature (Tang and Morrow, 1997). Factors that must be considered include asphaltene aggregation, rates of adsorption and desorption, and solubility of water in oil, all of which may vary with temperature.

One further factor is suggested by the observation that contact angles on mica can be lower at elevated aging temperature than at room temperature. This is the result that might be expected from the adhesion tests, especially for conditionally stable brine compositions. It is also consistent with more water-wet conditions in cores at high temperatures.

Why then are the opposite results observed on glass? The relative solubility of the two surfaces may provide some clues. Brady and House (1996) show solubility of crystalline quartz, SiO_2 glass, and muscovite at several temperatures in brines of varying pH. Approximate values at about pH 6 are summarized in **Table 2.1-3.** The rate for muscovite is cited at a higher temperature than that for the other materials. Nevertheless, it dissolves at a slower rate, especially near neutral pH. The soft glass of microscope slides probably dissolves at an even higher rate than SiO_2 glass cited here. Thus the contrast between dissolution rates of soft glass and muscovite at the temperatures used in this study is probably at least three orders of magnitude. It is possible that long aging times at elevated temperatures are causing corrosion of the glass surface, enhancing the effect of crude oil/solid interactions with glass.

Table 2.1-3. Dissolution rates of mica, quartz, and SiO_2 glass at pH 6 (from Brady and House, 1996).

Material	T°C	Rate of dissolution (mol cm^{-2} s^{-1})
SiO_2 glass	65	1×10^{-14}
Quartz	25	6×10^{-17}
Quartz	60	5×10^{-16}
Muscovite	70	3×10^{-17}

2.1.4.6 Ion-binding interactions with Moutray, a high acid number oil

An oil with high acid number and low base number can—in the presence of divalent cations—alter wetting of a negatively charged surface by an ion-binding mechanism. These interactions often seem to require longer aging times and cannot be predicted from the results of two-minute adhesion tests. Moutray crude oil has a high acid number and low base number; it should be a better candidate for ion binding with mica treated mica surfaces than A-93. The contact angle results shown in **Fig. 2.1-8** are consistent with this interpretation since, after aging in oil for about two weeks at 80°C, water-advancing angles on the Moutray-treated surfaces are much higher than those treated with varying concentrations of $CaCl_2$ brine and A-93 crude oil.

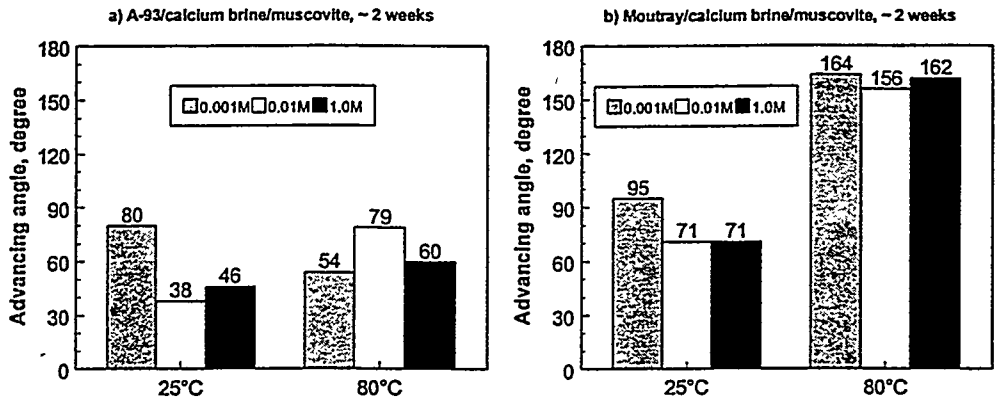

Figure 2.1-8. Alteration of wettability of muscovite aged in calcium brines and crude oils.

2.1.5 Summary

- Muscovite mica, whose surface structure is analogous to illite clay, is a good choice for standard tests of crude oil/brine/solid interactions with negatively charged reservoir minerals. It has the advantages of being widely studied, molecularly smooth, and very reproducible.

- The wetting of mica surfaces can be altered by exposure to crude oils. Two oils, A-93 from Prudhoe Bay and Moutray from West Texas, have been tested to compare their wettability altering capabilities, previously studied on glass surfaces, with similar conditions and mica surfaces.

- In the absence of water, intermediately-wet conditions result from exposure of mica surfaces to either A-93 or Moutray.

- With NaCl brines, acid/base interactions influence water-film stability. Film stability on mica is similar to that demonstrated previously on glass.

- Ion-binding interactions with an acidic oil (Moutray) can produce fairly oil-wet surfaces.

- There are small differences in interactions with muscovite and biotite mica surfaces. Macroscopic surface roughness is not detected by contact angle measurements on oil-treated surfaces.

- Changes in dissolution rates with pH and temperature for different substrate materials may have an impact on wettability alteration.

2.2 Alteration of Wetting in Square Glass Tubes

2.2.1 Introduction

Mixed wetting is increasingly accepted as a probable condition of oil reservoir rocks (Morrow, 1990; Cuiec, 1991; Buckley, 1996). Although most clean mineral surfaces are strongly water-wet, components from the crude oil can adsorb and alter wetting. Mixed wetting can occur if pore-lining minerals differ in their surface energetics or if fluid distribution affects patterns of adsorption. The latter case, first suggested by Salathiel (1973), can lead to bicontinuous oil-wet and water-wet paths through a rock. To characterize rocks with respect to their wetting condition, the amount of water (or oil) that will spontaneously imbibe and the rate of imbibition are often observed (Amott, 1959; Denekas *et al.*, 1959; Anderson, 1986; Morrow and McCaffery, 1978; Morrow *et al.*, 1994), but many questions remain regarding interpretation of the results of imbibition tests, especially for mixed-wet conditions.

Alteration of the wetting of high-energy surfaces exposed to brine and crude oil has been studied on smooth, flat surfaces (Anderson, 1986; Buckley, 1996), but relating contact angles to imbibition presents significant problems (Buckley *et al.*, 1996; Xie *et al.*, 1997). Capillary tubes of noncircular cross section provide a simple pore geometry for studies of mixed-wet conditions. For glass tubes, contact angles measured on flat glass surfaces can be used as a guide to the wetting alteration that should occur when tubes are exposed to brine and crude oils.

The purpose of this study is to assess the feasibility of generating mixed-wet conditions using brines and crude oils and of quantifying the results of wetting alteration in square glass tubes of capillary dimensions. This is a preliminary study in which a variety of procedures and measurements were examined including capillary rise of water against air and the rate, extent, and mechanisms of water imbibing into horizontal tubes containing oil.

2.2.1.1 Water film stability

To create a range of wetting conditions, A-93 crude oil from Prudhoe Bay was used with brines of varying pH and NaCl concentration. Interactions between these fluids and glass surfaces have been studied extensively (Liu and Buckley, 1997; Basu and Sharma, 1996; Xie, 1996).

Adhesion of crude oil to a solid surface is related to wettability alteration. Lack of adhesion may signify the presence of a water film, stabilized by double-layer repulsion between the crude oil and the solid surface. These forces are influenced by brine concentration and composition (Buckley *et al.*, 1989; Buckley and Morrow, 1990). In the absence of brine, polar interactions between oil components and solid can produce neutrally-wet surfaces. Other modes of interaction between oil and solid have been identified (Buckley *et al.*, 1997a). Because of the conditions selected for this study, the primarily interactions are likely to be (1) polar mechanisms that control interactions in the absence of water and (2) acid/base mechanisms that dominate when water is present, but lacks any divalent or multivalent ions.

Depending on the nature of the crude oil, different regimes of film stability are observed on a given solid surface. When water films are unstable, crude oil can contact the glass surface and adhesion and/or adsorption can occur. If the brine gives rise to stable water films, crude oil cannot contact the glass surface and adhesion does not occur. Between these two extremes is a region of brine compositions for which the films are conditionally stable. Whether or not the film breaks and crude oil contacts the surface can vary with experiment conditions. Stability regions for the A-93 crude oil used in this study were shown in the introduction in Fig. 1.

2.2.1.2 Menisci in noncircular capillary tubes

Noncircular capillary tubes have been the subject of many studies (*e.g.*, Lenormand *et al.*, 1983; Kovscek *et al.*, 1993). A meniscus in an angular tube can merge into liquid wedges in the corners. The MS-P method—so named by Mason and Morrow (1984) after the work of Mayer and Stowe (1965) and Princen (1969)—allows calculation of the shapes of wedging menisci.

Capillary systems can be divided into two groups. Nonwedging systems are those which have only a main terminal meniscus (MTM), bounded entirely by the solid perimeter, while wedging systems are those in which one or more arc menisci (AM) are formed and the MTM is bounded partly by solid and partly by liquid where it merges into the AMs (see **Fig. 2.2-1**).

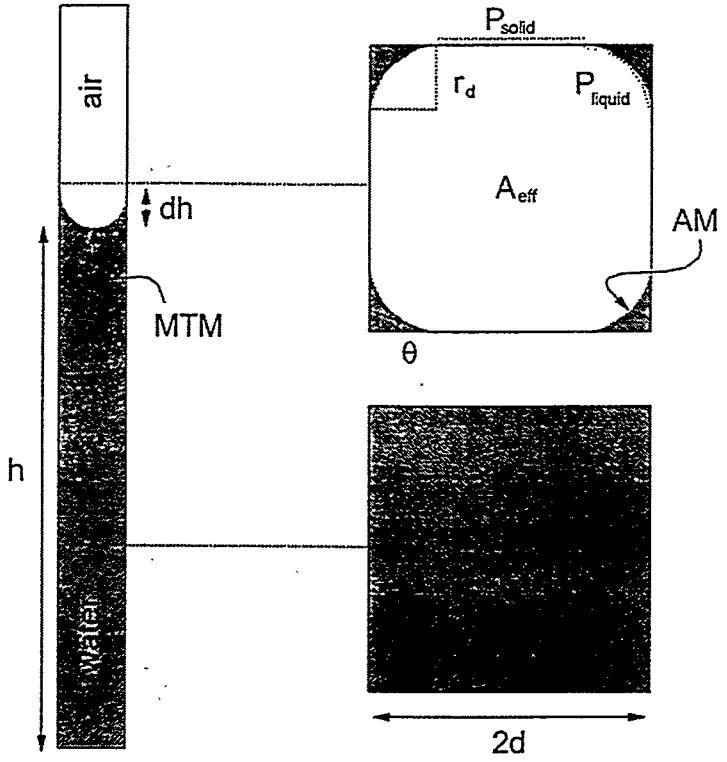

Figure 2.2-1. Main terminal meniscus (MTM), arc menisci (AM), radius of the AMs (r_d), contact angle (θ), effective area (A_{eff}), portions of liquid perimeter (P_{liquid}), and solid perimeter (P_{solid}) are illustrated for water rising against air in a square capillary.

At equilibrium, in the absence of gravitational forces, the curvature of the AMs must equal that of the MTM even though the shape of the MTM may be very complex. The simple geometry of the AM, with one radius of curvature equal to infinity, lends itself to analysis. The first experimental verification of the method was published by Mason *et al.* (1983). Since then, the method has been applied to a variety of pore geometries and wetting conditions (some examples include Mason and Morrow, 1984 and 1991; Walsh, 1989; and Ma *et al.*, 1996).

For a nonwedging system, the curvature of the main terminal meniscus equals the inverse of the hydraulic radius of the capillary. For a wedging system, the MS-P analysis can be applied to calculate curvatures. Consider the geometry defined in Fig. 2.2-1. The effective area of the cross-section shown above the MTM is not simply the cross-sectional area of the tube because the AMs occupy the corners, reducing the area available to the nonwetting phase. The presence of arc menisci also makes it necessary to consider the effective perimeter, P_{eff}, in parts: the solid

perimeter, ΣP_{solid}, is all the perimeter that is not contacted by the liquid wedges and the liquid perimeter, ΣP_{liquid}, is the sum of the arc lengths.

As the works cited above explain in detail, the MS-P equation can be derived from an energy balance approach, considering a small displacement, dh, of the MTM as shown in Fig. 2.2-1. The virtual work balance gives:

$$p_c A_{eff} dh = (\sigma_{SV} - \sigma_{SL}) \Sigma P_{solid} dh + \sigma_{LV} \Sigma P_{liquid} dh \tag{2.2-1}$$

Incorporation of Young's equation leads to the expression:

$$p_c A_{eff} = \sigma_{LV} \Sigma P_{solid} \cos\theta + \sigma_{LV} \Sigma P_{liquid} \tag{2.2-2}$$

The capillary pressure, p_c, across a point in an interface is given by the Young-Laplace equation:

$$p_C = \sigma \cdot C \tag{2.2-3}$$

Inserting this into Eq. 2.2-2 gives the following expression for the curvature:

$$C = \frac{\Sigma P_{solid} \cos\theta + \Sigma P_{liquid}}{A_{eff}} \tag{2.2-4}$$

If P_{eff} is defined as

$$P_{eff} = \Sigma P_{solid} \cos\theta + \Sigma P_{liquid} \tag{2.2-5}$$

Eq. 2.2-3 can be expressed as:

$$C = \frac{P_{eff}}{A_{eff}} \tag{2.2-6}$$

In a mathematical sense, the wedge will be infinitely long under constant curvature conditions. Thus, the arc menisci have radii of curvature of ∞ in the axial direction and r_d in the plane of cross-section, and thus:

$$C = \frac{1}{r_d} = \frac{P_{eff}}{A_{eff}} \tag{2.2-7}$$

A dimensionless expression for the curvature results if both sides of Eq. 2.2-7 are multiplied by some arbitrary characteristic tube dimension. For a square capillary the characteristic dimension is chosen to be half the width of the tube, d.

$$C_n = \frac{d}{r_d} = \frac{dP_{eff}}{A_{eff}} \tag{2.2-8}$$

Eq. 2.2-7 and 2.2-8 are both statements of the MS-P equation.

For the simple geometry of the $1mm^2$ tube under strongly water-wet conditions, the drainage radius r_d is 0.265 mm. The arc menisci held in the corners occupy 0.06 mm^2 or 6% of the cross-sectional area.

2.2.1.2a Square tube with nonzero contact angle and uniform wetting

Mason and Morrow (1984) applied MS-P theory to an n-sided tube with variable wetting. Appropriate expressions for A_{eff} and P_{eff} can be found from geometrical considerations. Substituting these into Eq. 2.2-8, with θ in radians, gives the following quadratic equation for (r_d/d):

$$\frac{1}{2}\left[\cos^2\theta - \cos\theta\,\sin\theta - \left(\frac{\pi}{4} - \theta\right)\right]\left(\frac{r_d}{d}\right)^2 - \cos\theta\left(\frac{r_d}{d}\right) + \frac{1}{2} = 0 \tag{2.2-9}$$

Solving this equation for (r_d/d) gives two roots, only one of which is physically meaningful. When the $(r_d/d)^2$ coefficient becomes zero, which happens when $\theta = 45°$, there are no real roots. This represents the point where the wedge menisci disappear, so the condition for

wedge menisci to occur in a square capillary is $\theta < 45°$. If the contact angle is less than 45° we have a wedging system, and the solution to the MS-P equation is:

$$C_n = \frac{d}{r_d} = \cos\theta + \sqrt{\frac{1}{2}\left[\sin 2\theta + \frac{\pi}{2} - 2\theta\right]} \qquad (2.2\text{-}10)$$

For contact angles in the interval $90° > \theta \geq 45°$, wedge menisci do not exist, and the curvature of the meniscus is equal to the curvature of a meniscus in a cylindrical capillary with radius d. If this curvature is converted to a dimensionless number, by multiplying by the characteristic dimension of the tube, the equation for meniscus curvature is:

$$C_n = \frac{d}{r_d} = 2\cos\theta \qquad (2.2\text{-}11)$$

2.2.1.2b Mixed-wet square tubes

The advantage of using noncircular tubes in this study is the opportunity they provide to produce and observe the effects of mixed-wet conditions. Adsorption of crude oil components is limited by the existence of water wedges; thus, after treatments with brine and crude oil, the corners remain more water-wet, while exposed portions of the glass surface may have high water-advancing contact angles.

The MS-P theory has been tested for mixed-wet conditions produced by using different materials to form different sides of pores (Walsh, 1989). Here an alteration of part of each pore wall to a less water-wet condition is envisioned, as illustrated in **Fig. 2.2-2.**

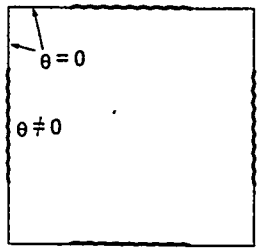

Figure 2.2-2. Square tube after exposure to brine and crude oil.

Curvatures calculated as a function of contact angle on the exposed surfaces in both uniform and mixed-wet tubes are shown in **Fig. 2.2-3.** For uniform wetting, curvatures were calculated using Eq. 2.2-10 for wedging systems and Eq. 11 for nonwedging systems. For the mixed-wet tubes, values are taken from the calculations of imbibition curvatures with hysteresis of Ma *et al.* (1996). Note that positive curvatures and spontaneous imbibition persist to contact angles greater than 90° for mixed-wet tubes.

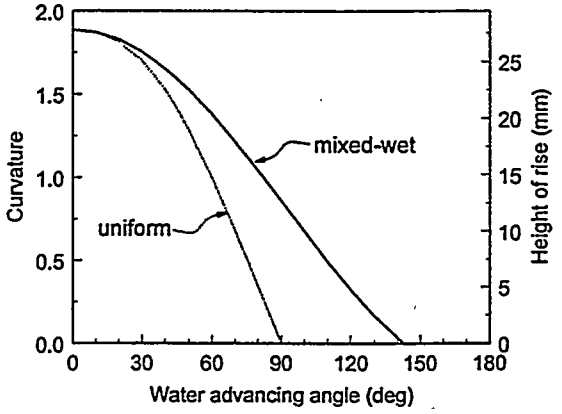

Figure 2.2-3. MS-P curvatures calculated for uniform and mixed-wet square capillaries.

2.2.1.3 Capillary rise

Capillary rise is a commonly used measure of wettability (Anderson, 1986). Most of the previous studies of capillary rise and flow in capillaries have been conducted using cylindrical tubes. Noncircular capillaries can also be used with the MS-P method to relate height to curvature.

The change in capillary pressure with height above a free liquid surface is given by:

$$\Delta p_c = \Delta \rho g h \tag{2.2-12}$$

Considering rise of liquid in a capillary above a datum level, Eq. 2.2-12 can be combined with the Young-Laplace equation (Eq. 2.2-3), and multiplied by d, to give:

$$C_n = d\left(\frac{1}{r_1}+\frac{1}{r_2}\right) = d\left(\frac{gh\Delta\rho}{\sigma}\right) \tag{2.2-13}$$

where r_1 and r_2 are radii of curvature of the main terminal meniscus. Using Eq. 2.2-13, the curvature of the MTM can be calculated from capillary rise experiments if the density difference and the interfacial tension between the fluids are known.

In a capillary rise experiment, the curvature varies with the height of rise due to the influence of gravity, so the constant curvature condition is not strictly met. However, if the capillary forces are much greater than the gravitational forces, MS-P theory can still be applied. In a simple capillary rise experiment, the capillary forces will be governed by the relationship between the height of rise and the dimensions of the tube, and by wettability. For strongly wetting conditions, gravitational forces will be negligible if the height of rise is much larger than the characteristic dimensions of the tube (i.e. h/d>>1). However, Mason *et al.* (1983) demonstrated that the method provides a good approximation even outside this range. For other wetting conditions such a criterion is more difficult to establish.

2.2.1.4 Spontaneous imbibition

The rate and amount of spontaneous imbibition are the basis of many commonly used measures of the wettability of core samples. The core is said to be strongly water-wet if large volumes of brine are rapidly imbibed, while lower rates and smaller volumes usually imply a more weakly water-wet core. If no water is imbibed the core is either oil-wet or neutrally wet (Anderson, 1996). Between these extremes are many wetting conditions of practical interest that might well be discerned from imbibition rate and extent, if we understood better how to interpret the data. While square quartz capillaries are not representative of many of the complexities of natural porous media, they have two important advantages as models in which to study imbibition. One is transparency, which allows us to see what is happening during imbibition, and the other is the existence of corners in which water can form wedges.

The rate of imbibition of a wetting fluid displacing air was given for cylindrical tubes by Washburn (1921). Flow of a wetting fluid in noncircular tubes was investigated by Ransohoff and Radke (1988). A dimensionless resistance factor was introduced to account for corner geometry and roundedness. Dong (1995) calculated and measured the rate of imbibition into square tubes,

for both zero and nonzero contact angles in uniformly-wetted tubes. The effects on imbibition rate of a viscous nonwetting phase and of mixed-wet surface conditions remain to be investigated.

A dimensionless number, referred to as the spontaneous imbibition index (SI) is introduced. This number is defined as the ratio of the amount of oil produced by spontaneous imbibition in a given test to the amount of oil produced in the analogous strongly water-wet case. In most cases the SI index was not greatly different from the displacement efficiency, since the strongly water-wet tests were very efficient in these straight tubes.

2.2.2 Experimental materials and procedures

2.2.2.1 Materials

2.2.2.1a Fluids

Brines used for aging of the capillaries prior to treatment with A-93 crude oil were prepared according to the method described by Liu (1993). Brines ranged in pH from 4 to 8 and in ionic strength from 0.01 to 1 *M*. In this report, brine compositions are labeled using the shorthand notation {pH, I}. Properties of A-93 crude oil are summarized in **Tables 2.2-1** and **2.2-2.**

Table 2.2-1. Chemical and physical properties of the A-93 crude oil.

Source	ρ at 25°C g/cm^3	μ at 25°C cP	Asphaltenes (wt%) precipitated by: n-C_5	n-C_6	n-C_7
Prudhoe Bay	0.8945	26.7	11	7	4

Table 2.2-2. Gravity, acid and base numbers for the A-93 crude oil.

°API	Acid number (mg KOH/g oil)[a]	Base number (mg KOH/g oil)b
25.5	0.14 ± 0.04	2.42 ± 0.33

[a]ASTM D664-89; [b]ASTM D2896-88

A 3 vol % solution of red food color in distilled water was the aqueous phase in the capillary rise experiments. The physical and interfacial properties of the dyed water are given in **Tables 2.2-3** and **2.2-4.**

Table 2.2-3. Viscosities and densities for the dyed water/decane system.

Chemical	ρ g/cm^3	μ cP
distilled water	0.9982[c]	1.002[c]
dyed, distilled water	0.9989d	
{8,0.01} brine		0.94 ± 0.06
{8,1} brine		0.99 ± 0.06
decane	0.7300[c]	0.92[c]
dyed decane		0.92 ± 0.05

[c]CRC Handbook of Chemistry and Physics, 1st Student ed., 1988 (at 20°C); [d]measured at 20°C

Table 2.2-4. Interfacial tensions.

Phases	IFT at 20°C mN/m
distilled water / air	74.0±0.4
dyed, distilled water/air	72.3±0.2
dyed decane / {8,0.01} brine	27.4
dyed decane / {8,1} brine	28.9
A-93 / {8,0.01} brine	26.5
A-93 / {8,1} brine	25.5

In water-oil experiments, an oil dye, Oil Red O from Sigma, was used to enhance the visibility of the decane phase. Excess dye was equilibrated with decane and the mixture was centrifuged to remove undissolved dye particles. Interfacial tensions and viscosities are given in Tables 2.2-3 and 2.2-4. Contact angles between {8,0.01} and {8,1} brines and dyed decane are in **Table 2.2-5.**

Table 2.2-5. Contact angles.

Phases	θ_A (deg)	θ_R (deg)
{8,0.01} / dyed decane	22.1 ± 1.9	20.0 ± 1.25
{8,1} / dyed decane	20.1 ± 1.8	18.7 ± 0.8

2.2.2.1b Glass capillaries

The capillaries used in these experiments were obtained from Wilmad glass. The 10 cm long square capillaries had a nominal inner dimension of 1 mm^2 (V=0.1mL). The inner dimensions of the square capillaries were measured to be 0.98±0.02 mm^2. Details of these measurements are given in **Table 2.2-6.** The 10 cm long rectangular tubes had nominal inner dimensions of 1 mm by 10 mm (V=1mL).

Table 2.2-6. Measurement of the tube inner dimensions

Test number	Length of tube (mm)	Volume of water contained (mL)	Estimated side length (mm)
1	99.5	0.1017	1.01
2	100.0	0.0922	0.96
3	110.0	0.1006	0.99
4	100.0	0.0947	0.97
5	110	0.0963	0.98
	Average		0.98 ± 0.02

Prior to use, the capillaries were cleaned in an ultrasonic bath for at least 15 minutes in a solution composed of 9 parts hydrogen peroxide (30%) and 1 part ammonium hydroxide (20%). After cleaning, they were rinsed with copious amounts of distilled water and dried.

2.2.2.2 Exposure of capillaries to brine and oil

Aging in either brine or A-93 crude oil was accomplished by submerging the completely filled capillaries in a closed container of brine or crude oil. Tubes were oriented vertically during aging periods. Two different treatment sequences were tested:

- Some tubes were completely filled with oil with no initial water saturation (S_{wia}=0, where S_{wia} is the initial water saturation during aging in oil).

- Others were aged in brine for 24 hours, drained to an S_{wi} of approximately 6%, then filled with oil ($S_{wia} \neq 0$).

For tests of capillary rise (water vs. air), tubes were washed, first with toluene, then with decane, to remove the crude oil. Finally, the tubes were dried. To test drainage, dried tubes were refilled with water.

Some of the spontaneous imbibition (water vs. oil) tests started with similarly washed and dried capillaries, after they had been refilled with oil. Imbibition thus began with no initial water saturation ($S_{wii}=0$, where S_{wii} denotes the initial water saturation at the start of imbibition). Other brine-treated tubes were drained, filled with crude oil, allowed to age in oil for a period of time t_a, then submerged directly in the imbibing brine, without the rinsing and refilling steps. The water saturation at the start of these imbibition tests was not zero, but the value to which the tubes were drained before aging in oil ($S_{wii}=S_{wia} \neq 0$).

2.2.2.3 Capillary rise

The height of capillary rise was measured from the datum level to the bottom of the air/water meniscus (as shown in **Fig. 2.2-4**) using a ruler with 1 mm graduations. The accuracy of the measurement is ± 0.5 mm. The volume of the tubes, and of the water that rose during these experiments, was small compared to the total volume in the beaker, so no change in the datum level was observed during the experiments. More exacting experimental procedures (as described by Walsh, 1989) would be required for completely quantitative results. Several of the experiments were repeated to check reproducibility. For unexposed tubes, 10 measurements of capillary rise were performed. From these a mean value of 26±3 mm was calculated for the height of rise. Results are given in **Table 2.2-7**. Reproducibility is better in the square capillaries than in rectangular ones. The spontaneous influx of water began rapidly, but declined after approximately 30 seconds. Constant height of the water column was usually reached after 30-60 minutes. The height of the column was measured for as long as 24 hours, but no changes in height were observed after 1 hour.

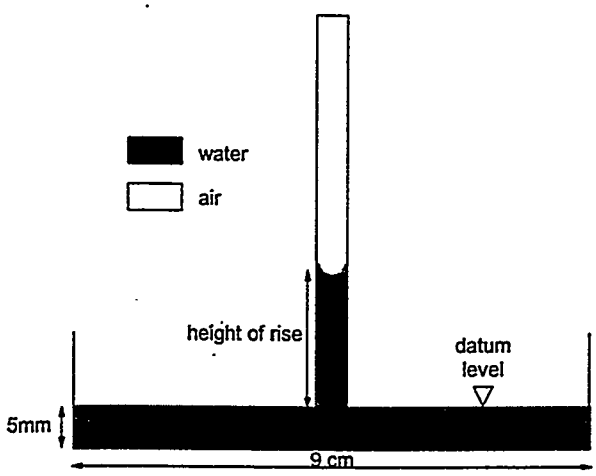

Figure 2.2-4. Schematic of the experimental setup for measuring capillary rise.

Table 2.2-7. Results for unexposed square capillaries.

Experiment #	Capillary rise (mm)
1	25.0
2	28.0
3	24.5
4	24.0
5	24.0
6	31.0
7	26.0
8	28.5
9	21.0
10	23.0
average	25.5 ± 2.9

2.2.2.4 Spontaneous imbibition

A syringe was used to fill treated capillaries with oil (either dyed decane or crude oil). Capillaries were secured in a holder—a small block of stainless steel into which a groove the size of the outer dimensions of the capillary tube was cut. Over the capillary, a piece of plexiglass was held in place with two screws. The whole assembly was submerged horizontally in the invading brine. The weight of the stainless steel block kept the tube submerged and horizontal. A piece of heat-shrinkable Teflon tubing was used to connect the capillary to the syringe. The connection to the syringe was cut at the start of the imbibition experiment, leaving a piece of heat-shrinkable

tubing around one end of the capillary. This end of the capillary was preferentially oil-wet, and water imbibed only from the other end, as illustrated in **Fig. 2.2-5.**

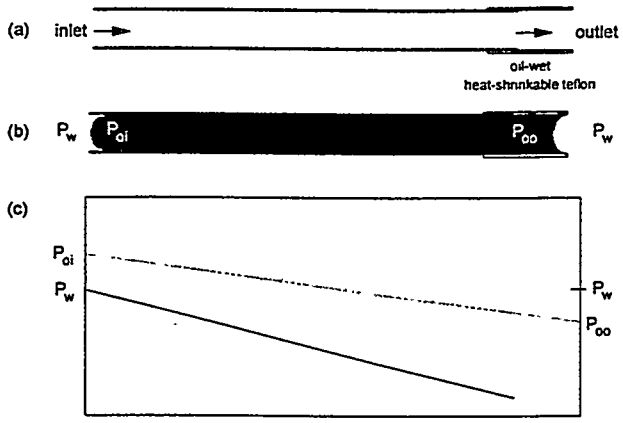

Figure 2.2-5. Inlet and outlet conditions for imbibition into glass capillary plus teflon.

Imbibition was monitored using a microscope and a video camera. Lengths of brine-invaded regions and lengths of oil droplets were measured with a scale in the microscope eyepiece lens. Altering the microscope focus produced a three-dimensional view of the tube and the fluids within it. It was therefore possible, to some extent, to see where remaining oil was situated (oil films on the walls, oil blobs extending from one wall of the capillary to the other, oil blobs sticking to one of the walls but not to the other, etc.), and thus to estimate the volume of oil produced. The estimated volume of oil produced is reported as a percentage of original oil in place (%OOIP). All procedures in the aging sequences and imbibition tests were conducted at ambient temperature.

2.2.3 Air/water capillary rise experiments

2.2.3.1 Observations

2.2.3.1a Imbibition into clean tubes

The highest rise observed was for water in clean capillary tubes. Water rose to an average height of 25.5 mm (see Table 2.2-7), corresponding to $C_n = 1.72 \pm 0.07$, or to $\theta_A = 28.5°$. Contact angle measurements with dyed water and air on flat glass surfaces confirm that glass is strongly wetted by water ($\theta_A = 0°$) which would give $C_n = 1.886$ in a perfectly square tube. Quantitative

application of this method will require that this difference between the expected and measured heights of rise be explained. Some possible factors include the effect of gravity, effects of temperature changes, a nonzero contact angle of dyed water in the cleaned tubes, variation in the actual dimensions of the tube, rounding of the corners, and accuracy of measured surface tension and density.

2.2.3.1b Meniscus height in brine and oil-treated square tubes

In all cases, treatment of capillaries with oil led to reduction of the meniscus height for water imbibing. The height of capillary rise decreased as the pH and salinity of the aging brine decreased and as the aging time in crude oil increased. The lowest meniscus heights were found for tubes aged in {4,0.01} brine followed by aging in A-93 crude oil. Drainage tests showed that hysteresis between θ_A and θ_R is significant. Details of these measurements are summarized in **Table 2.2-8.**

Table 2.2-8. Meniscus height, curvature, and contact angles in square capillaries. The aging period in brine was 24 hrs; t_a is the aging time in A-93 crude oil.

Brine	pH	t_a	Imbibition				Drainage			
pH/[NaCl]	measured	(hr)	h (mm)	C_n	$\theta_{uniform}$	θ_{mixed}	h (mm)	C_n	$\theta_{uniform}$	θ_{mixed}
4, 0.01	4.01	12	7.8	0.53	75	108				
4, 0.01	3.77	24	6.0	0.41	78	115	24.0	1.63	35	42
4, 0.01	4.01	48	5.0	0.34	80	119	26.0	1.76	25	29
4,0.01		528	3.0			128	24.5	1.66	32	39
4, 1	3.89	12	12.5	0.85	65	90				
4, 1	3.89	24	8.5	0.58	73	105	26	1.76	25	29
4, 1	3.82	46	6.5	0.44	77	113				
6, 0.01	6.06	12	16.0	1.08	57	78				
6, 0.01	6.06	24	7.5	0.51	75	109				
6, 0.01	6.06	24	7.5	0.51	75	109				
6, 0.01	6.06	46	7.5	0.51	75	109	27	1.83	18	19
6, 1	5.55	12	13.0	0.91	63	87				
6, 1	5.55	24	13.5	0.91	63	87				
6, 1	6.90	24	12.5	0.85	65	90				
6, 1	5.55	46	8.5	1.08	57	78				
8, 0.01	8.40	12	16.0	1.08	57	78				
8, 0.01	8.40	24	15.0	1.02	60	81				
8, 0.01	8.40	48	12.5	0.85	65	90				
8, 1	8.14	12	15.0	1.02	60	81				
8, 1	8.14	24	12.5	0.85	65	90				
8, 1	8.14	48	12.0	0.81	66	93				

Figure 2.2-6 shows the influence of aging time for all six brines. The effect of pH is shown in **Fig. 2.2-7** for tubes aged in crude oil for 48 hours.

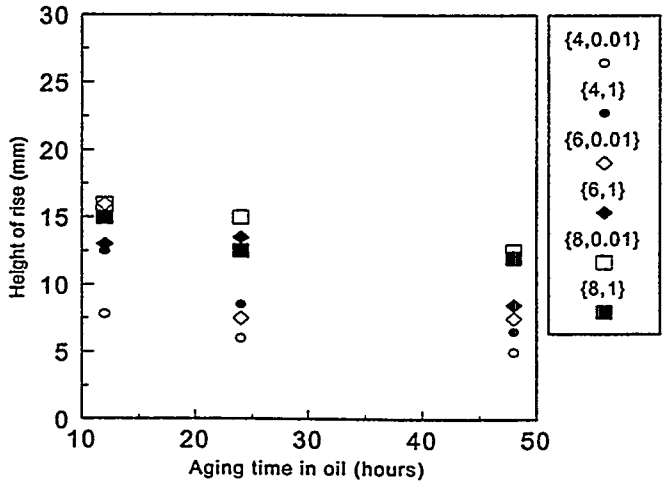

Figure 2.2-6. Meniscus height in square tubes aged in different brines as a function of aging time in crude oil.

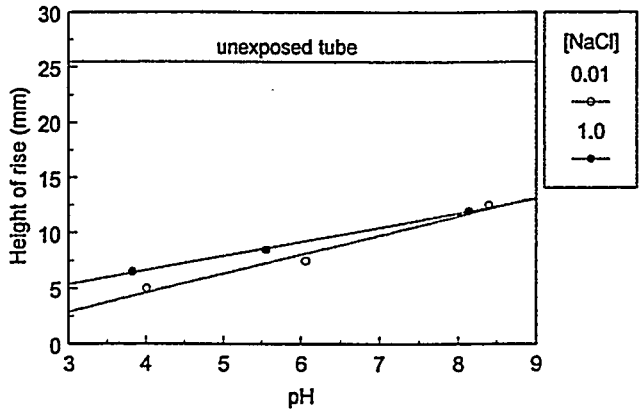

Figure 2.2-7. Capillary rise as a function of pH for tubes aged for 48 hours in A-93 crude oil.

According to Eq. 2.2-10, a uniformly wetted system is wedging only if the normalized meniscus curvature C_n, calculated from capillary rise experiments, is less than 1.414. In many cases, however, wedges could be seen above menisci with lower curvature, indicating that mixed wetting existed. The contact angles ($\theta_{uniform}$) calculated from Eq. 2.2-11 and those estimated from the hysteresis analysis of Ma *et al.* (1996) (θ_{mixed}) are included in Table 2.2-8, giving a lower and upper limit on estimates of both imbibition (water advancing) and drainage (water receding) angles.

Additional evidence for mixed wetting was obtained by rotating the tubes 90° from vertical to horizontal orientation and observing the rearrangement of water and air in the absence of gravity. Depending on wetting, results ranged from very little rearrangement to water advancing in the corners over the full tube length. Details of these observations are summarized in **Table 2.2-9**. The extent of water wedge formation in the pH 6- and 8-treated tubes indicates that the corners have remained water-wet.

Table 2.2-9. Observations of fluid rearrangement in square capillaries turned from vertical to horizontal orientation after measurements of the height of rise.

Brine {pH,[NaCl]}	Oil aging time (hrs)	Water and air rearrange?	Furthest extent of water into corners (mm)	Observation time	Other observations
{4,0.01}	48	y	9	< 1 hr	
{6,1}	12	y	80	>4.5 hrs	Wedges were visible before tube was turned. Wedges extended rapidly after turning the tube. Experiment terminated because water was evaporating.
{6,1}	24	y	80	1-2 hrs	Isolated water droplets form in corners when tube is turned. Droplets are reconnected by advancing water wedges.
{6,1}	48	y			Water wedge in one corner only.
{8,0.01}	12	y	100	< 5 min	Wedges are not of uniform thickness, develop very rapidly, and can break up.
{8,0.01}	24	y			Like {8,0.01} aged for 12 hrs.
{8,0.01}	48	y	100?		Wedges advance more slowly than in the other two {8,0.01} cases. Water reaches the outlet, but continuity is not always clearly observed.
{8,1}	12	y	100	1 - 2 min	Continuous films that vary in color depending on thickness.
{8,1}	24	y			Like {8,1} aged for 12 hrs.
{8,1}	48	y			Like {8,1} aged for 12 or 24 hrs.

2.2.3.1c Capillary rise in brine and oil-treated rectangular tubes

Detailed results from the measurements of capillary rise in rectangular tubes are given in **Table 2.2-10**. Interpretation of the results of capillary rise experiments in rectangular tubes is problematic. For each interface, a maximum value (measured near a corner) and a minimum height are reported. Higher rise near the corners may illustrate mixed wetting, but variability of the tube dimensions is probably the limiting factor in these experiments.

Table 2.2-10. Rectangular capillary results. t_a(b) is the aging period in brine and t_a(co) is the aging time in crude oil. Max = highest point of capillary rise in the corners, min = lowest point on the water meniscus

Brine	Measured pH	t_a (b)	t_a (co)	Capillary rise (mm) minimum	maximum	Repeated measurements min - max
unexposed tube				18.0	21.3	
4, 0.01	4.16	24h	12h	9.5	10.5	
4, 0.01	4.16	24h	24h	9.0	9.5	
4, 1	4.04	24h	12h	9.0	11.0	
4, 1	4.04	24h	24h	8.5	10.5	Initially deformed, but flattens out
4, 1	4.04	24h	48h	9.0	10.0	8.5 - 11.5
6, 0.01	5.99	24h	12h	7.0	7.7	8.0 - 10.0
6, 0.01	5.99	24h	24h	10.0	18.0	10.5 - 18.5
6, 0.01	6.00	46h	24h	10.0	11.3	10.0 - 18.0
6, 0.01	5.99	24h	48h	7.0	10.5	
6, 1	5.55	24h	12h	10.0	11.0	
6, 1	5.55	24h	24h	9.5	12.7	
6, 1	5.55	24h	48h	10.5	12.0	
8, 0.01	8.40	24h	12h	9.0	12.5	
8, 0.01	8.40	24h	24h	9.0	12.5	
8, 0.01	8.40	24h	48h	7.5	17.5	
8, 1	8.14	24h	12h	11.0	13.0	
8, 1	8.14	24h	24h	10.5	12.5	
8, 1	8.14	24h	48h	8.5	14.0	

2.2.3.2Discussion of capillary rise experiments

When the wettability of a glass surface is altered by exposure to crude oil in the presence of water, a nonuniform or mixed wettability state can be generated. The average water saturation of tubes after drainage and before introduction of oil was estimated by a series of measurements to be 6% ± 3%, in very good agreement with the amount predicted from a calculation of the MS-P drainage radius of perfectly wetted square tubes. Detail of these measurements are summarized in **Table 2.2-11.**

Table 2.2-11: Measurements of the S_{wi} before the tube was aged in crude oil

Test number	Measured length (mm)	Weight of water remaining (g)	S_{wi} (%)
1	100	0.0060	6.02
2	100	0.0057	5.71
3	104	0.0075	7.23
4	99	0.0043	4.36
5	110	0.0018	6.41
6	100	0.0078	7.82
7	109	0.0093	8.56
8	110	0.0021	1.91
9	100	0.0059	5.92
10	109	0.0064	5.87
11	100	0.0082	8.22
12	110	0.0058	5.29
average	104±5		6±3

Bulk water residing in the corners can maintain strongly water-wet surfaces. If the aging brine gives rise to stable water films, the flat walls of the capillary can also remain water-wet. Thus, situations ranging from protection of most of the capillary from crude oil adsorption to exposure of most of the tube can be generated by appropriate brine selection.

Contact angles resulting from crude oil treatments were more dependent on the pH and salinity of the aging brine than on the aging time in A-93 crude oil. None of the tubes became oil-wet at the aging temperature (25°C) and relatively short aging periods used in these experiments. Wettability of the originally strongly water-wet capillary was altered towards a less water-wet condition as the pH of the brine was decreased and the aging period in crude-oil increased. Capillaries pretreated with {4,0.01}, {6,0.01}, or {4,1} brines produce higher contact angles, while those pretreated with {8,0.01}, {6,1}, or {8,1} brines produce lower contact angles. Given the A-93/NaCl brine/glass stability diagram (Fig. 1), the observed trends are reasonable since {4,0.01} and {6,0.01} brines give rise to unstable water films, {4,1}, {8,0.01} and {6,1} brines form conditionally stable films and {8,1} brines produce stable films.

Mixed wetting has been demonstrated by the existence of wedges even when the curvature is low. High hysteresis and changes in wetting with aging time are all consistent with previous contact angle observations. The extent of alteration is somewhat surprising in view of the low

temperatures used in all of these experiments. Greater differentiation between stable and unstable combinations of oil and brine might have been expected. It is likely that the procedure subsequent to oil exposure—i.e., rinsing with toluene and decane, followed by drying—does not entirely preserve strongly water-wet conditions in the corners.

2.2.4 Spontaneous imbibition of brine into oil-filled tubes

Visual observations of water displacing oil in horizontally oriented tubes were made to observe filling mechanisms, rate, and extent of the spontaneous invasion of water into capillaries containing only oil or both oil and water. Results are reported for dry tubes treated with crude oil and for capillaries that were aged first in brine (pH 4 to 8 and varying ionic strength), then in A-93 crude oil. Strongly water-wet conditions were tested using dyed decane.

2.2.4.1 Observations of filling mechanisms and rates

Two classes of interface movement were observed, piston-like motion of the MTM and snap-off by water in the AMs. These two types of movement are illustrated in **Fig. 2.2-8**. When snap-off and bypassing occurred, the remaining oil took on a variety of shapes, as illustrated in **Fig. 2.2-9**. Volumes have been estimated based on lengths, but in the more irregular cases, these volumes are necessarily somewhat subjective.

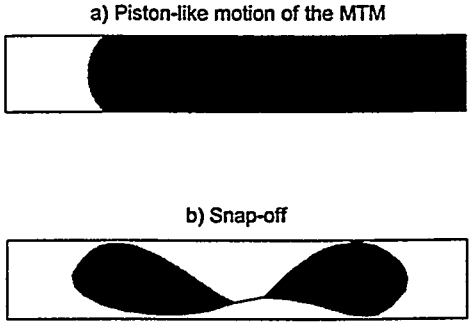

Figure 2.2-8. The two kinds of meniscus displacement observed during imbibition. a) Piston-like motion was generally observed for tubes with no initial water saturation. b) Snap-off was more commonly observed in tubes with an initial water saturation at the beginning of imbibition, and is the result of water advancing in the corners.

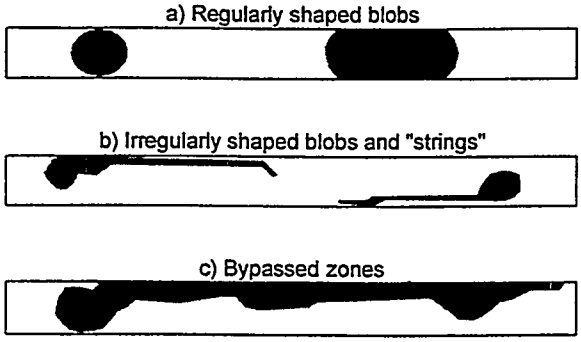

Figure 2.2-9. Different shapes of bypassed oil.

2.2.4.1a Strongly water-wet capillaries

Experiments with dyed decane as the oil phase were performed as the water-wet base cases for comparison to subsequent experiments with crude oil. The results of these experiments are summarized in **Table 2.2-12**; base case numbers are assigned for reference in later sections of this report. **Figure 2.2-10** shows oil production as a function of imbibition time for the experiments where {8,1} was the imbibing brine. Snap-off occurred in all tubes containing initial water (i.e. $S_{wii} \neq 0$) in the corners at the onset of the imbibition experiment (Fig. 2.2-10b).

Table 2.2-12. Oil produced (%OOIP) from decane-filled tubes pretreated with different brines and with different initial conditions.

Aging brine	S_{wia} (%)	S_{wii} (%)	Imbibing brine	Amount of oil produced (%OOIP)	Base case number
None	0	0	{8,0.01}	95	1
None	0	0	{8,1}	96	2
{4,1}	6	0	{8,0.01}	100	3
{8,1}	6	0	{8,0.01}	100	4
{4,1}	6	0	{8,1}	100	5
{8,0.01}	6	0	{8,1}	95	
{8,1}	6	0	{8,1}	100	6
Distilled water	6	6	{8,1}	99	
{4,1}	6	6	{8,1}	99	7
{8,0.01}	6	6	{8,1}	90	
{8,1}	6	6	{8,1}	84	8

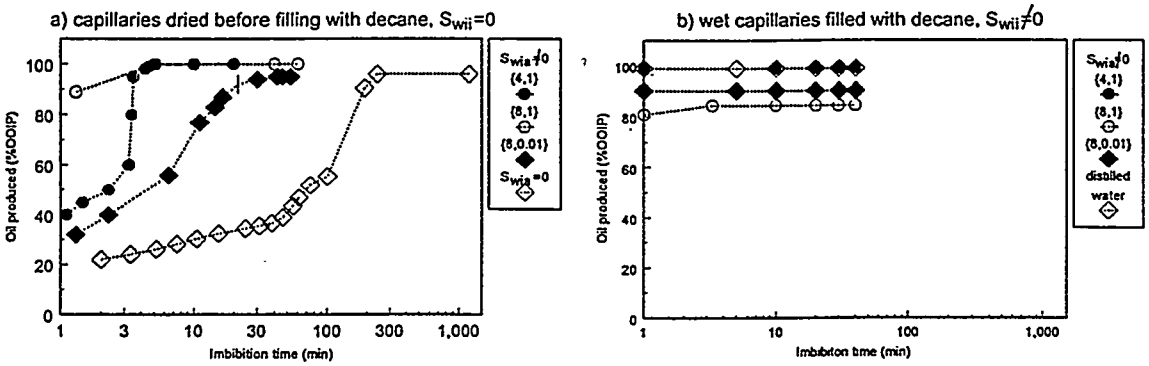

Figure 2.2-10. Decane produced as a function of imbibition time. {8,1} brine imbibing into (a) tubes dried before filling with decane (S_{wii}=0) and (b) tubes with an initial water saturation ($S_{wii}\neq 0$).

2.2.4.1b A-93 crude oil tests

In the following section, the results of treatment of square capillary tubes, either dry or wet, with crude oil are presented in terms of the rate of imbibition of two different brines. Preliminary experiments showed that almost no distilled water or pH 4 brine imbibed. However, if pH 8 brines were used, spontaneous imbibition was observed. Variables included the brine compositions used to pretreat the tubes, the aging time (t_a) in A-93 crude oil, and the presence or absence of an initial water saturation at the start of imbibition.

Initially dry capillaries (S_{wia}=0)

No aging (t_a=0): Capillary tubes were submerged in brine immediately after filling with oil; aging time in oil was therefore only a matter of minutes (nominally t_a=0). Neither distilled water nor pH 4 and 6 brines imbibed. The {8,0.01} and {8,1} brines both imbibed. Some characteristic features of the imbibition process included:

(1) piston-like motion of the MTM (see Fig. 2.2-8a),

(2) an oil/water interface that appeared to be nearly flat during the displacement, and

(3) little or no movement of water in the corners ahead of the MTM.

For the first one or two hours, the moving interface left no oil behind. However, during the later stages of the imbibition process with {8,1} brine, oil began adhering to the walls of the capillary, leaving microscopic drops and oil films which became increasingly prevalent until finally

the interface movement stopped. Results from the experiments are given in **Table 2.2-13.** In **Fig. 2.2-11** the amount of oil produced (%OOIP) is plotted as a function of time.

Table 2.2-13. Amount of oil produced by spontaneous imbibition of brine. $S_{wia}=S_{wii}=0$, $t_a=0$.

Experiment	Imbibing brine {pH, [NaCl]}	Amount of oil produced (%OOIP)	Spontaneous imbibition index (SI)
Decane-filled (base case 1)	{8,.0.01}	95±1	1
1	{8,.0.01}	18±1	
2	{8,.0.01}	24±1	0.20±0.04
3	{8,.0.01}	16±1	
Decane-filled (base case 2)	{8,1}	96±1	1
1	{8,1}	23±1	
2	{8,1}	87±1	0.6±0.4
3	{8,1}	74±1	

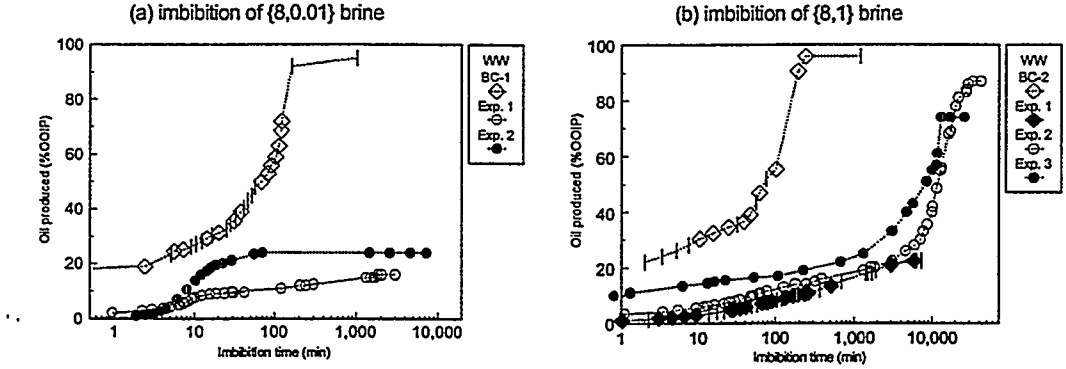

Figure 2.2-11. Crude oil produced by spontaneous imbibition of brine into capillaries with no initial water ($S_{wia}=S_{wii}=0$) or aging ($t_a=0$), plotted as a function of time for (a) {8,0.01} brine and (b) {8,1}.

Capillaries aged in crude oil ($t_a\neq0$): If capillaries were allowed to age in oil before initiation of imbibition, the amount of water imbibed was significantly lower than for the $t_a = 0$ experiments, although the patterns of imbibition were similar. The results from the experiments are given in **Table 2.2-14** and **Fig. 2.2-12.**

Table 2.2-14. Amount of oil produced by spontaneous imbibition of {8,1} brine. $S_{wia}=S_{wii}=0$, $t_a\neq0$.

Aging period in A-93 (hrs)	Imbibing brine {pH,[NaCl]}	Amount of oil produced (%OOIP)	Spontaneous imbibition index SI
Decane-filled (base case 2)	{8,1}	96±1	1
1	{8,1}	42±1	0.44±0.02
2.5	{8,1}	7±1	0.07±0.02
4	{8,1}	8±1	0.08±0.02
6	{8,1}	21±1	0.22±0.02
16	{8,1}	5±1	0.05±0.02

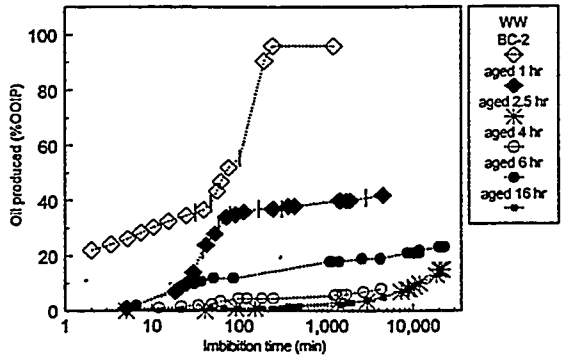

Figure 2.2-12. Oil produced by spontaneous imbibition of {8,1} brine into capillaries aged in crude oil but not in brine ($S_{wia}=S_{wii}=0$; $t_a\neq0$); plotted as a function of imbibition time.

Capillaries aged with connate water ($S_{wia}\neq0$)

Tubes cleaned and refilled with oil before imbibition ($S_{wii}=0$): Brine composition effects were investigated with tubes aged in {4,1}, {6,1}, {8,0.01}, and {8,1} brines. Little or no imbibition occurred in tubes pretreated with either {6,1} or {8,0.01} brine. However, tubes aged in either {4,1} or {8,1} brine imbibed either {8,0.01} or {8,1} brine for all aging times investigated.

In the tubes that imbibed, the interface shape initially appeared to be flat, similar to the shape of the oil/water interface during imbibition into dry tubes. Often this shape changed to a more rounded appearance after about 30 to 60 min, when water started advancing into the corners. If water imbibed uniformly into all four corners, the meniscus shape was symmetric. If not, the distortion of the interface was greatest in the corner which had the highest water

saturation. Further water movement in the corners led to snap-off (see Fig. 2.2-8b) by filling from the corners, followed by bypassing of oil. The bypassed oil either appeared as regularly shaped blobs or as irregularly shaped blobs, "strings" or "zones (see Fig. 2.2-9 and Spildo, 1997). Results from these experiments are given in **Table 2.2-15**. The general trend was towards a decrease in the amount of water imbibed as the aging period in crude oil increased. Plots showing the amount of oil produced as a function of time for tubes aged in {8,0.01} and {8,1} brine are given in **Fig. 2.2-13**.

Table 2.2-15. Amount of oil produced by spontaneous imbibition of brine. $S_{wia}\neq 0$, $S_{wii}=0$.

Aging period in A-93	Imbibing brine {pH,[NaCl]	Amount of oil produced (%OOIP)	SI index
{4,1} as the aging brine			
Decane-filled (base case 3)	{8,0.01}	100±1	1
12	{8,0.01}	39±2	0.39±0.03
48	{8,0.01}	18±2	0.18±0.03
Decane-filled (base case 5)	{8,1}	100±1	1
12	{8,1}	16±1	0.24±0.06
37	{8,1}	0	0
{8,1} as the aging brine			
Decane-filled (base case 4)	{8,0.01}	100±1	1
12	{8,0.01}	66±2	0.66±0.03
24	{8,0.01}	55±1	0.55±0.03
48	{8,0.01}	30±1	0.30±0.03
50	{8,0.01}	26±1	0.26±0.03
Decane-filled (base case 6)	{8,1}	100±1	1
12	{8,1}	80±2	0.78±0.04
12	{8,1}	75±2	
24	{8,1}	41±1	
24*	{8,1}	55±1	0.47±0.07
24*	{8,1}	46±1	
50	{8,1}	24±1	0.24±0.06

*No initial MTM.

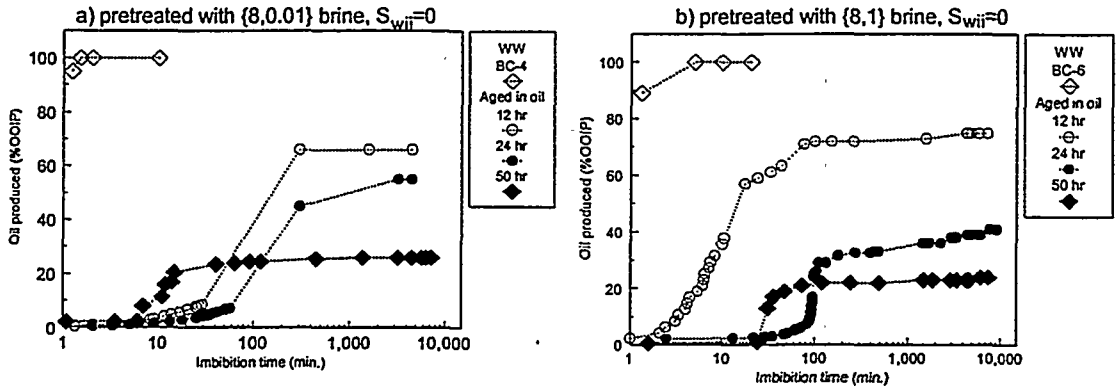

Figure 2.2-13. Oil produced by spontaneous imbibition of brine into capillaries aged in brine and crude oil (S_{wii} = 0), plotted as a function of imbibition time.

Cleaning step omitted (S_{wii}≠0): A more realistic situation with respect to imbibition into an oil reservoir is that an initial water saturation exists. In the remaining experiments, water was present in the corners at the start of imbibition. Tubes were pretreated with {4,0.01}, {4,1}, {6,0.01}, and {8,1} as the aging brines. Only capillaries aged in the {8,1} brine imbibed significantly. In these tubes, the imbibition mechanism was found to be significantly different from those with no initial water saturation at the beginning of imbibition. The most striking differences were (a) water advancement into the corners, leading to snap-off, usually started in the first few minutes after submersion of the capillary, (b) imbibition rates were much faster (see **Fig. 2.2-14**), (c) snap-off events were more frequent, and (d) all the bypassed oil appeared as regular-shaped blobs. Similarity to reported imbibition rate measurements in Berea sandstone cores treated with crude oil (*e.g.*, Zhou et al., 1996; Tang and Morrow, 1996) can be noted and will be discussed later in this report.

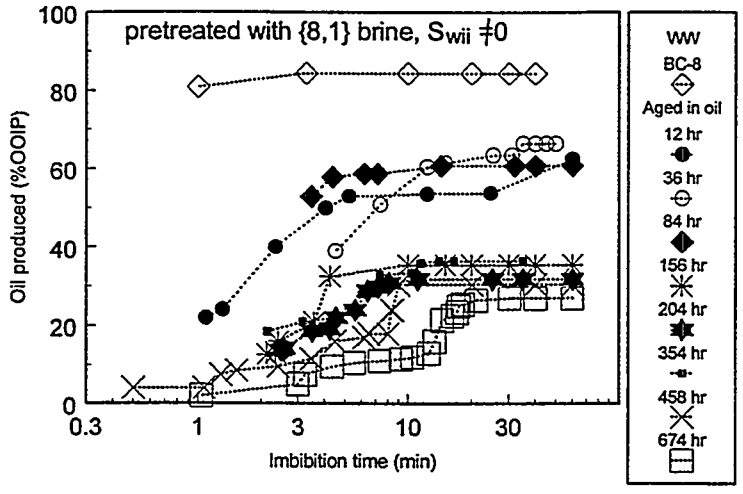

Figure 2.2-14 Oil produced by spontaneous imbibition of {8,1} brine into capillaries aged in brine and crude oil ($S_{wii}\neq 0$), plotted as a function of imbibition time.

Less water imbibed into capillaries aged in {4,1} brine prior to crude oil aging than into those aged in {8,1} brine and water advancement in the corners was less pronounced; no snap-off's were observed. The results from these experiments are summarized in **Table 2.2-16**.

Table 2.2-16. Amount of oil produced by spontaneous imbibition of {8,1} brine. $S_{wii} \neq 0$.

Aging period in A-93 (hrs)	Amount of oil produced (%OOIP)	Spontaneous imbibition index (SI)
{4,1} as the aging brine		
Decane-filled (base case 7)	100±1	1
12	10±1	0.10±0.04
37	3±1	0.03±0.03
{8,1} as the aging brine		
Decane-filled (base case 8)	84±1	1
12	63±1	0.75±0.04
36	66±1	0.78±0.04
60	39±1	0.46±0.04
84	61±1	0.73±0.04
90	45±1	0.54±0.04
156	36±1	0.43±0.04
204	32±1	0.38±0.04
235	34±1	0.40±0.04
354	36±1	0.43±0.04
384	41±1	0.49±0.04
458	30±1	0.36±0.04
674	27±1	0.32±0.04

2.2.4.2 Discussion of the spontaneous imbibition tests

2.2.4.2a Reproducibility of imbibition measurements

The outcome of a particular spontaneous imbibition test is variable, even when tubes have been similarly treated. Some variability in tube dimensions is unavoidable. Another source of variability in many of the tests reported here is the amount and distribution of water remaining after tubes have been drained. The average of 6% for S_{wi} in a strongly water-wet drainage is in good agreement with the expected amount, but the standard deviation was 3% so there can be significant differences between replicate tests. Vertical orientation of the tubes during aging means that gravity effects played a role in distribution of the fluids.

Variations in initial water saturation can affect the outcome of these tests in two distinct ways. First, the extent of wetting alteration depends on the amount, distribution, and composition of the brine in place during aging in crude oil, and second, the rate of imbibition and probability of snap-off events are both influenced by S_{wi}. These two different effects are recognized in the notation used here, with S_{wia} signifying the water saturation during crude-oil aging and S_{wii} indicating the water present in the tube at the onset of imbibition.

Whether or not there is an initial MTM influences the course of imbibition. In most cases, compression and expansion of the teflon tube as it was cut to separate the oil-filled capillary from the filling syringe caused a small amount of water to enter at the tube inlet and form an initial MTM. The only exceptions are two tests marked in Table 2.2-15.

2.2.4.2b Imbibition into water-wet square capillaries

When decane is used as the oil phase, the capillaries remained water-wet and water or brine always imbibed. The course of that imbibition varied, however, depending on whether or not there was an initial water saturation. Two experiments with no initial water saturation are compared in **Fig. 2.2-15** (see also Table 2.2-12 and Fig. 2.2-10). As

expected, brine composition makes no difference; the rates and amounts of water imbibed are almost identical. Decane was displaced by steady advancement of the MTM from inlet to outlet. No water was seen advancing in the corners ahead of the MTM.

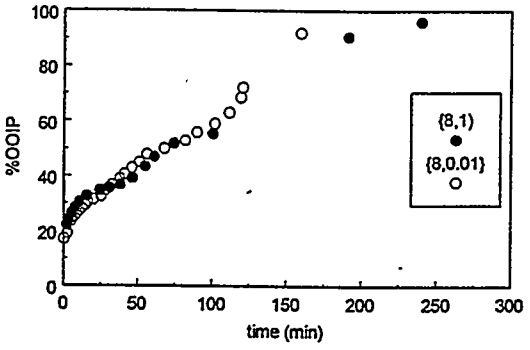

Figure 2.2-15. Imbibition of brine into decane-filled tubes.

Since θ_A for water and dyed-decane was only about 20°, wedges should be able to form, but they do not. The relative permeability to the water invading an oil-filled corner is very low and limits the rate at which water can fill the corner wedges. Evidently, for a contact angle on the order of 20°, filling of the corner wedges is slower than the rate at which the MTM moves to fill the tube with water. If $\theta_A = 0°$, the wedges should fill rapidly and trap some decane. That they do not is evidence that $\theta_A > 0°$, as confirmed by contact angle measurements.

If the capillaries were first filled with brine, flushed with decane to S_{wi}, then cleaned and dried before refilling with 100% decane, in the same sequence as was used for some of the tubes exposed to crude oil, imbibition rates were significantly faster (see Fig. 2.2-10a). There are two possible explanations: (1) salt dried in the corners of the tube helps to maintain more water-wet conditions ($\theta_A < 20°$), or (2) the salt dried in the corners might introduce an osmotic effect that assists in formation of corner wedges. Mennella *et al.* (1995) showed that a salt-coated glass plate had less tendency to adsorb crude oil components than a clean plate, but the contact angles reported were greater than 20°, so it is not obvious how this observation affects interpretation of the dyed-decane results. Additional work is needed to distinguishing between the contributions from these two possibilities.

The fastest imbibition times were for capillaries containing connate water. Again, there are two possible effects. The presence of water films may limit adsorption of dye on the capillary walls, maintaining more water-wet conditions and higher relative permeability to water in the water-filled corners permits more rapid imbibition. Imbibing water rapidly swelled the wedges. At some point, the swollen wedges reached the limiting curvature at which the AMs touch to form an unstable cylindrical interface. The imbibing liquid then spontaneously redistributed, snapping off segments of the nonwetting phase. Since the snap-off events reflect instabilities that can occur anywhere in the tube, the amount of oil produced varied in replicate experiments.

2.2.4.2c Capillaries contacted with crude oil

In capillaries that have been contacted with crude oil, the wetting conditions that develop are complex. For a given oil, the mechanisms of interaction can depend on brine composition and the history of exposure (including aging time, aging temperature, and water saturation).

Polar interactions in dry capillaries

When a clean, dry capillary tube was filled with crude oil, adsorption of polar material from the oil onto the glass surface began. Analogous tests on flat surfaces have been reported (Buckley *et al.*, 1997a). In those tests, water advanced over a decane-covered surface at 77° after only one day of aging in A-93 crude oil at 25°C. After 20 days of aging, the contact angle was essentially unchanged (θ_A=80°). Polar interactions between crude oil and solid typically occur quickly (on the order of a few hours) and make glass surfaces intermediately wet. Since there is no initial water in these tubes, wetting is altered uniformly. The effects of polar interactions are evident in **Fig. 2.2-16**. After 16 hours of aging in oil, very little water imbibes and the SI is less than 0.1, consistent with uniformly neutral wetting.

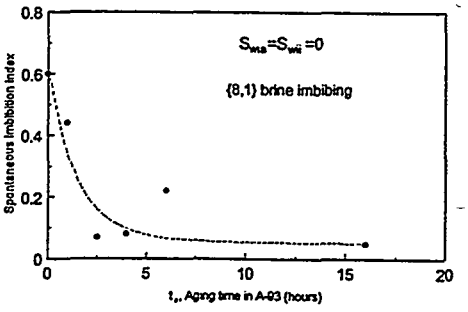

Figure 2.2-16. SI index as a function of aging time.

Acid/base interactions in wet capillaries

Interactions by the acid/base mechanism are dominant between a high base number, medium gravity oil—of which A-93 is a good example—and an acidic silicate surface (Buckley *et al.*, 1997a). In the presence of a brine phase, interactions between oil and solid are largely dependent on the composition of the brine. These interactions can continue to change surface wetting for days or even weeks.

In each experiment, there are two brine compositions: the brine in which the tube is aged and the imbibing brine. These two brines can be the same or they may be different. Aging brines tested included {4,1}, {6,1}, {8,0.01}, and {8,1}. Three of these are in the conditionally stable region (Fig. 1). Only {8,1} produces stable water films with A-93 crude oil.

As shown in **Table 2.2-17**, aging brine plays an important role in determining whether or not a treated tube imbibes. For tubes aged in {6,1} or {8,0.01} brine and crude oil, no imbibition of water was observed. Those aged in {4,1} or {8,1} did imbibe.

Table 2.2-17. Brine combinations tested, S_{wii}=0

Aging brine	Imbibing brines	Imbibed? (hours of aging)	Water moves in: MTM	AMs
{4,1}	{8,0.01}	yes (12, 48)	X	X
{6,1}	{8,0.01}	no		
{8,0.01}	{8,0.01}	no		
{8,1}	{8,0.01}	yes (12, 24, 48, 50)	X	X
{4,1}	{8,1}	yes (12), no (37)	X	
{6,1}	{8,1}	no		
{8,0.01}	{8,1}	no		
{8,1}	{8,1}	yes (12, 24, 50)	X	X

The composition of the imbibing brine also influences the rate and amount of brine imbibed, as shown in **Fig. 2.2-17**. Imbibition of {8,0.01} and {8,1} brines are compared for tubes that were aged initially in {8,1} brine. Effects of both aging time and brine compositions on the amount of oil produced are shown in **Fig. 2.2-18**, where the variation in the SI index is plotted as a function of aging time in crude oil for tubes aged in {4,1} and {8,1} brines. Aging brine composition has the stronger influence, in agreement with the results of Tang and Morrow (1996).

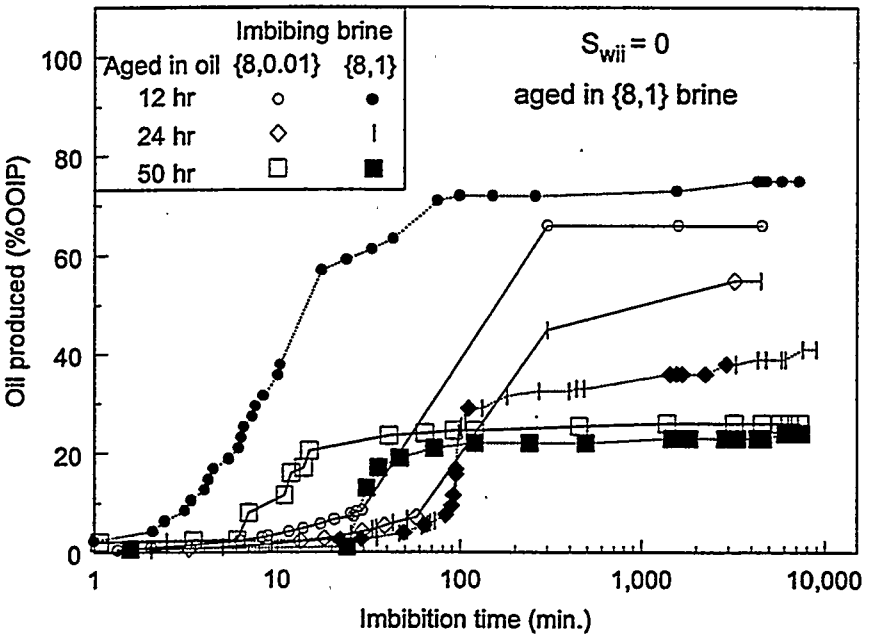

Figure 2.2-17. Influence of brine composition on imbibition rates.

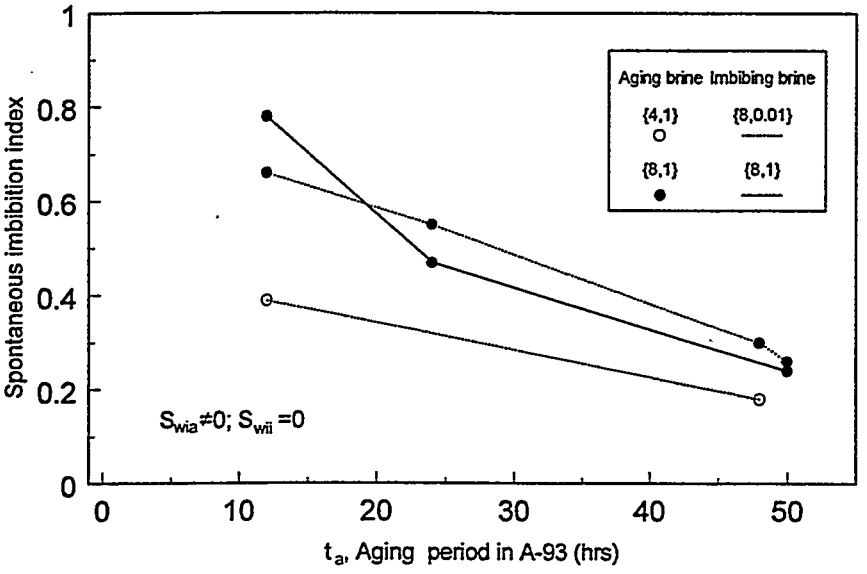

Figure 2.2-18. SI index as a function of aging time in A-93 crude oil.

Although these capillary tubes were cleaned and dried before filling with oil for the imbibition tests, the flow of water into these tubes was quite different from that into tubes which had never contained brine. Dry tubes that were treated with crude oil became uniformly altered in wetting and did not develop arc menisci. In the cleaned tubes that had

first been treated with brine, then with oil, water wedges were almost always noted. The corners remained more water-wet than other parts of the tube.

Several tests were performed with $S_{wii} \neq 0$. The brine that was present during aging in oil was not dried, nor was the oil replaced before beginning imbibition. **Figure 2.2-19** shows the effect of aging time on the spontaneous imbibition index. Imbibition is much faster in these tubes with water already occupying the corners (*cf.*, Fig. 2.2-14). An MTM sweeps the tube until snap-off from AM growth occurs, trapping oil and creating new MTMs. Fluid movement ceased in an hour or less.

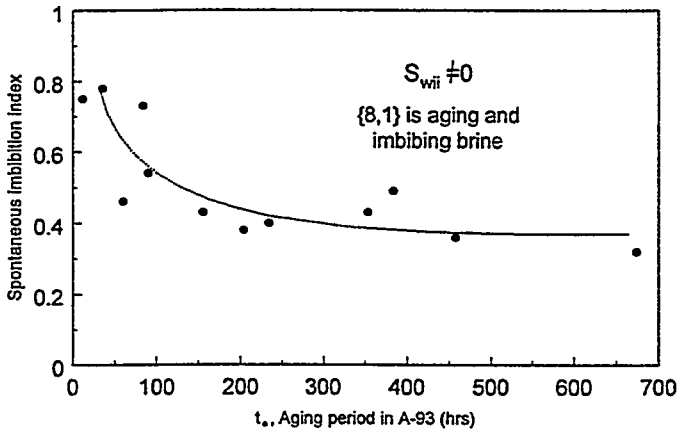

Figure 2.2-19. SI index as a function of aging time for capillaries with an initial water saturation at the start of imbibition.

These tests illustrate an effect of aging time, which is similar to that reported for aging Berea sandstone cores in A-93 crude oil (Zhou *et al.*, 1996, and references cited therein). Cores and tubes were most water-wet for short aging times, and imbibed less water as the aging time increased. Changes in the rate of imbibition continued over the 29 days of aging tested here. All of the tubes remain weakly water-wet.

Another feature found in imbibition rate curves for both square tubes and cores is the appearance of an induction time in the first stages of imbibition for weakly water-wet conditions (Zhou *et al.*, 1996). In the square tubes, induction times are most marked for those systems that develop AMs, starting from $S_{wii} = 0$ (cf. Figs. 2.2-11, 12, and 13), although induction periods are also apparent in the more directly comparable case of aged

tubes with $S_{wii} \neq 0$ (Fig. 2.2-14). In the square tubes, this induction period represents the time required to swell AMs before significant oil is swept out by movement of MTMs. It would be of interest to know to what extent this might also be true in cores.

2.2.5 Summary

Square tubes, exposed to brine and crude oil, become mixed wet. Water rising against air can form corner wedges even though the average contact angle, calculated from the height of rise, assuming uniform wetting, indicates that wedges should not form. A second set of contact angles, calculated from a mixed-wet model, are higher and show more differentiation between tubes treated with different aging brines. High hysteresis is observed, consistent with previous contact angle observations of glass surfaces contacted with brine and crude oil.

Oil displacement by a main terminal meniscus and the formation, extension, and swelling of arc menisci during spontaneous displacements of decane or crude oil by brine have been documented. A variety of conditions were tested. Variables included compositions of aging and imbibing brines, aging times in oil, and presence or absence of an initial water saturation.

The mechanism of displacement by imbibition depends on whether water wedges form in the corners. If the tube is preferentially water-wet, but water wedges are absent, oil recovery by movement of the main terminal meniscus can approach 100% in these straight capillaries. When water wedges are present, snap-off events exert a dominant, and sometimes unpredictable, influence over the amount of oil that is trapped.

Water wedges formed in all mixed-wet tubes. Only capillaries that were made uniformly neutral in wetting by aging in the absence of water failed to imbibe some water into the corners.

Imbibition rates were estimated by measuring lengths of brine and oil-filled sections of the capillary tube, with results that showed similarities to the rate of imbibition

in much more complex porous media. An induction time during which water filled the corner wedges with little accompanying movement of oil was observed. Suppression of both the rate and amount of imbibition was reminiscent of results reported with this same crude oil in Berea sandstone cores.

The amounts of oil produced were compared using a spontaneous imbibition index. A consistent trend of decreased oil production with increased aging time emerged. Wetting alteration by polar and acid/base interactions was generally consistent with previous contact angle observations. Often the brine that produced the most stable water films with glass and A-93 crude oil was the only one that maintained sufficiently water-wet conditions to guarantee some imbibition of water.

In the future, baseline studies of very strongly water-wet conditions will help to distinguish between the possible effects of dye adsorption and the suggested contributions of salinity and osmotic effects. Other improvements in experimental techniques are needed; for example, better control over the initial water saturation. The focus will be on situations where S_{wia} and S_{wii} both are nonzero. Triangular tubes, which drain to give higher S_{wi}, might be more directly comparable to the angular pore spaces in most sandstones than the square tubes used in this study.

There are a wealth of unexplored combinations of brine and crude oils, including brines containing divalent ions and crude oils with different acidic and basic characteristics, that could be studied in noncircular capillaries. Coupling independent measurements of contact angles to measurements of the rate, extent, and patterns of imbibition will help to elucidate imbibition mechanisms and their dependence on the details of wetting conditions in cores and in oil reservoirs.

CONCLUSIONS AND FUTURE WORK

Considerable progress has been made during the second year of this project, especially toward the first two goals, as presented in sections 1 and 2 of this report. To reiterate the most important points, the following summary of conclusions is presented.

Part 1. Chemical Evaluation of Crude Oils

The results of wettability tests with four medium gravity oil samples, for which surface precipitation should not be a factor, are consistent with expectations based on their G-AB profiles. Spraberry, with a high base number and low acid number, participates in acid/base interactions with the acidic mica surface. These interactions are strongest when ionic strength is low.

As additional experience is gained with oils that have an increasingly wide range of G-AB profiles, we expect to be able to define more closely the properties associated with oils that have the highest and lowest propensity to alter wetting of solid surfaces.

Determining when asphaltene precipitation is likely to be an important factor has led to the refractive index approach. In this area, some important conclusions from our recent work are that the solubility parameters of several hydrocarbons have the dependence on RI as predicted for London dispersion interactions, that the density dependence of the RI can be accurately estimated by the Clausius-Mossotti or Lorenz-Lorentz equations over the pressure range of interest in petroleum reservoirs, that the difference between the RIs of hydrocarbons, extrapolated to zero frequency, can be estimated from the differences between the RIs measured at the sodium-D line if the hydrocarbons have similar absorption frequencies. This may not be valid for asphaltenes since they absorb in the frequencies of visible light.

The F_{RI} of mixtures of a crude oil or its asphaltenes with hydrocarbon solvents and precipitants are a linear function of the volume fraction of the crude oil as predicted by the Clausius-Mossotti and Lorenz-Lorentz equations. This makes it possible to estimate the RI of the crude oil or asphaltene when it is too opaque to measure directly.

The RI of live crude oil during pressure depletion can be calculated from the RI of STO, molar refraction of the separator gas, the formation volume factor, B_o, and the solution gas/oil ratio, R_s.

For a number of crude oils with RI in the range, 1.51 ± 0.04, precipitation with addition of *n*-heptane begins when the mixture RI is less than the average P_{RI} of 1.44 ± 0.02. Note that the value of P_{RI} is more nearly constant than is the RI of the original oils.

In a model system with the pure hydrocarbons, hexabenzobenzene and toluene, addition of *n*-heptane initiates precipitation when the RI drops below 1.4275. This value of P_{RI} is within the range of values observed for crude oil systems. Thus precipitation phenomena analogous to asphaltene precipitation occurs in a system with no polar interactions. This is evidence that polar interactions are not necessary for asphaltene precipitation.

The addition of the aromatic solvent, α-methylnaphthalene, to crude oil allows more dilution with isooctane before precipitation occurs, but the values of P_{RI} is unchanged. Thus AMN is an analog of a resin in its solvating power for the asphaltenes even though AMN has no polar groups to contribute to solvation due to polar interactions. This is evidence that the aromatic character of the resins is responsible for the solvating properties of the resins.

Part 2. Wettability Assessment

Muscovite mica, whose surface structure is analogous to illite clay, is a good choice for standard tests of crude oil/brine/solid interactions with negatively charged reservoir minerals. It has the advantages of being widely studied, molecularly smooth, and very reproducible.

The wetting of mica surfaces can be altered by exposure to crude oils. Two oils, A-93 from Prudhoe Bay and Moutray from West Texas, have been tested to compare their wettability altering capabilities, previously studied on glass surfaces, with similar conditions and mica surfaces.

In the absence of water, intermediately-wet conditions result from exposure of mica surfaces to either A-93 or Moutray. With NaCl brines, acid/base interactions influence water-film

stability. Film stability on mica is similar to that demonstrated previously on glass. Ion-binding interactions with an acidic oil (Moutray) can produce fairly oil-wet surfaces.

There are small differences in interactions with muscovite and biotite mica surfaces. Macroscopic surface roughness is not detected by contact angle measurements on oil-treated surfaces. Finally, we find that changes in dissolution rates with pH and temperature for different substrate materials may have an impact on wettability alteration.

We have shown that square tubes, exposed to brine and crude oil, become mixed wet. Thus we can use COBR interactions to produce simple mixed-wet porous media for study of the effects of wetting alteration on imbibition, a necessary step to bridge the gap between surface wetting studies and the effects of wetting on multiphase flow in porous media.

The mechanism of displacement by imbibition depends on whether water wedges form in the corners. If the tube is preferentially water-wet, but water wedges are absent, oil recovery by movement of the main terminal meniscus can approach 100% in these straight capillaries. When water wedges are present, snap-off events exert a dominant, and sometimes unpredictable, influence over the amount of oil that is trapped.

Water wedges formed in all mixed-wet tubes. Only capillaries that were made uniformly neutral in wetting by aging in the absence of water failed to imbibe some water into the corners.

Imbibition rates were estimated by measuring lengths of brine and oil-filled sections of the capillary tube, with results that showed similarities to the rate of imbibition in much more complex porous media. An induction time during which water filled the corner wedges with little accompanying movement of oil was observed. Suppression of both the rate and amount of imbibition was reminiscent of results reported with this same crude oil in Berea sandstone cores.

Future Work

Work continues in both the chemical characterization of crude oils and in the wetting assessment areas. Oils continue to be added to our data base of chemical properties as they

become available. New tools being developed that will be reported on during year 3 include the following.

- The capability to observe the onset of precipitation at high temperature and pressure is being extended to lower molecular weight precipitants, including propane and CO_2, and to continue investigations of the effects of temperature and pressure.
- FT-IR techniques are being tested to quantify differences between crude oils and the materials that adsorb from them.
- Assessment of surface wetting is being extended to elevated temperatures and pressures.
- Atomic forces microscopy is being used to provide a direct measure of the material that adsorbs from crude oils onto solid surfaces.

In cores, the effects of mixed wetting on end-point fluid saturations and relative permeability to water are being studied.

NOMENCLATURE

a_a	molecular radius of asphaltene molecule
A_{eff}	effective area available to nonwetting phase
AM	arc meniscus
B_o	formation volume factor (RB/STB)
C	coefficient, defined in Eq. 1.2-3
C	curvature, $1/r_d$
C_i	molar concentration of component i
C_i^o	molar concentration at a reference condition where the RI is evaluated
C_n	normalized curvature, d/r_d
C_Σ	sum of molar concentrations (Eq. 1.2-14)
COBR	crude oil/brine/rock
d	half width of square tube
D	distance from a molecule to a surface
DLVO	Derjaguin-Landau-Verwey-Overbeek
f_V	volume fraction
F_{RI}	function of n, $F_{RI} = (n^2-1)/(n^2+2)$
g	acceleration due to gravity
h	height of meniscus above free water surface
h	Plank's constant
ΔH^M	heat of interaction between asphaltene and remainder of crude oil
I_o	Amott index to oil
I_w	Amott index to water
I_{w-o}	Amott-Harvey index
MS-P	Mayer & Stowe - Princen
MTM	main terminal meniscus
n	refractive index
N_A	acid number (mg KOH/g of oil)
N_B	base number (mg KOH/g of oil)
N_o	Avogadro's number
P	pressure
P_b	bubble point pressure
P_c	capillary pressure
P_{eff}	effective perimeter = $\Sigma P_{liquid} + \Sigma P_{solid} \cos\theta$
P_{liquid}	arc menisci lengths
P_{solid}	solid perimeter lengths
pH	-log of hydrogen ion concentration
pK_a	pH at equivalence point
P_{RI}	refractive index at onset of asphaltene precipitation
P_{RI}*	P_{RI} calculated from solvent-to-precipitant ratio
PVT	pressure-volume-temperature
r	distance between centers of two molecules (Eq. 1.2-3)
R	radius of spherical particle (Eq. 1.2-5)
R	gas constant
r_d	drainage radius calculated using MS-P theory
r_1, r_2	radii of curvature
R_i	molar refraction of component i
R_s	dissolved gas content (scf/STB)
RI	refractive index
RI_{oil}	refractive index of oil
S_w	saturation of water
S_{wia}	S_{wi} during aging in oil
S_{wii}	S_{wi} at the start of imbibition
S_{wi}	initial water saturation
SARA	saturates-aromatics-resins-asphaltenes
T	temperature (°C)
t_a	aging time in oil
t_b	aging time in brine
USBM	United States Bureau of Mines
V	volume
V	molar volume
$V_{f,oil}$	oil volume fraction
w	interaction energy (molecules)
W	interaction energy (surfaces)
w_a	weight percent
X	mole fraction
α	electronic polarizability
χ	Flory-Huggins interaction parameter
δ	solubility parameter
ε_o	permittivity of free space
Δ_{RI}	= RI_{oil} - P_{RI}
θ	contact angle through water (deg)
θ_A	water-advancing contact angle (deg)
θ_R	water-receding contact angle (deg)
θ_{mixed}	contact angle calculated from curvature assuming hysteresis
$\theta_{uniform}$	contact angle calculated from curvature assuming uniform wetting
ρ	number density
ρ	density (g/ml)
σ	hard sphere diameter
ν_e	absorption frequency in the uv
σ_{LV}	liquid-vapor interfacial tension
σ_{SL}	solid-liquid interfacial tension
σ_{SV}	solid-vapor interfacial tension

subscripts

a	asphaltene
i	component i
o	oil
s	solvent

REFERENCES

Amott, E.: "Observations Relating to the Wettability of Porous Rock," *Trans.*, AIME (1959) **216**, 156-162.

Anderson, W.G.: "Wettability Literature Survey—Part 2: Wettability Measurement," *JPT* (Nov. 1986b) **38**, No. 12, 1246-1262.

ASTM D664-89: "Standard Test Method for Acid Number of Petroleum Products by Potentiometric Titration," *ASTM* (1989).

ASTM D1218-92: "Standard Test Method for Refractive Index and Refractive Dispersion of Hydrocarbon Liquids," *ASTM* (1992) 409-412.

ASTM D2007-80: "Standard Test Method for Characteristic Groups in Rubber Extender and Processing Oils by the Clay-Gel Adsorption Chromatographic Method," *ASTM* (1980).

ASTM D2896-88: "Standard Test Method for Base Number of Petroleum Products by Potentiometric Perchloric Acid Titration, *ASTM* (1988).

Barton, Allan F. M.: *CRC Handbook of Solubility Parameters and Other Cohesion Parameters*, 2nd ed. CRC Press, Boca Raton (1991).

Basu. S. and Sharma, M.M.: "Measurement of Critical Disjoining Pressure for Dewetting of Solid Surfaces," *J. Colloid. Interface Sci.* (1996) **181**, 443-455.

Basu, S. and Sharma, M.M.: "Characterization of Mixed-Wettability States in Oil Reservoirs by Atomic Force *SPEJ* (Dec. 1997) **2**, 527-435.

Bichard, J.A.: "Oil Solubility," presented at the 19th Canadian Chem. Engr. Conf. and 3rd Symp. on Catalysts, Edmonton, Alberta, Oct. 19-22, 1969.

Brady, P.V. and House, W.A.: "Surface-Controlled Dissolution and Growth of Minerals," in *Physics and Chemistry of Mineral Surfaces*, P.V. Brady, Ed. CRC Press (1996) 225-305.

Brown, R.J.S. and Fatt, I.: "Measurements of Fractional Wettability of Oilfield Rocks by the Nuclear Magnetic *Trans.*, AIME (1956) **207**, 262-64.

Buckley, J.S.: "An Etched Glass Micromodel: Description and Displacement Mechanisms," PRRC #93-14, Quarterly Report on "Evaluation of Reservoir Wettability and Its Effect on Oil Recovery," Jan.-March, 1993.

Buckley, J.S.: "Microscopic Investigation of the Onset of Asphaltene Precipitation," *Fuel Sci. & Tech. Internat.*(1996) **14**, 55-74.

Buckley, J.S.: "Mechanisms and Consequences of Wettability Alteration by Crude Oils," PhD Thesis, Heriot-Watt University, Edinburgh, Scotland (1996).

Buckley, J.S., Bousseau, C., and Liu, Y.: "Wetting Alteration by Brine and Crude Oil: From Contact Angles to Cores," *SPEJ* (Sept. 1996) **1**, No. 3, 341-350.

Buckley, J.S., Liu, Y., and Monsterleet, S.: "Mechanisms of Wetting Alteration by Crude Oils," *SPEJ* (Mar. 1998) 54-61.

Buckley, J.S., Liu, Y., Xie, X., and Morrow, N.R.: "Asphaltenes and Crude Oil Wetting—The Effect of Oil Composition," *SPEJ* (June, 1997) 107-119.

Buckley, J.S. and Morrow, N.R.: "Characterization of Crude Oil Wetting Behavior by Adhesion Tests," paper SPE/DOE 20263 presented at the 1990 SPE/DOE EOR Symposium, Tulsa, April 23-25.

Buckley, J.S., Takamura, K., and Morrow, N.R.: "Influence of Electrical Surface Charges on the Wetting Properties of Crude Oils," *SPEFE* (August 1989) 332-340.

Burke, N.E., Hobbs, R.D., and Kashou, S.F.: "Measurement and Modeling of Asphaltene Precipitation," *JPT* (1990) 1440-1446.

Christenson, H.K. and Israelachvili, J.N.: "Direct Measurements of Interactions and Viscosity of Crude Oils in Thin Films between Model Clay Surfaces," *J. Colloid Interface Sci.* (1987) **119**, 194.

Cimino, R., Correra, S., Sacomani, P.A., and Carniani, C.: "Thermodynamic Modelling for Prediction of Asphaltene Deposition in Live Oils," paper SPE 28993 presented at the 1995 SPE International Symposium on Oilfield Chemistry, San Antonio, TX, 14-17 February.

Cimino, R., Correra, S., Del Bianco, A., and Lockhart, T.P.: "Solubility and Phase Behavior of Asphaltenes in Hydrocarbon Media," *Asphaltenes: Fundamentals and Applications*, E.Y. Sheu and O.C. Mullins (eds.), NY: Plenum Press (1995) 97-130.

Cuiec, L.: "Restoration of the Natural State of Core Samples," paper SPE 5634 presented at the 1975 ATCE, Dallas, Sept. 28 - Oct. 1.

Cuiec, L.: "Evaluation of Reservoir Wettability and Its Effects on Oil Recovery," in *Interfacial Phenomena in Oil Recovery*, N.R. Morrow, ed., Marcel Dekker, Inc., New York City (1991), 319-375.

Denekas, M.O., Mattax, C.C., and Davis, G.T.: "Effect of Crude Oil Components on Rock Wettability," *Trans.*, AIME (1959) **216**, 330-333.

Dong, M.: "A Study of Film Transport in Capillaries with an Angular Cross-Section," PhD Thesis, University of Waterloo, 1995.

Ducker, W.A., Xu, Z., and Issraelachvili, J.N.: "Measurements of Hydrophobic and DLVO Forces in Bubble- *Langmuir* (1994) **10**, 3279-3289.

Dubey, S.T. and Doe, P.H.: "Base Number and Wetting Properties of Crude Oils," *SPERE* (Aug. 1993) 195-200.

Dubey, S.T. and Waxman, M.H.: "Asphaltene Adsorption and Desorption from Mineral Surfaces," *SPERE* (Aug. 1991) 389-395.

Espinat, D. and Ravey, J.C.: "Colloidal Structure of Asphaltene Solutions and Heavy-Oil Fractions Studied by Small-Angle Neutron and X-Ray Scattering," paper SPE 25187 presented at the 1993 SPE International Symposium on Oilfield Chemistry, New Orleans, March 2-5.

Feynman, R.P., Leighton, R.B., and Sands, M.: *The Feynman Lectures on Physics*, Vol. II (1989) Addison-Wesley Publishing Co.

Gaudin, A.M., Witt, A.F., and Biswas, A.K.: "Hysteresis of Contact Angles in the System Organic Liquid-Water-Rutile," *Trans.*, SME (March 1964) 1-5.

Heithaus, J.J.: "Measurement and Significance of Asphaltene Peptization," *J. Institute of Petroleum* (Feb. 1962) **48** No. 458, 45.

Herron, M.M., Matteson, A., and Gustavson, G.: "Dual-Range FT-IR Mineralogy and the Analysis of Sedimentary Formations," paper SCA 9730 presented at the 1997 Int. Symp., Calgary, 7-10 Sept.

Hildebrand, J.H. and Scott, R.L.: *The Solubility of Nonelectrolytes*, (1964) Dover Publications, Inc.

Hirasaki, G.J.: "Structural Interactions in the Wetting and Spreading of van der Waals Fluids," in *Contact Angle, Wettability and Adhesion*, Mittal, K.L. (ed.) VSP, Utrecht, 1993.

Hirschberg, A., deJong, L.N.J., Schipper, B.A., and Meijer, J.G.: "Influence of Temperature and Pressure on Asphaltene Flocculation," *SPEJ* (June 1984) 283-293.

Hotier, G. and Robin, M.: "Effects of Different Diluents on Heavy Oil Products: Measurement, Interpretation, and a Forecast of Asphaltene Flocculation," *Revue de l'IFP* (1983) **38**, 101.

Hough, D.B. and White, L.R.: "The Calculation of Hamaker Constants from Lifshitz Theory with Applications to Wetting Phenomena," *Advances in Colloid and Interface Science*, **14** (1980) 3-41.

Hurst, A.: "Problems of Reservoir Characterization in Some North Sea Sandstone Reservoirs Solved by the Application of Microscale Geological Data," *North Sea Oil & Gas Reservoirs*, Trondheim (Dec. 2-4, 1985), Graham & Trotman, Ltd., London (1987), 153-167.

Israelachvili, J.N.: *Intermolecular and Surface Forces*, 2nd Ed., Academic Press, San Diego (1991).

Jadhunandan, P. and Morrow, N.R.: "Spontaneous Imbibition of Water by Crude Oil/Brine/Rock Systems," *In Situ* (1991) **15**, No. 4, 319-345.

Jadhunandan, P. and Morrow, N.R.: "Effect of Wettability on Waterflood Recovery for Crude Oil/Brine/Rock Systems," *SPERE* (1995) **10**, No. 1, 40-46.

Kovscek, A.R., Wong, H., and Radke, C.J.: "A Pore-Level Scenario for the Development of Mixed Wettability in Oil Reservoirs," *AIChE J.* (June 1993) **39**, No. 6, 1072-1085.

Lenormand, R., Zarcone, C., and Sarr, A.: "Mechanisms of the Displacement of One Fluid by Another in a Network of Capillary Ducts," *J. Fluid Mech.* (1983) **135**, 337-353.

Leontaritis, K.J. and Mansoori, G.A.: "Asphaltene Flocculation During Oil Production and Processing: A Thermodynamic-Colloidal Model," paper SPE 16258 presented at the 1987 SPE International Symposium on Oilfield Chemistry, San Antonio, 4-6 Feb.

Liu, L.: "Interactions of Crude Oils with Model Mineral Surfaces," MS Thesis, New Mexico Institute of Mining and Technology, Socorro, NM (1997).

Liu, Y.: "Wetting Alteration by Adsorption from Crude Oils," MS Thesis, New Mexico Institute of Mining and Technology, Socorro, NM (1993).

Liu, Y. and Buckley, J.S.: "Evolution of Wetting Alteration by Adsorption from Crude Oil," *SPEFE* (Mar. 1997) 5-11.

Ma, S., Mason, G., and Morrow, N.R.: "Effect of contact angle on drainage and imbibition in regular polygonal tubes," *Colloids and Surfaces A* (1996) **117**, 273-291.

MacMillan, D.J., Tackett, J.E., Jr., Jessee, M.A., and Monger-McClure, T.G.: "A Unified Approach to Asphaltene Precipitation: Laboratory Measurement and Modeling," paper SPE 28990 presented at the 1995 SPE International Symposium on Oilfield Chemistry, San Antonio, 14-17 Feb.

Mason, G., Nguyen, M.D., and Morrow, N.: "Effect of Contact Angle on the Meniscus Between Two Equal *J. Colloid Interface Sci.* (1983) **95**, No. 2, 494-501.

Mason, G. and Morrow, N.R.: "Effect of Contact Angle on Capillary Displacement Curvatures in Pore Throats Formed by Spheres," *J. Colloid Interface Sci.* (1984) **168**, No. 1, 130-141.

Mason, G. and Morrow, N.R.: "Capillary Behavior of a Perfectly Wetting Liquid in Irregular Triangular Tubes," *J. Colloid Interface Sci.* (1991) **141**, No. 1, 262-274.

Mayer, R.P. and Stowe, R.A.: "Mercury Porosimetry—Breakthrough Pressure for Penetration Between Packed *J. Coll. Interface Sci.* (1965) **20**, 893-911.

Mennella, A., Morrow, N.R., and Xie, X.: "Application of the Dynamic Wilhelmy Plate to Identification of Slippage at a Liquid-Liquid-Solid Three-Phase Line of Contact," *J. Pet. Sci. Eng.* (1995) **13**, 179-192.

Morrow, N.R.: "Wettability and Its Effect on Oil Recovery," *JPT* (Dec. 1990) 1476-1484.

Morrow, N.R., Cram, P.J., and McCaffery, F.G.: "Displacement Studies in Dolomite with Wettability Control by Octanoic Acid," *SPEJ* (1973) **255**, 221.

Morrow, N.R., Lim, H.T., and Ward, J.S.: "Effect of Crude-Oil-Induced Wettability Changes on Oil Recovery," *SPEFE* (Feb. 1986) 89-103.

Morrow, N.R., Ma, S., Zhou, X., and Zhang, X.: "Characterization of Wettability from Spontaneous Imbibition Measurements," paper CIM 94-47 presented at the 1994 Petr. Soc. of CIM Ann. Tech. Meeting and AOSTRA 1994 Ann. Tech. Conf., Calgary, June 12-15.

Morrow, N.R. and McCaffery, F.G.: "Fluid Displacement Studies in Uniformly Wetted Porous Media," in *Wetting, Spreading and Adhesion*, J.R. Padday, ed., New York: Academic Press (1978) 289-319.

Pan, H. and Firoozabadi, A.: "A Thermodynamic Micellization Model for Asphaltene Precipitation: Part I: Micellar Size and Growth," paper SPE 36741 presented at the 1996 ATCE, Denver, 6-9 Oct.

Parkash, S., Moschopedis, S., and Speight, J.: "Physical Properties and Surface Characteristics of Asphaltenes," *Fuel* (1979) **58**, 877-882.

Princen, H.M.: "Capillary Phenomena in Assemblies of Parallel Cylinders. I. Capillary Rise between Two *J. Coll. Interface Sci.* (1969) **30**, 69-75.

Ransohoff, R.C. and Radke, C.J.: "Laminar Flow of a Wetting Liquid Along the Corners of a Predominantly Gas- *J. Coll. Interface Sci.* (1988) **121**, 392-401.

Rassamdana, H., Dabir, B., Nematry, M., Farhani, M., and Sahimi, M.: "Asphalt Flocculation and Deposition: I. *AIChE Journal* (Jan. 1996) **42**, 10.

Reichert, C., Fuhr, B.J., and Klein, L.L.: "Measurement of Asphaltene Flocculation in Bitumen Solutions," *J. Cnd. Pet. Tech.* (Sept.-Oct. 1986) 33-37.

Salathiel, R.A.: "Oil Recovery by Surface Film Drainage in Mixed-Wettability Rocks," *J. Pet. Tech.* (Oct. 1973) 1216-24; *Trans.*, AIME, **255**.

Spildo, K.: "Spontaneous Imbibition of Brine into Crude Oil-Filled Square Capillaries," Video, PRRC, July 1997.

Tang, G.Q. and Morrow, N.R.: "Salinity, Temperature, Oil Composition, and Oil Recovery by Waterflooding," *SPE RE* (Nov. 1997) 269-276.

Thiyagarajan, P., Hunt, J.E., Winans, R.E., Anderson, K.B., and Miller, T.: "Temperature-Dependent Structural Changes of Asphaltenes in 1-Methylnaphthalene," *Energy & Fuels* (1995) **9**, 829-833.

Thomas, M.M., Clouse, J.A., and Longo, J.M.: "Adsorption of Organic Compounds on Carbonate Minerals 1. Model Compounds and their Influence on Mineral Wettability," *Chem. Geol.* (1993) **109**, 201-213.

Vedam, K. and Limsuwan, P.: "Piezo- and Elasto-optic Properties of Liquids under High Pressure. II Refractive Index vs. Density," *J. Chem. Phys.* (1978) **69** (11), 4772-4778.

Victorov, A.I. and Firoozabadi, A.: "Thermodynamics of Asphaltene Precipitation in Petroleum Fluids by a Micellization Model," *AIChE J.* (1996) **42**,1753.

Walsh, T.J.: "Capillary Properties of Model Pores," PhD Dissertation, Loughborough University of Technology, 1989.

Washburn, E.W.: "The Dynamics of Capillary Flow," *Phys. Rev.* (1921) **17**, 274-5.

Weast, R.C.: *CRC Handbook of Chemistry and Physics*, 68th ed. (1987) CRC Press, Inc.

Wiehe, I.A.: "Two-Dimensional Solubility Parameter Mapping of Heavy Oils," *Fuel Sci. & Tech. Int.* (1996) **14**, 289-312.

Xie, X.: "Application of the Dynamic Wilhelmy Plate Technique to Investigation of Oil/Brine/Quartz Wetting Alteration by Adsorption from Crude Oil," PhD thesis, University of Wyoming, Laramie, WY (1996).

Xie, X., Morrow, N.R., and Buckley, J.S.: "Crude Oil/Brine Contact Angles on Quartz Glass," to be presented at the 1997 SCA Internat. Symp., Calgary, 11-13 Sept.

Yildiz, H.Ö.: "Effect of Brine Composition on Oil Recovery by Waterflooding," PhD Thesis, New Mexico Institute of Mining and Technology, Socorro, NM (1995).

Zhou, X., Morrow, N.R., and Ma, S: "Interrelationship of Wettability, Initial Water Saturation, Aging Time, and Oil Recovery by Spontaneous Imbibition and Waterflooding," paper SPE 35436 presented at the 1996 SPE/DOE IOR Symposium, Tulsa, 21-24 April.

Zhou, X., Torsæter, O., Xie, X., and Morrow, N.R.: "The Effect of Crude-Oil Aging Time and Temperature on the Rate of Water Imbibition and Long-Term Recovery by Imbibition," *SPEFE* (Dec. 1995)259-265.